Universität Bremen

GRAIN-SIZE COMPOSITION OF QUATERNARY SOUTH ATLANTIC SEDIMENTS AND ITS PALEOCEANOGRAPHIC SIGNIFICANCE

Dissertation zur Erlangung des Doktorgrades der Naturwissenschaften

am Fachbereich Geowissenschaften der Universität Bremen

Vorgelegt von Michael Frenz

Bremen, 2003

Tag des Kolloquiums:

20. Juni 2003

Gutachter:

1. Prof. Dr. Rüdiger Henrich
2. Priv.-Doz. Dr. Rüdiger Stein

Prüfer:

1. Prof. Dr. Dieter Fütterer
2. Dr. Jan-Berend W. Stuut

Table of contents

Abstract

The grain-size composition is an fundamental property of sediments. The grain-size signature contains information about the history of a deposit such as sediment source, input mechanism, accumulation, redistribution, modification or alteration of sediment compounds. In previous studies mainly downcore results of grain-size distributions were used to infer climate variability from the changes of sediment input or current intensity. The spatial aspect of sediment input and distribution is often neglected. The use of grain-size composition in carbonate-dissolution studies in most previous studies is restricted to the sand content as a dissolution indicator. The detailed grain-size distribution of the calcareous sediment compounds is rarely used for paleoceanographic reconstructions. Hitherto, the direct link between the size distributions and the particles behind is very rough.

The present study presents the spatial distribution of grain-size signatures of sediments from the South Atlantic in two time slices: modern (surface samples) and Last Glacial Maximum (LGM). First the overall texture of the sediments was determined (sand, silt, clay contents), followed by the detailed analysis of the grain-size distribution of the bulk and terrigenous silt fraction (63-2 μm) using a Micromeritics SediGraph 5100. From these results the carbonate silt grain-size distribution was calculated. The main results are presented in three manuscripts according to regional and thematic settings.

(#1) At the South American continental margin a modern terrigenous sample set with a relative high sample coverage is available. Together with bulk geochemical parameters of the sediments (carbonate, organic carbon) the spatial variations in the grain-size distributions give a plausible model for the sedimentation pattern in the SW Atlantic, which is in good agreement with the modern oceanography in this area. Relatively high carbonate contents at water depths between 2000 and 4000 m are typical for the southward flow of North Atlantic Deep Water (NADW) traced down to 48°S. This carbonate-rich band is interrupted by a narrow N-S-striking corridor between 52 and 54°W with high contents of organic carbon and a characteristic grain-size signature. This corridor is interpreted to be the sedimentary imprint of the Malvinas (Falkland) Brazil Confluence. Very coarse sediments along the Argentine outer shelf and continental slope reveal strong sediment sorting caused by the vigorous Malvinas Current. In contrast, at the southern base of the Santos Plateau and in the southern Brazil Basin very fine-grained sediments accumulate under relatively weak current conditions.

(#2) Pelagic calcareous oozes show a generally bimodal grain-size distribution in the silt fraction with a prominent minimum at 8 μm. According to scanning-electron microscopical investigations (SEM) the modes were attributed to foraminifer fragments and juvenile foraminifer tests (> 8 μm) on the one hand and coccoliths (< 8 μm) on the other. Including the carbonate content of the sand and clay fractions the contribution of foraminifer and coccolith carbonate was calculated. The relatively fertile region of the equatorial upwelling is characterised by high contributions of foraminifer carbonate, whereas the sediments in the oligotrophic centre of the subtropical gyre are rich in coccoliths. In contrast to the coarse silt (cf. #3), the grain size of the fine silt mode is regionally very stable and independent from water depth. This phenomenon is attributed to nearly identical coccolith assemblages within the respective provinces and the relative dissolution resistance of coccoliths. A comparison to the results of census and biometrical data retrieved from

separated silt samples revealed the following results: Relatively small (nominal diameter < 4 µm) and in bulk samples exceptionally abundant species like *E. huxleyi* und *F. profunda* are highly depleted in the silt and therefore enriched in the clay fraction (equivalent spherical diameter < 2 µm). In the southernmost province the fine silt mode is almost exclusively composed of *C. leptoporus*. To infer the position (grain size) of this species in the other provinces its nominal diameter (mean length of the placcoliths) and its equivalent spherical diameter (modal grain size of fine silt) are linked by a shape factor. By fitting of more normal distributions to measured size distributions it is possible to attribute the Gaussian distributions to single coccolith species. The area below the curve gives the mass contribution of the species, respectively.

(#3) The observed water-depth dependence of the coarse silt mode is used to reconstruct carbonate dissolution for modern and LGM sediments. The basic assumption is that carbonate dissolution causes fragmentation of foraminifer tests and that these fragments become successively smaller with increasing dissolution intensity. This causes not only a relative decrease in sand content, but a decrease in coarse silt contribution and its mean and modal grain size as well. If the samples are ordered to ecologic provinces and their relative position to the Atlantic deep-sea basins a critical water depth can be observed below which the mentioned parameters indicate a significant change in the grain-size composition of the sediments. This critical depth coincides with the sedimentary lysocline. For the modern situation the vertical position of the lysocline was determined at a water depth of about 4100 m for the Brazil and Cape Basins. In the Angola Basin the lysocline is about 500 m deeper. This asymmetry in the carbonate preservation pattern is connected to the restricted intrusion of Antarctic Bottom Water into the Angola Basin due to submarine barriers. According to the present data the lysocline was situated at a water depth of about 3100 m during the LGM, and the present asymmetry in carbonate preservation between the basins did not exist. These results support ocean circulation models, which rely on a reduced production of NADW and a vertical extension of carbonate corrosive Southern Component Water during glacial periods.

Kurzfassung

Die Korngrößenzusammensetzung ist eine fundamentale Eigenschaft von Sedimenten. Sie enthält Informationen über die Geschichte der Ablagerung wie die der Sedimentquelle, des Eintragsmechanismus, Umlagerung, Modifizierung oder der Alteration von Sedimentbestandteilen. In bisherigen Studien wurden meist Zeitreihen von Korngrößenverteilungen benutzt, um anhand der Variabilität des Sedimenteintrags oder der Strömungsintensität auf Klimaänderungen zu schließen. Dagegen wird der räumliche Aspekt des Sedimenteintrags und der Verbreitung meist vernachlässigt. Der Einsatz der Korngrößenzusammensetzung in Karbonatlösungsstudien beschränkt sich in älteren Arbeiten meist auf den Anteil der Sandfraktion als Lösungsindikator. Hingegen wird die detaillierte Korngrößenverteilung des karbonatischen Sedimentanteils selten zu paläoozeanographischen Rekonstruktionen herangezogen. Des weiteren wird die direkte Verbindung zwischen der Korngrößenverteilung und den zugehörigen Partikeln meist sehr pauschal beurteilt.

Die vorliegende Arbeit behandelt die räumliche Verteilung der Korngrößensignaturen von Sedimenten aus dem Südatlantik zweier Zeitscheiben: rezente Sedimente (Oberfläche) und Sedimente des Letzten Glazialen Maximums (LGM). Zunächst wurde das Gesamtkorngrößengefüge der Sedimente erfasst (Anteile von Sand, Silt und Ton). Daran schloss sich die detaillierte Analyse der Siltfraktion an. Mit Hilfe des Micromeritics SediGraph 5100 wurden nacheinander die Korngrößenverteilungen des Gesamtsilts und des terrigenen Silts ermittelt. Aus beiden Verteilungen wurde die der karbonatischen Siltfraktion berechnet. Die Ergebnisse dieser Korngrößenanalysen sind in drei Manuskripten regional und thematisch zusammengefasst.

(#1) Vom südamerikanischen Kontinentalrand liegt ein räumlich dichter Datensatz für terrigene Oberflächensedimente vor. Gemeinsam mit geochemischen Parametern der Sedimente (Karbonatgehalt, Anteil des organischen Kohlenstoffs) ergibt ihre räumliche Verteilung ein plausibles Gesamtbild für die Sedimentation im SW Atlantik, welches gut mit der modernen ozeanographischen Konstellation übereinstimmt. Relativ hohe Karbonatgehalte zwischen 2000 und 4000 m Wassertiefe charakterisieren den südwärtigen Fluss von Nordatlantischem Tiefenwasser (NADW) bis 48°S. Dieses karbonatreiche Band wird durch einen engen N-S-streichenden Korridor zwischen 52 und 54°W mit hohen Gehalten an organischem Kohlenstoff und einer typischen Korngrößensignatur unterbrochen. Dieser Korridor wird als sedimentologisches Abbild der Malvinas- (Falkland-) Brasil-Konfluenz interpretiert. Sehr grobe Sedimente am äußeren argentinischen Schelf und Kontinentalhang belegen die starke sedimentsortierende Wirkung des Malvinasstroms. Am südlichen Fuß des Santos Plateaus und im südlichen Brasilbecken werden hingegen sehr feinkörnige Sedimente unter relativ ruhigen Strömungsbedingungen abgelagert.

(#2) Pelagische Karbonatschlämme weisen in der Siltfraktion generell eine bimodale Korngrößenverteilung mit einem markanten Minimum bei 8 µm auf. Anhand von rasterelektronenmikroskopischen Untersuchungen wurden die Modi Foraminiferenfragmenten und juvenilen Foraminiferen (> 8 µm) einerseits und Coccolithen (< 8 µm) andererseits zugeordnet. Unter Einbeziehung der karbonatischen Sand- und Tonfraktion wurde der Beitrag von Foraminiferen- und Coccolithenkarbonat berechnet. Dabei zeichnet sich der mesotrophe Bereich des äquatorialen Auftriebs durch hohe Anteile an Foraminiferenkarbonat aus, während die Sedimente in den oligotrophen Bereichen

im Zentrum der subtropischen Gyre coccolithenreich sind. Die Korngröße des Feinsiltmodus' ist im Gegensatz zu der des Grobsilts (siehe #3) regional sehr stabil und wassertiefenunabhängig. Dieses Phänomen wird auf nahezu identische Coccolithenvergesellschaftungen innerhalb der Provinzen und die relative Karbonatlösungsresistenz der Coccolithen zurückgeführt. Ein Abgleich mit Auszählungs- und Biometriedaten an Siltproben ergab folgende Resultate: Relativ kleine (Nominaldurchmesser < 4 µm) und in Gesamtproben außerordentlich häufige Coccolithenarten wie *E. huxleyi* und *F. profunda* sind in der Siltfraktion stark ab-, dafür in der Tonfraktion (äquivalent sphärischer Durchmesser < 2 µm) stark angereichert. In der südlichsten Provinz wird der Feinsiltmodus fast ausschließlich von *C. leptoporus* gebildet. Um die Position (Korngröße) dieser Population in anderen Provinzen zu ermitteln wurden sein Nominaldurchmesser (durchschnittliche Länge des Placcolithen) und sein äquivalent sphärischer Durchmesser (Modalkorngröße des Feinsilts) mit einen Formfaktor verbunden. Durch Angleichung weiterer Normalverteilungen an die gemessenen Korngrößenverteilungen ist es möglich, einzelne Gauß-Verteilungen weiteren Coccolithenarten zuzuordnen und deren Gewichtsbeitrag anhand der Fläche unter der Kurve zu bestimmen.

(#3) Die beobachtete Wassertiefenabhängigkeit des Grobsiltmodus' wird benutzt, um Karbonatlösung für rezente und LGM-zeitliche Sedimente zu rekonstruieren. Man geht davon aus, dass Foraminiferengehäuse durch Karbonatlösung fragmentieren und diese Fragmente bei höherer Lösungsintensität kleiner werden. Das hat zur Folge, dass nicht nur der relative Anteil der Sandfraktion abnimmt, sondern auch der Grobsiltanteil sowie dessen mittlere und modale Korngröße. Ordnet man die Proben in den ökologischen Provinzen entsprechend ihrer Position zu den atlantischen Tiefseebecken, kann man eine kritische Wassertiefe ermitteln, unterhalb welcher die genannten Parameter eine signifikante Änderung der Korngrößenzusammensetzung der Sedimente anzeigen. Diese fällt mit der sedimentären Lysokline zusammen. Für die moderne Situation wurde die vertikale Position der Lysokline bei einer Wassertiefe von etwa 4100 m für das Brasil- und das Kap-Becken bestimmt. Im Angola-Becken liegt diese etwa 500 m tiefer. Diese Asymmetrie im Karbonaterhaltungsmuster hängt mit dem durch submarine Barrieren eingeschränkten Zufluss von karbonatuntersättigtem Antarktischen Bodenwasser in das Angola-Becken zusammen. Entsprechend der vorliegenden Daten lag die Lysokline dagegen während des LGM bei etwa 3100 m Wassertiefe, und es existierte keine Asymmetrie der Karbonaterhaltung zwischen den Becken. Diese Ergebnisse stützen ozeanische Zirkulationsmodelle, die von einer reduzierten Produktion von NADW und einer vertikalen Ausdehnung von karbonatkorrosivem Südkomponentenwasser während Kaltphasen ausgehen.

PART I

INTRODUCTION

With the establishment of the "Global Conveyor Belt" (Broecker, 1987), a vivid model was provided to explain the global transfer of heat, gas, salt and nutrients. Especially by the rate of inter-hemispheric heat exchange and the coupling to green house gases/CO_2 (uptake and release) the global thermohaline circulation is seen to be most relevant and sensitive for past and future climate changes (e.g. Manabe and Stouffer 1993). Including the Atlantic sector of the Southern Ocean the Atlantic takes a key role in the global circulation because the main intermediate and deep-water masses are produced in its high latitudes. In the vicinity of the South Atlantic freshly build deep-water masses of southern and northern origin come across each other. The South Atlantic is best qualified to study the physical and chemical properties of the deep-water masses because, compared to the Indian and Pacific Ocean it is situated in relative proximity to their formation regions.

On the other hand, the flow of water masses leaves its imprint in the sediments. The conditions of the upper ocean control the biogenic production. The climatic framework steers quality and amount of the of terrigenous input. The deep water masses are responsible for (re-) distribution and modification of this primary input (e.g. current sorting, carbonate dissolution). Additionally, the isotopic signature of the water masses are impressed on the shells of planktic and benthic organisms. Therefore, the sediment record serves as an archive of past climatic and oceanic leftovers from which paleoceanographers and sedimentologists with the help of modellers read the past of our planet and make predictions for future development.

To shed some more light on the complex interactions of present and past ocean circulation at a global key position the German Research Foundation (*Deutsche Forschungs-gemeinschaft*) funded the Collaborative Research Centre (*Sonderforschungsbereich*) 261 "The South Atlantic in the Late Quaternary: Reconstruction of material budget and current systems". The present thesis is integrated in its subproject B2 "Palaeo-circulation of deep and bottom waters" directed by D. Fütterer. This subproject monitored and interpreted the

imprints of the deep circulation on the chemical and textural properties of the sediments. Methodical focuses were the isotopic signature of calcareous microfossils, sediment grain-size distributions and clay mineral assemblages.

1 The circulation of the Atlantic Ocean as a key part of the global conveyor

The global ocean circulation is mainly driven by differences in the density of seawater. Since the density of the seawater is controlled by temperature and salinity it is referred to as global thermohaline circulation. A simplified model of the global thermohaline circulation is the Conveyor Belt (Gordon, 1986; Broecker, 1987, Fig. 1).

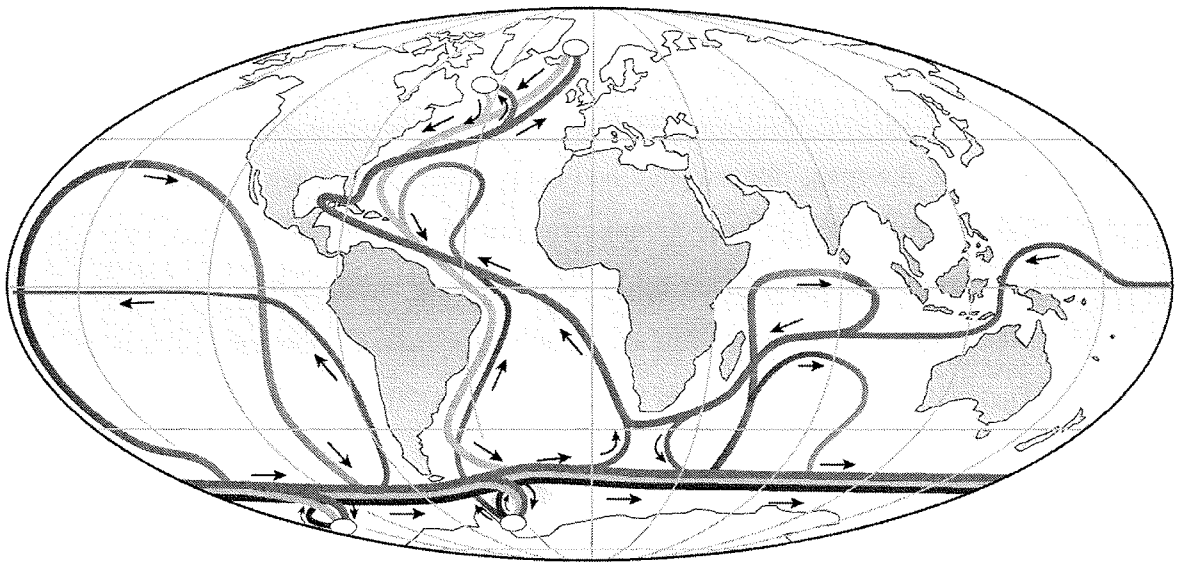

Fig. 1: *Simplified large-scale ocean circulation redrawn from Rahmsdorf (2002) as a modified version of the global conveyor belt of Broecker (1987). Medium grey lines: surface currents, light grey lines: deep currents, dark grey lines: bottom currents; white ovals: formation regions of deep and bottom waters.*

In contrast to the Pacific and Indian Oceans where heat is moved from low to high latitudes in both, in the northern and southern hemispheres, in the Atlantic Ocean warm and salty near-surface water shows an overall net northward transport. This anomalous heat transport causes 4°C higher sea-surface temperatures in the northern North Atlantic compared to similar latitudes in the Pacific (Levitus, 1982). The comfortable side-effect of this North Atlantic "heat piracy" (Berger and Wefer, 1996) are the mild northern Europe air temperatures which are about 10°C warmer compared to adequate Pacific regions (Roemmich and Wunsch, 1985; Manabe and Stouffer, 1988).

In the Norwegian and Labrador Seas the cooled surface waters convectively sink to the deep ocean (Dickson and Brown, 1994). This newly build relatively warm and saline North Atlantic Deep Water (NADW) is characterised by a high oxygen but low nutrient contents. As a Western Boundary Current it is exported to the south at water depths of roughly 2000 to 4000 m until it is incorporated in the Antarctic Circumpolar Current (ACC, Warren, 1981).

Over the entire depth range the ACC system flows eastward all around the Antarctic continent with intense mixing of adjoining waters and several equator-ward loops in the Atlantic, Indian and Pacific Oceans. Thereby it experiences a decrease in oxygen and salinity whereas the nutrient content increases. The ACC returns to the Atlantic sector through the Drake Passage as Circumpolar Deep Water (CDW) with a density range similar to NADW. Extreme cooling of CDW proportions below the ice sheets and mixing with cold waters from the ice shelfs of the Ross a and Weddell Seas results in sinking of these water masses. These are exported to the north and east as Lower CDW and Weddell Sea Deep Water. Both together often are referred to as Antarctic Bottom Water (AABW).

In the southeast Pacific and southwest Atlantic a cold, highly oxygenised and low saline surface water slides below the thermocline central waters. This Antarctic Intermediate Water in the Atlantic is derived from the surface circumpolar layer in the region of the Drake Passage and the Malvinas (Falkland) Current (Stramma and England, 1999). This water moves northward together with the Upper CDW which is separated from the LCDW by the intruding NADW.

1.1 Upper Ocean circulation of the South Atlantic

The South Atlantic surface circulation is dominated by Subtropical Gyre (e.g. Peterson and Stramma, 1991; Stramma and England, 1999). At its southern boundary the South Atlantic Current moves east parallel to the ACC across the Subantarctic Front. At the southern tip of Africa the South Atlantic Current encounters the Agulhas Current which imports warm surface water from the Pacific and Indian Oceans. The Benguela and the South Equatorial Current are responsible for the transatlantic transport towards the northeast, where it splits in two. (1) The Northern Brazil Current moves proportions of this warm waters to the north and across the equator and producing the mentioned Atlantic heat transfer anomaly. (2) The southern branch, the Brazil Current moves to the southwest where it encounters the cold Malvinas Current at the Brazil Malvinas Confluence roughly off the mouth of the Rio de La Plata. The sedimentological impact of this oceanographic feature is portrayed by Frenz et al. (in press, Manuscript #2). Driven by the trade winds in the tropics a complex

set of northern and southern Equatorial Currents and counter currents accompany the Equatorial Divergence and Inner Tropical Convergence Zones. In the northeast of the South Atlantic the cyclonic Angola Gyre transports warm surface waters along the coast southwards. At about 16°S this current encounters the Benguela Current at the Angola Benguela Front.

Major consequences of this flow pattern are the contrasts between strong nutrient depletion in the oligotrophic central areas of the Subtropical Gyre and the increased fertility at the meso- and eutrophic upwelling areas at the equatorial divergence and the costal Benguela upwelling system. Accordingly, the production pattern in the upper ocean and its traces in the sedimentary record differs significantly between these areas as recorded in Manuscripts #2 and #3 (Frenz et al., submitted; Frenz and Henrich, submitted).

1.2 Intermediate and deep-water circulation of the South Atlantic

The AAIW is characterised by an oxygen maximum and a salinity minimum just below (e.g. Reid, 1996, Tab. 1). It occupies water depths between 500 and 1200 m (Boebel et al., 1999). Commonly used meridional profiles of the Atlantic water mass structure (e.g. Fig. 2) suggest a continuous northward flow of the AAIW. Recent studies of the World Ocean Circulation Experiment confirmed that the circulation of the AAIW roughly follows subtropical gyre of the surface circulation, and consequently moves southward with the Brazil Current (Boebel et al., 1997; Boebel et al., 1999; Stramma and England, 1999).

Table 1: *Selected Source Water Type characteristics of Larqué et al. (1997), used to unmix the contributions of these water masses from measured values. These may serve as water mass characteristic values.*

	AAIW	UCDW	NADW	LCDW	WSDW
T, °C	4.0	2.5	3.0	1.5	-0.2
S, psu	34.2	34.6	34.92	34.76	34.68
O_2, ml/l	5.6	4.6	5.6	4.75	5.25
PO_4, µmol/kg	1.9	2.2	1.7	1.8	2.2
SiO_2, µmol/kg	20	70	30	102	121
NO_3, µmol/kg	26.5	29.0	23.5	29.0	31.0

When moving northward the CDW is divided into an Upper and Lower branch by the southward moving NADW. AAIW and UCDW reveal a low carbonate ion concentration (Fig. 2) and are weakly under-saturated with respect to aragonite. Therefore they are traced by their low aragonite preservation which can be revealed by means of ultra-structural investigations of pteropod shells (Gerhardt and Henrich, 2001).

The relatively warm and saline water mass of NADW (Tab. 1) can further be subdivided into an Upper and Lower layer. UNADW is build mainly in the Labrador Sea, and on its way south additionally it receives heavily saline but warm Mediterranean Outflow Water (Reid, 1996). The denser, since colder LNADW is build further north in the Norwegian-Greenland Sea. NADW moves south mainly as a Deep Western Boundary Current in terms of Stommel (1958) at mid-depth of roughly 2000 to 4000 m as far as 39°S (e.g. Peterson and Whitworth III, 1989; Maamaatuaiahutapu et al., 1992). Due to its carbonate-ion super-saturation (> 110 µmol/l, Broecker and Peng, 1982; Dittert et al., 1999, Fig. 2) NADW shows a high carbonate preservation potential. Therefore, it leaves a core of sediments with relatively high carbonate contents along the western boundary. However, in contrast to the modern oceanographic trace of NADW, in the sediments of the South American continental margin this core can be followed down to 48°S (Frenz et al., in press, Manuscript #1).

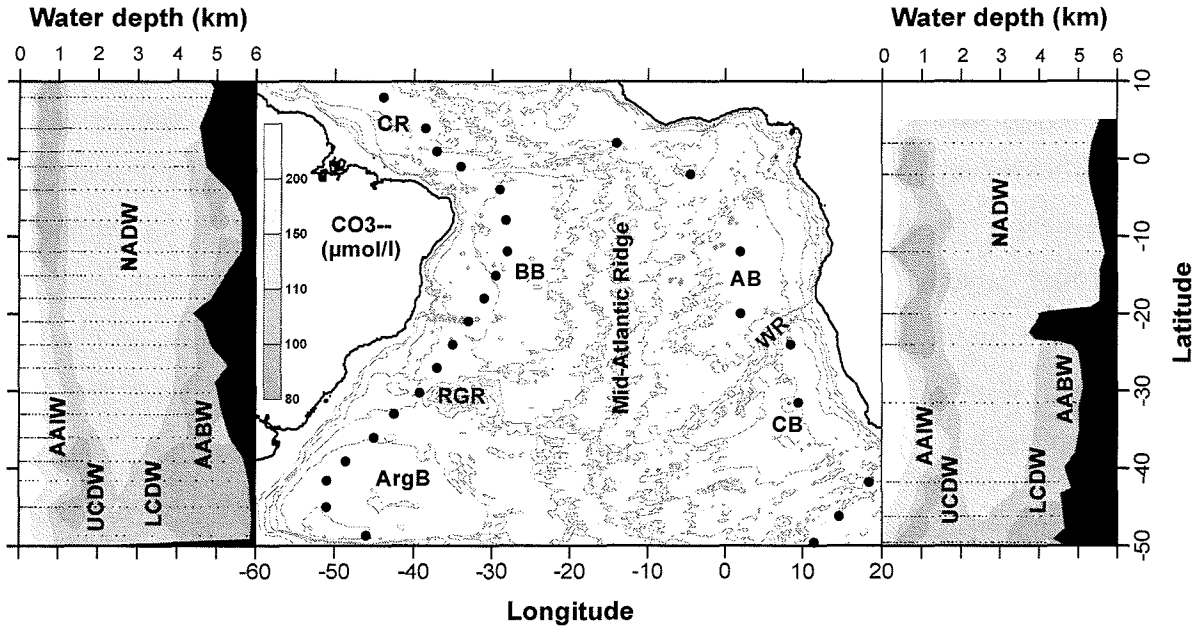

Fig. 2: Present water mass distribution of the eastern and western South Atlantic according to interpolated carbonate-ion concentrations taken from GEOSECS (1999). Note the asymmetry between the Brazil and Angola Basins. The dots in the centered map indicate the position of the GEOSECS stations along which the profiles run. Essential bathymetric features are indicated as follows: AB – Angola Basin, ArgB – Argentine BB – Brazil Basin, CB – Cape Basin, CR – Ceará Rise, RGR – Rio Grande Rise, WR – Walvis Ridge; adopted from Frenz and Henrich (submitted)

Antarctic Bottom Water (i.e. LCDW and WSDW) intrudes the western South Atlantic via the Georgia Basin (WSDW) and over the Falkland Plateau (LCDW, Arhan et al., 1999). It spreads west then north in the Argentine Basin as a Deep Western Boundary Current below a water depth of roughly 4000 m before it is blocked by the Santos Plateau/Rio Grande Rise. One proportion of AABW is recirculated in the Argentine Basin (Saunders and King, 1995; Coles et al., 1996). Another proportion escapes through the sills of the Vema and

Hunter Channels into the Brazil Basin (e.g. Speer et al., 1992; McDonagh et al., 2002). In the northern Brazil Basin another bifurcation occurs. As one part moves further through the Ceará Abyssal Plain to the northern hemisphere (McCartney and Curry, 1994). Another smaller proportion flows via the Romanche and Chain Fracture Zones into the Sierra Leone, Guinea and Angola Basins (Mercier et al., 1994). According to Tucholke and Embley (1984) the eastern route of AABW leads around the Atlantic-Indic and Agulhas Ridges into the Cape Basin.

AABW is strongly undersaturated with respect to carbonate and therefore reveals poor carbonate preservation. In the western basins of the South Atlantic the interface of AABW and carbonate conservative NADW coincides with the level of increased carbonate dissolution referred to as the sedimentary lysocline at water depths of about 4200 m (Thunell, 1982). Due to the AABW blockage by the submarine barriers of the Mid Atlantic and Walvis Ridges only minor amounts of AABW can pass the sills of the Walvis Passage (about 4200 m) and Romanche Fracture Zone (about 4350 m) and intrude into the Angola Basin. Therefore, the deep Angola Basin is mainly filled with NADW (Van Bennekom and Berger, 1984; Shannon and Chapman, 1991; Warren and Speer, 1991; Mercier et al., 1994). Consequently, in the deep parts of the Angola Basin the sedimentary lysocline is situated deeper compared to the Brazil Basin causing an asymmetry in the carbonate preservation pattern. In recent, carbonate preservation studies went further into this phenomenon in the South Atlantic by means of ultrastructural breakdown of planktic foraminifer tests (*G. bulloides*) (Volbers and Henrich, 2002; Volbers and Henrich, submitted) and by means of grain-size analyses of the carbonate sediment fraction .

1.3 Variability of the Atlantic circulation regime in the late Quaternary

From many studies there is evidence that during glacial periods climatic conditions and ocean circulation differed considerably from the present pattern. It is well documented in gas inclusions of ice cores that during glacials the atmospheric CO_2 content was lower tan today (e.g. Neftel et al., 1988; Barnola et al., 1991). During glacial periods large amounts of ice are locked in the ice sheets at high latitudes. So during the Last Glacial Maximum (LGM 19-23 ka BP, Mix et al., 2001) 50 10^6 km^3 sea water were stored as ice, which accordingly lowered the sea level of 120 m (e.g. Stocker, 1998). Three modes of circulation are suggested to have prevailed in the Atlantic (Sarnthein et al., 1994; Alley and Clark, 1999) of which the interstadial (warm) and stadial (cold) modes according to models correspond to the modern and LGM situations (e.g. Ganopolski et al., 1998). During interstadials NADW formed in the northern North Atlantic as described above. In the

stadials, in contrast, it may have formed in the subpolar North Atlantic and its production rate and southward flow are assumed to have been lower (Rutberg et al., 2000). Accordingly, it was less dense and sank less deep, wherefore it is referred to Glacial North Atlantic Intermediate Water (GNAIW, Boyle and Keigwin (1987), Oppo and Lehman (1995)). For compensation, the layer of southern origin below (Southern Component Water, SCW) may have expanded to shallower water depths in the southern and equatorial Atlantic (e.g. Duplessy et al., 1988; Bickert, 1992; Labeyrie et al., 1992; Sarnthein et al., 1994). Consequently, the interface of water masses with good and poor carbonate preservation potential (GNAIW/SCW) must have shoaled. This pattern was confirmed using the preservation states of *G. bulloides* (BDX', Volbers and Henrich, submitted), and as well as by means of grain-size distributions of the carbonate fraction of LGM sediments from the South Atlantic (Frenz and Henrich, submitted, Manuscript #3)

2 Grain-size characteristics as a palaeoceanographic tool

Particle size is a fundamental property of sediments. It tells much about the origin and history of a deposit, especially about the dynamics of transport and deposition. Additionally, if the biogenic fraction is considered, production and dissolution patterns can be revealed. From the multitude of applications of variations in grain-size composition in marine sediments the key approaches are introduced in this chapter. However, this list is by far not exhaustive.

2.1 Discrimination of sedimentary environments

The processes that lead to a certain grain-size composition of sediments are multifold. They are mainly steered by climatic controlled input and sorting parameters which vary spatially and with time. Generally, the sediment grain size decreases with distance from the source. Additionally, the highly variable and laterally rapidly changing sediment facies nearshore and on the inner shelf becomes successively more homogenous towards outer shelf, the continental rise and the abyssal plain. Major sediment transport processes found in the marine environment include local fluvial discharge, eolian dust input, ice rafting, wave and storm currents, littoral and geostrophic currents, submarine mass movements and pelagic and hemipelagic settling. According to the marine setting the importance of one or more prevalent processes varies, which is reflected by the decrease of sorting and the development of typical modes in the grain-size distributions. To ease the interpretation usually the terrigenous (lithogenous/siliciclastic) sediment fraction is considered separately. Eliminating the biogenic carbonate fraction and, where necessary the biogenic

opal, removes size effects which are caused by variations in the production rate of the different plankton groups and their preservation character.

From the grain-size distributions of a set of surface samples Rea and Hovan (1995) distinguished between eolian and mainly hemipelagic sediments in the abyssal North Pacific. The eolian signal (prominent peak at 2 μm, well sorted) appeared to be more prominent further downwind in the central Pacific in contrast to the more hemipelagic sediments (flat size distribution, poor sorting) close to the continental margins. In a similar study on sediments from the Bermuda Rise and the Blake Outer Ridge Joseph et al. (1998) delineated among turbidites, (hemi-) pelagic interlayers and drift sediments. In addition to characteristic grain-size distributions the magnetic fabric of the sediments revealed grain alignment due to random settling (hemi-/pelagic) and transport along the sea floor.

A useful tool to distinguish between eolian and fluvial sediment supply and current sorting is the so called Koopmann Index (Koopmann, 1981). It utilises the relationship between the modal grain size of the coarse terrigenous fraction (> 6 μm) and the proportion of this fraction relative to the bulk terrigenous sediment. The Koopmann Index identifies well-sorted eolian dust by an increase of the modal grain size with increasing proportion of coarse silt. In contrast, high amounts of clay and fine grain size are indicative for flivial discharge. In addition, relative high contents of coarse silt and moderate modal grain sizes characterise sediments which experienced removal of the fine share due to winnowing by currents. Applying Koopmanns concept Tiedemann et al. (1989) traced the climatic record of dust supply versus riverine input in sediments off northwest Africa back to the Late Miocene. Besides in the subtropical North Atlantic Sirocko and Sarnthein (1989) showed the applicability of the Koopmann Index in Holocene sediment records of the northwestern Indian Ocean. A much more simple derivative, namely the proportion of the size fraction > 6 μm already gives valuable information about the temporal and spatial distribution patterns of eolian dust and allowed to decipher variations in the strength of the atmospheric circulation in the subtropical North Atlantic (Tetzlaff and Peters, 1986) and the Southwest Pacific (Stein and Robert, 1985; Stein, 1986).

At the pacific side of the South American continent, Lamy et al. (1998a; 1998b) combined (silt) grain-size analyses with (clay) mineralogical results to infer the spatial and temporal variations in the mode of sediment input (eolian vs. fluvial) along the Chilean continental margin. The modern sediments (Lamy et al., 1998b) revealed a meridional segmentation according to the geologic, morphologic and climatic features of the hinterland. The grain-size composition is controlled by the primary grain size of the source rocks

(plutonic/volcanic rock type, chemical/physical weathering) and the mode of sediment input (eolian in the subtropical north, fluvial further south). The Late Quaternary time series of the northern part (Lamy et al., 1998a) shows cyclic variations between arid climates (finer grained) and more humid conditions (coarser grained) over the past 120 ka. However, often different input processes and transport phenomena may have affected the sediments. This makes the identification of the individual processes and their relative contribution very complicated. A solution for this problem is offered by the concept of end-member modelling (Weltje, 1997). This algorithm provides a mathematical tool to decompose (e.g.) particle-size distributions into a limited number of subpopulations. This unmixing technique has been successfully applied to a variety of sedimentary environments. For example it has been used to discriminate proximal and distal eolian input and fluvial discharge in the Arabian Sea (Prins and Weltje, 1999; Prins et al., 2000), iceberg discharge and current sorted sediments in the North Atlantic (Prins et al., 2001; Prins et al., 2002) and eolian dust and hemipelagic mud in the eastern South Atlantic (Stuut et al., 2002b).

All theses studies base on downcore grain-size variations of the bulk terrigenous sediment fractions measured with laser particle sizers. Frenz et al. (in press, Manuscript #1) for the first time, applied the end-member modelling algorithm to silt size distributions of surface samples from the South American continental margin in the western South Atlantic. Although the size range was limited to the silt spectrum a three-end-member model separated (1) the very coarse bedload tongue of the Rio de la Plata and the strongly winnowed sediments under the influence of the vigorous Malvinas Current, (2) the hemipelagic settled suspended river discharge of the La Plata along the Brazil Malvinas Confluence and (3) very fine-grained abyssal sediments at the deeper Santos Plateau and southern Brazil Basin.

2.2 Reconstruction of current strength

Most studies using sediment grain-size distributions intend to infer the variability of bottom currents. The basic assumption behind this is that faster currents leave coarser sediments behind due to the resuspension and removal (winnowing) or non-deposition of finer grains. In this concern the terrigenous silt fraction is emphasised. The development and progress of sediment grain size as a paleocurrent indicator is closely linked to the names of M. Ledbetter and N. McCave and their co-workers. First records of the grain size – current speed relation came from the Vema Channel in the southwest Atlantic in the second half of the 1970's (Ledbetter and Johnson, 1976; Ellwood and Ledbetter, 1977;

Ellwood and Ledbetter, 1979; Ledbetter, 1979). The grain size and grain alignment records revealed a fine mean grain size (16 μm) where slow flowing NADW moves to the South and a coarser mean grain size (> 20 μm) where AABW passes northward this narrower cross section in the gap of the Rio Grande Rise. Their time series indicated fluctuations in the water depth of the NADW/AABW interface as well as in AABW currents strength with no clear trends to warm or cold climates. Later this method was applied to the Argentine Basin to deduce current speed and pathways of AABW in this area (Ledbetter, 1986; Ledbetter and Klaus, 1987; Ledbetter, 1993).

McCave and co-workers investigated drift sediments in the northeast Atlantic. They found the terrigenous (and carbonate) silt grain size to be bimodal distributed showing a prominent minimum at about 10 μm (Robinson and McCave, 1994; McCave et al., 1995b). They interpreted the fine terrigenous silt (< 10 μm) to settle flocculated and being harder to be remobilised by currents due to its cohesive behaviour. Therefore it was concluded that its size distribution is not sensitive for current sorting. Finally these authors referred to the terrigenous fraction 63-10 μm to as "sortable silt" and its mean (and modal) grain size indicative for current strength. A large number of publications manifests the applicability of this paleoceanographic tool for the reconstruction of deep-ocean flow in the context of climate variability (e.g. McCave et al., 1995a; Revel et al., 1996; McCave, 1997; Bianchi and McCave, 1999; Bianchi et al., 2001; Yokokawa and Franz, 2002; Gröger et al., submitted).

These studies have in common to attribute relative size variations to relative variations in current strength, assuming no significant changes of the input variables. However, variability of the sources need to be considered. For example, at higher latitudes IRD input will significantly change the sediment grain-size independently of differences in current strength. This needs to be inspected using estimations for this input like content or composition of the coarse fraction, > 63 μm, > 125 μm (e.g. Henrich et al., 1989; Thiede et al., 1998; Austin and Evans, 2000). The grain-size distributions of sediments influenced by IRD can not directly be considered for current estimations. Before doing this the IRD influence needs to be suppressed (Hass, 2002) or unravelled with an end-member algorithm (Prins et al., 2002). Of course, similar impacts on grain-size distributions must be considered close to rivers and areas of significant eolian dust supply.

2.3 Grain size of the calcareous sediment fraction

The Atlantic Ocean is regarded as the largest present-day carbonate sink as it serves as a huge carbonate depocenter with an average deep lysocline (Milliman, 1993). Therefore carbonate-rich sediments cover a large part of the South Atlantic. Variations in the grain-size composition of the calcareous compounds may result from a variety of processes, among which ecology and production rates of carbonate particles and their preservation potential are most important.

One central aspect of the grain size of calcareous sediments is the possibility to trace carbonate dissolution. It has been shown by several studies that the sand content of deep-sea carbonates is sensitive to carbonate dissolution with a continuous decrease of sand contents with progressive dissolution (e.g. Berger et al., 1982; Yasuda et al., 1993; Tiedemann and Franz, 1997; Franz and Tiedemann, 2002). This observation bases on the fact that the sand-sized shells of carbonate producers – in the pelagic environment mainly planktic foraminifers – become more fragmented with increasing dissolution intensity and are therefore transferred to finer size fractions, decreasing the relative sand content. Additionally, the ratio in the number of bulk foraminifer tests relative to foraminifer fragments decreases, providing an estimation for carbonate dissolution (e.g. Rühlemann et al., 1996; Gröger et al., submitted). Stuut et al. (2002a) related the abundance of whole foraminifer tests to that of fragments by means of two distinct size fractions in calcareous sediments on the Walvis Ridge. The log ratio of the fraction > 90 μm (whole tests) to the size fraction to 25-90 μm (mainly fragments) is indicative for dissolution intensity. In a new approach this fragmentation and size transfer has been traced down to the silt fraction (Frenz and Henrich, submitted, Manuscript #3) This study has shown that increased carbonate dissolution results in a more intense fragmentation and therefore smaller grain sizes of the fragments in the coarse silt fraction. With this tool it was possible to trace the vertical position of the sedimentary lysocline for the Holocene and the LGM in the deep basins of the South Atlantic. However, using bulk dissolution proxies one needs to rule out or consider effects that may result from dilution with non-carbonate material, lateral transfer and climatic induced ecological changes of the community (Henrich et al., in press).

Another approach to use the grain-size distributions of the carbonate share of sediments is the decomposition into its compounds, and the possibility to quantify them respectively. Generally, in the pelagic open ocean carbonate production is almost exclusively planktic which furthermore can be subdivided into four groups: foraminifers, pteropods,

coccolithophores and calcareous dinoflagellates (Baumann et al., in press). Hitherto, estimations of the carbonate contribution of the diverse groups base on the carbonate content of empirical size classes like for example the fractions > 63 µm for foraminifers (e.g. Baumann et al., in press) or < 32 µm for coccoliths (e.g. Broerse et al., 2000). However, these include a certain unknown amount of contamination by other groups. When analysing drift sediments in the northeast Atlantic Robinson and McCave (1994) and McCave et al. (1995b) found a general minimum in the size distribution of the carbonate silt fraction at about 10 µm. They attributed the carbonate fraction coarser than this distinctive size to foraminifer fragments and the finer share to coccoliths. In a study Frenz et al. (submitted, Manuscript #2) modified and applied this method on surface sediments of the Mid-Atlantic Ridge of the South Atlantic. For this area, stretching from the equator to 40°S the contribution of foraminifer and coccolith carbonate was calculated, accepting slight contaminations by pteropods at shallow water depths. In this study, for the first time single peaks in the size distribution of the fine silt (< 10 µm) could be attributed to a distinct single coccolith species. These findings have been confirmed by SEM observations of silt separates. This might represent a new way to separate restricted coccolith assemblages as suggested by previous studies (Paull and Thierstein, 1987; Paull et al., 1988; Stoll and Ziveri, 2002) in order to infer isotope fractionation by species.

3 Methods

In the duration of this PhD study altogether 394 sediment samples from the South Atlantic were analysed with respect to their grain-size distribution. The samples originate from 25 cruises of the Research Vessel METEOR between 1988 and 2000. Out of the bulk sample set 180 samples represent sediment surface. 214 samples originate from 57 sediment cores covering the time interval of LGM according to the "LGM-Liste" (Niebler et al., submitted). By kind permission of R. Höppner the grain-size data of another 81 surface samples enabled to condense the sample coverage at the South American continental margin and the Mid-Atlantic Ridge (Fig. 3).

All samples were processed according to the analytical procedure given in the flow chart of Figure 4.

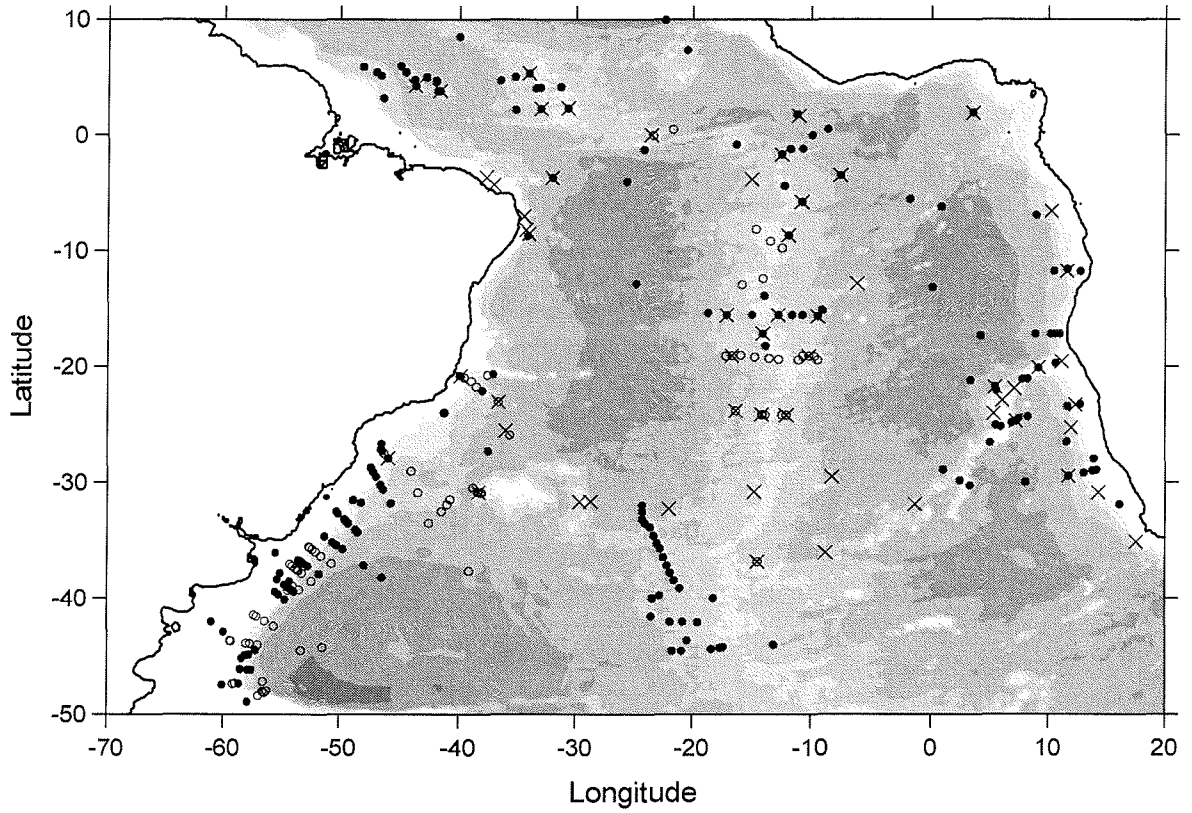

Fig. 3: Locations of the investigated samples in the South Atlantic. The symbols indicate surface samples (•), LGM bearing cores (X) and results of surface samples used by permission of R. Höppner (○). The shaded depth intervals are multiples of 1000 m with the black solid shoreline.

The samples were wet-split into sand (coarse fraction) and mud (fine fraction) using a 63 µm mesh. The dried and weighed sand fraction is available for further investigations like coarse fraction analyses, isotopic investigations or carbonate dissolution studies (Volbers and Henrich, submitted) etc.. The fine fraction suspension was left alone to settle for about one week before it was concentrated by sucking off excess water.

In a further step the fine fraction was split into silt (63-2 µm) and clay (< 2 µm) according to Stokes' Law in Atterberg settling cylinders (cf. Gessner, 1931). Sodium carbonate (Na_2CO_3, 0.25 g/l) was used as a dispersing agent and to prevent carbonate corrosion. The settling time varied between 19 and 24 h depending on the current temperature and the fixed settling height (29 cm). 15 to 40 load/extraction cycles were necessary to remove the clay fraction thoroughly. After every cycle the clay suspension was spiked with magnesium chloride ($MgCl_2$) solution in order to accelerate aggregation of particles and their settling. The $MgCl_2$ was removed by rinsing and centrifuging the clay sample before drying and weighing. The clay fraction can further be used for clay mineral analyses (Diekmann et al., 2003). For this purpose it is decarbonised using acetic acid. Quantitatively done, the weight loss represents the preliminary value for the carbonate content of the clay fraction.

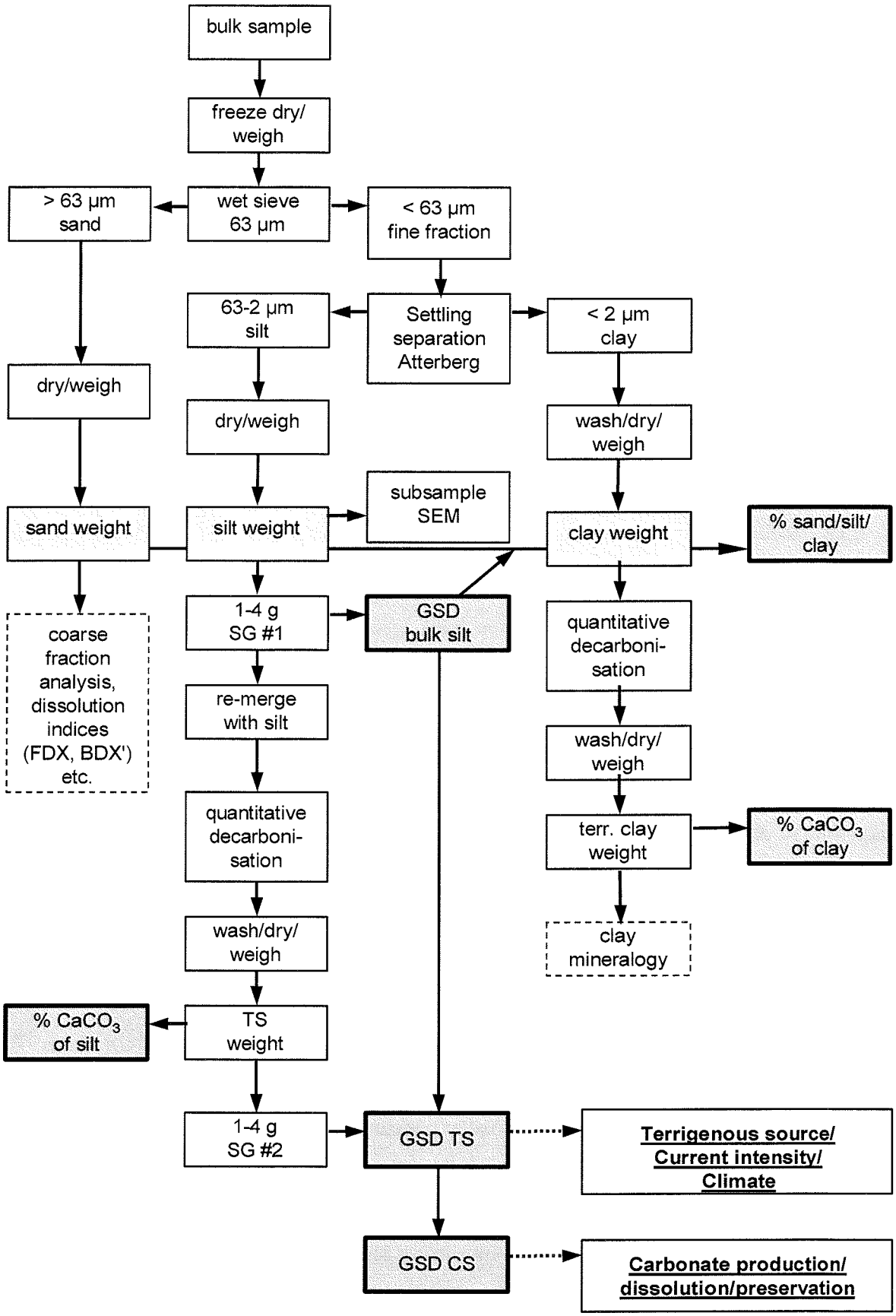

Fig. 4: *Flow chart of the analytical methods as used in this study. Abbreviations as follows, SEM: scanning electron microscopy, SG #1/2: SediGraph analysis run number, GSD: grain-size distribution, TS terrigenous silt, CS: carbonate silt. FDX and BDX' are foraminiferal dissolution indices. See text for further detailed information.*

The grain-size distribution of the silt fraction was measured with a Micromeritics SediGraph 5100. This device measures the particle concentration in a suspension by the attenuation of a collimated x-ray beam. The particles are assumed to settle in the sedimentation cell in accordance to Stokes' Law. Therefore with elapsing time the detected x-ray intensity increases by decreasing particle concentration due to sedimentation. For further information on the detailed principles of the SediGraph technique confer expert publications (e.g. Stein, 1985; Coakley and Syvitski, 1991; McCave and Syvitski, 1991). The SediGraph is regarded as a precise device within the different size analytical techniques (Stein, 1985; Jones et al., 1988; Singer et al., 1988; Bianchi et al., 1999). Among the pros and cons for the use of the SediGraph one of each may be emphasized. Generally, in settling techniques grain shape and density become integral components of size given as the Equivalent Spherical Diameter (ESD, Stokes diameter). This avoids discussions about "size" (e.g. Winkelmolen, 1982) and particle shape effects of other techniques (e.g. Konert and Vandenberghe, 1997).

The SediGraph measurement is restricted to the scope of Stokes' Law. Gibbs et al. (1971) give a complex settling equation which includes effect of increasing Reynolds numbers at greater diameters, indicating good agreement with Stokes' law below 100 µm. According to these findings the working range of the SediGraph is restricted to < 100 µm, compared to the official range of 300-0.1 µm (Micromeritics, 1996). A lower border is given by the cohesive behaviour of very small particles. Therefore, usually the clay fraction (< 2 µm) is removed. Additionally, samples rich in biogenic opal or smectite must be avoided due to the tendency of aggregate building (Stein, 1985). Therefore, the SediGraph is constrained to a distinct size window, whereas e.g. laser techniques, measuring in turbulent flow, have no general restrictions in size spectrum.

Each sample was measured twice, if the minimal sample amount of 1 g was given. For the first SediGraph measurement, a representative subsample (1-4 g) of the dried and weighed silt was disaggregated in 50 ml of 0.05 % calgon solution (sodium polyphosphate) as suggested by the manufacturer (Micromeritics, 1996). Assuming a sample density of 2.65 g/cm^3 and a liquid volume of 70-80 ml (includes 20-30 ml for sample transfer) the resulting concentrations in the analysed suspension are between 0.5 and 2.1 vol.-% as advised by Stein (1985) to minimise hindered settling.

Prior to the second SediGraph run the silt fraction was decarbonised using concentrated hydrochloric acid. The weight difference of the sample before and after the decarbonisation gave the preliminary carbonate content of the silt fraction. Alternatively,

the carbonate contents of silt (and clay) can be determined using a subsample (Robinson and McCave, 1994). Preparation and execution of the second SediGraph run are identical to the first one.

However thorough the extraction of the clay fraction in the Atterberg settling tubes appears to be, the Sedigraph detects a certain amount of residual clay in the silt fraction (< 10 %). This detected clay content in both SediGraph runs must be considered for the silt and clay contents as well as for the contents of carbonate in these two subfractions by subtracting this amount from the silt and adding it to the clay.

The unreduced report files generated with the Micromeritics software are converted into 50 equal-spaced (0.1 Φ) size classes from 4 to 9 Φ (62.5-2 μm) using the SediMac programme written by G. Kuhn (AWI, Bremerhaven). The grain-size distribution of the carbonate silt was calculated by subtracting the relative terrigenous silt size distribution from that of the bulk silt distribution in each size class. This method was suggested by Paull et al. (1988) and adopted later by Robinson and McCave (1994) and McCave et al. (1995b). For data presentation the statistical parameters mean and modal grain size, sorting (standard deviation) and skewness were calculated according to the momentum method of Krumbein (1936).

4 References

Alley, R.B. and Clark, P.U., 1999. The deglaciation of the northern hemisphere: A global perspective. Annu. Rev. Earth Planet. Sci., 27: 149-182.

Arhan, M., Heywood, K.J. and King, B.A., 1999. The deep waters from the Southern Ocean at the entry to the Argentine Basin. Deep Sea Research Part II: Topical Studies in Oceanography, 46(1-2): 475-499.

Austin, W.E.N. and Evans, J.R., 2000. Benthic foraminifera and sediment grain size variability at intermediate water depths in the Northeast Atlantic during the late Pliocene-early Pleistocene. Marine Geology, 170(3-4): 423-441.

Barnola, J.-M., Pimieta, P., Ranaud, D. and Korotkevich, Y.S., 1991. CO_2-climate relationship as deduced from the Vostok ice core: a re-examination based on new measurements and on a re-evaluation of the air dating. Tellus B, 43B: 83-90.

Baumann, K.-H., Böckel, B., Donner, B., Gerhardt, S., Henrich, R., Vink, A., Volbers, A.N.A., Willems, H. and Zonneveld, K.A.F., in press. Contribution of calcareous plankton groups to the carbonate budget of South Atlantic surface sediments. In: S. Mulitza, V. Ratmeyer and G. Wefer (Editors), The South Atlantic in the late Quaternary: Reconstruction of material budget and current systems. Springer, Berlin Heidelberg New York.

Berger, W.H., Bonneau, M.C. and Parker, F.L., 1982. Foraminifera on the deep-sea floor: lysocline and dissolution rate. Oceanologica Acta, 5: 249-258.

Berger, W.H. and Wefer, G., 1996. Central themes of South Atlantic circulation. In: G. Wefer, W.H. Berger, G. Siedler and D.J. Webb (Editors), The South Atlantic: Present and past circulation. Springer, Berlin Heidelberg New York.

Bianchi, G.G., Hall, I.R., McCave, I.N. and Joseph, L., 1999. Measurement of sortable silt current speed proxy using the Sedigraph 5100 and Coulter Multisizer IIe: precision and accuracy. Sedimentology, 46: 1001-1014.

Bianchi, G.G. and McCave, I.N., 1999. Holocene periodicity in North Atlantic climate and deep-ocean flow south of Iceland. Nature, 397: 515-517.

Bianchi, G.G., Vautravers, M. and Shackleton, N.J., 2001. Deep flow variability under apparently stable North Atlantic Deep Water production during the last interglacial of the subtropical NW Atlantic. Palaeogeography, 6(3): 306-316.

Bickert, T., 1992. Rekonstruktion der spätquartären Bodenwasserzirkulation im östlichen Südatlantik über stabile Isotope benthischer Foraminiferen. Berichte, Fachbereich Geowissenschaften, 27. Universität Bremen, Bremen, 205 pp.

Boebel, O., Davis, R.E., Ollitrault, M., Peterson, R.G., Richardson, P.L., Schmid, C. and Zenk, W., 1999. The intermediate depth circulation of the western South Atlantic. Geophysical Research Letters, 26(21): 3329-3332.

Boebel, O., Schmid, C. and Zenk, W., 1997. Flow and recirculation of Antarctic Intermediate Water across the Rio Grande Rise. Journal of Geophysical Research, 102(C9): 20967-20986.

Boyle, E. and Keigwin, L.D., 1987. North Atlantic thermohaline circulationduring the past 20,000 years linked to high-latitude surface temperature. Nature, 30: 35-40.

Broecker, W.S., 1987. The biggest chill. Natural History Magazine: 74-82.

Broecker, W.S. and Peng, T.H., 1982. Tracers in the sea. Eldigio Press, New York, 689 pp.

Broerse, A.T.C., Ziveri, P., van Hinte, J.E. and Honjo, S., 2000. Coccolithophore export production, species composition, and coccolith-CaCO3 fluxes in the NE Atlantic (34°N 21°W and 48°N 21°W). Deep Sea Research Part II: Topical Studies in Oceanography, 47(9-11): 1877-1905.

Coakley, J.P. and Syvitski, J.P.M., 1991. SediGraph technique. In: J.P.M. Syvitski (Editor), Principles and methods of geological particle size analysis. University Press, Cambridge, pp. 129-142.

Coles, V.J., McCartney, M.S., Olson, D.B. and Smethie Jr., W.M., 1996. Changes in Antarctic Bottom Water properties in the western South Atlantic in the late 1980s. Paleoceanography, 101(C4): 8957-8970.

Dickson, R.R. and Brown, J., 1994. The production of North Atlantic Deep Water: Sources, rates, and pathways. Jour. Geophysical Res., 99(C6): 12319-12341.

Diekmann, B., Fütterer, D.K., Grobe, H., Hillenbrand, C.D., Kuhn, G., Michels, K., Petschick, R. and Pirrung, M., 2003. Terrigenous sediment supply in the polar to temperate South Atlantic: Land-ocean links of environmental changes during the late Quaternary. In: S. Mulitza, V. Ratmeyer and G. Wefer (Editors), The South Atlantic in the late Quaternary: Reconstruction of material budget and current systems. Springer, Berlin Heidelberg New York.

Dittert, N., Baumann, K.-H., Bickert, T., Henrich, R., Huber, R., Kinkel, H. and Meggers, H., 1999. Carbonate dissolution in the deep-sea: methods, quantification and paleoceanographic application. In: G. Fischer and G. Wefer (Editors), Use of proxies in paleoceanography: examples from the South Atlantic. Springer, Berlin Heidelberg.

Duplessy, J.C., Shackleton, N.J., Fairbanks, R.G., Labeyrie, L., Oppo, D. and Kallel, N., 1988. Deepwater source variations during the last climatic cycle and their impact on the global deepwater circulation. Paleoceanography, 3(3): 343-360.

Ellwood, B.B. and Ledbetter, M.T., 1977. Antarctic Bottom Water fluctuations in the Vema Channel: effects of velocity changes on particle alignment and size. Earth and Planetary Science Letters, 35: 189-198.

Ellwood, B.B. and Ledbetter, M.T., 1979. Paleacurrent indicators in deep-sea sediment. Science, 203: 1335-1337.

Franz, S.O. and Tiedemann, R., 2002. Depositional changes along the Blake-Bahama Outer Ridge deep water transect during marine isotope stages 8 to 10 - links to the Deep Western Boundary Current. Marine Geology, 189(1-2): 107-122.

Frenz, M., Baumann, K.-H., Boeckel, B., Höppner, R. and Henrich, R., submitted. Quantification of foraminifer and coccolith carbonate in South Atlantic surface sediments by means of carbonate grain-size distributions.

Frenz, M. and Henrich, R., submitted. Carbonate dissolution revealed by silt grain-size distribution: comparison of Holocene and Last Glacial Maximum sediments from the pelagic South Atlantic.

Frenz, M., Höppner, R., Stuut, J.-B., Wagner, T. and Henrich, R., in press. Surface sediment bulk geochemistry and grain-size composition related to the oceanic circulation along the South American continental margin in the Southwest Atlantic. In: S. Mulitza, V. Ratmeyer and G. Wefer (Editors), The South Atlantic in the late Quaternary: Reconstruction of material budget and current systems. Springer, Berlin Heidelberg New York.

Ganopolski, A., Rahmsdorf, S., Petoukhov, V. and Claussen, M., 1998. Simulation of modern and glacial climateswith a coupled global model of intermediate complexity. Nature, 391: 351-356.

GEOSECS, 1999. Pangaea data set ID: 55389.

Gerhardt, S. and Henrich, R., 2001. Shell preservation of Limacina inflata (Pteropoda) in surface sediments from the Central and South Atlantic Ocean: a new proxy to determine the aragonite saturation state of water masses. Deep Sea Research Part I: Oceanographic Research Papers, 48(9): 2051-2071.

Gessner, H., 1931. Die Schlämmanalyse. Akademische Verlagsgesellschaft mbH, Leipzig, 244 pp.

Gibbs, R.J., Matthews, M.D. and Link, D.A., 1971. The relationship between sphere size and settling velocity. Journal of Sedimentary Petrology, 41(1): 7-18.

Gordon, A.L., 1986. Interocean exchange of thermocline water. Journal of Geophysical Research, 91(C4): 5037-5046.

Gröger, M., Henrich, R. and Bickert, T., submitted. Glacial-interglacial variability and long-term changes in the lower circulation loop of North Atlantic Deep Water: Inference from silt grain-size analysis and carbonate preservation studies at Ceará Rise, western equatorial Atlantic.

Hass, H.C., 2002. A method to reduce the influence of ice-rafted debris on a grain size record from northern Fram Strait, Arctic Ocean. Polar Research, 21(2): 299-306.

Henrich, R., Baumann, K.-H., Gerhardt, S., Gröger, M. and Volbers, A.N.A., in press. Carbonate preservation in deep and intermediate water masses in the South Atlantic: evaluation and geological record (a review). In: S. Mulitza, V. Ratmeyer

and G. Wefer (Editors), The South Atlantic in the late Quaternary: Reconstruction of material budget and current systems. Springer, Berlin Heidelberg New York.

Henrich, R., Wolf, T., Bohrmann, G. and Thiede, J., 1989. Cenozoic paleoclimatic and changes in the northern hemisphere revealed by variability of coarse fraction composition in sediments from the Voring Plateau - ODP Leg 104 drill sites. In: E. Taylor (Editor), Proceedings of the Ocean Drilling Program, Scientific Results, 104. Ocean Drilling Program, College Station, TX.

Jones, K.P.N., McCave, I.N. and Patel, P.D., 1988. A computer-interfaced sedigraph for modal size analysis of fine-grained sediment. Sedimentology, 35: 163-172.

Joseph, L.H., Rea, D.K. and Pluijm, B.A., 1998. Use of grain size and magnetic fabric analyses to distinguish among depositional environments. Palaeogeography, 13(5): 491-501.

Konert, M. and Vandenberghe, J., 1997. Comparison of laser grain size analysis with pipette and sieve analysis: a solution for the underestimation of the clay fraction. Sedimentology, 44(3): 523-535.

Koopmann, B., 1981. Sedimentation von Saharastaub im subtropischen Nordatlantik während der letzten 25.000Jahre. "Meteor" Forschungsergebnisse, C(35): 23-59.

Krumbein, W.C., 1936. Application of logarithmic moments to size frequency distributions of sediments. Journal of Sedimentary Petrology, 6: 35-47.

Labeyrie, L.D., Duplessy, J.C., Duprat, J., Juillet-Leclerc, A., Moyes, J., Michel, E., Kallel, N. and Shackleton, N.J., 1992. Changes in the vertical structure of the North Atlantic Ocean between glacial and modern times. Quaternary Science Reviews, 11: 401-413.

Lamy, F., Hebbeln, D. and Wefer, G., 1998a. Late Quaternary precessional cycles of terrigenous sediment input off the Norte Chico, Chile (27.5[deg]S) and palaeoclimatic implications. Palaeogeography, Palaeoclimatology, Palaeoecology, 141(3-4): 233-251.

Lamy, F., Hebbeln, D. and Wefer, G., 1998b. Terrigenous sediment supply along the Chilean continental margin: modern regional patterns of texture and composition. Geologische Rundschau, 87: 477-494.

Larqué, L., Maamaatuaiahutapu, K. and Garçon, V., 1997. On the intermediate and deep water flows in the South Atlantic Ocean. Journal of Geophysical Research, 102(C6): 12425-12440.

Ledbetter, M.T., 1979. Fluctuations of Antarctic Bottom Water velocity in the Veam Channel during the last 160,000 years. Marine Geology, 33(1/2): 71-89.

Ledbetter, M.T., 1986. Bottom-current pathways in the Argentine Basin revealed by mean silt particle size. Nature, 321: 423-425.

Ledbetter, M.T., 1993. Late Pleistocene to Holocene fluctuations in bottom-current speed in the Argentine Basin mudwave field. Deep-Sea Research II, 40(4/5): 911-920.

Ledbetter, M.T. and Johnson, D.A., 1976. Increased transport of Antarctic Bottom Water in the Vema Channel during the last ice age. Science, 194: 837-839.

Ledbetter, M.T. and Klaus, A., 1987. Influence of bottom currents on sediment texture and sea-floor morphology in the Argentine Basin. In: P.P.E. Weaver and J. Thomson (Editors), Geology and geochemistry of abyssal plains. SEPM (Society for Sedimentary Geology) Special Publication 31, pp. 23-31.

Levitus, S., 1982. Climatological atlas of the world ocean. NOAA Professional Paper, 13. US Government Printing Office, Washington, D.C., 173 pp.

Maamaatuaiahutapu, K., Garçon, V.C., Provost, C., Boulahdid, M. and Osiroff, A.P., 1992. Brazil-Malvinas Confluence: Water mass composition. Journal of Geophysical Research, 97(C6): 9493-9505.

Manabe, S. and Stouffer, R.J., 1988. Two stable equilibria of a coupled ocean-atmosphere mode. Journal of Climate, 1(841-866).

McCartney, M.S. and Curry, W.B., 1994. Transequatorial flow of Antarctic Bottom Water in the western Atlantic Ocean: Abyssal geostrphy at the equator. Journal of Physical Oceanigraphy, 23(6): 1264-1276.

McCave, I.N., 1997. Recent sedimentation beneath the Deep Western Boundary Current off northern New Zealand. Deep-Sea Research I, 44(7): 1203-1237.

McCave, I.N., Manighetti, B. and Beveridge, N.A.S., 1995a. Circulation in the glacial North Atlantic inferred from grain-size measurements. Nature, 374: 149-152.

McCave, I.N., Manighetti, B. and Robinson, S.G., 1995b. Sortable silt and fine sediment size/composition slicing: Parameters for palaeocurrent speed and palaeoceanography. Paleoceanography, 10(3): 593-610.

McCave, I.N. and Syvitski, J.P.M., 1991. Principles and methods of geological particle size analysis. In: J.P.M. Syvitski (Editor), Principles, methods and application of particle size analysis. University Press, Cambridge, New York, Port Chester, Melbourne, Sydney, pp. 3-21.

McDonagh, E.L., Arhan, M. and Heywood, K.J., 2002. On the circulation of bottom water in the region of the Vema Channel. Deep Sea Research Part I: Oceanographic Research Papers, 49(7): 1119-1139.

Mercier, H., Speer, K.G. and Honnorez, J., 1994. Tracing the Antarctic Bottom Water throug the Romanche and Chain Fracture Zones. Deep Sea Research, 41: 1457-1477.

Micromeritics, 1996. SediGraph 5100 Particle size analysis system, Operator's manual, pp. 238.

Milliman, J.D., 1993. Production and accumulation of calcium carbonate in the ocean: budget of nonsteady state. Global Biogeochemical Cycles, 7(4): 927-957.

Mix, A.C., Bard, E. and Schneider, R., 2001. Environmental processes of the ice age: land, oceans, glaciers (EPILOG). Quaternary Science Reviews, 20(4): 627-657.

Neftel, A., Oeschger, H., Staffelbach, T. and Stauffer, B., 1988. CO_2 record in the Byrd ice core 50,000 - 5,000 years BP. Nature, 331: 609-611.

Niebler, H.-S., Mulitza, S., Donner, B., Arz, H., Pätzold, J. and Wefer, G., submitted. Sea-Surface Temperatures in the Equatorial and South Atlantic Ocean during the Last Glacial Maximum (23-19 ka). Paleoceanography.

Oppo, D.W. and Lehman, S.J., 1995. Suborbital timescale variability of North Atlantic Deep Water during the past 200,000 years. Paleoceanography, 10(5): 901-910.

Paull, C.K., Hills, S.J. and Thierstein, H.R., 1988. Progressive dissolution of fine carbonate particles in pelagic sediments. Marine Geology, 81: 27-40.

Paull, C.K. and Thierstein, H.R., 1987. Stable isotopic fractionation among particles in Quaternary coccolith-sized deep-sea sediments. Paleoceanography, 2(4): 423-429.

Peterson, R.G. and Stramma, L., 1991. Upper-level circulation in the South Atlantic Ocean. Progress in Oceanography, 26: 1-73.

Peterson, R.G. and Whitworth III, T., 1989. The Subantarctic and Polar Fronts in relation to deep water masses through the Southwestern Atlantic. Journal of Geophysical Research, 94(C8): 10817-10838.

Prins, M.A., Bouwer, L.M., Beets, C.J., Troelstra, S.R., Weltje, G.J., Kruk, R.W., Kuijpers, A. and Vroon, P.Z., 2002. Ocean circulation and iceberg discharge in the glacial North Atlantic: inferences from unmixing of sediment size distribution. Geology, 30(6): 555-558.

Prins, M.A., Postma, G. and Weltje, G.J., 2000. Controls on terrigenous sediment supply to the Arabian Sea during the late Quaternary: the Makran continental slope. Marine Geology, 169: 351-371.

Prins, M.A., Troelstra, S.R., Kruk, R.W., Borg van der, K., Jong de, A.J. and Weltje, G.J., 2001. The Late Quaternary sediment record from Reykjanes Ridge, North Atlantic. Radiocarbon, 43(2B): 939-947.

Prins, M.A. and Weltje, G.J., 1999. End-member modelling of siliciclastic grain-size distributions:the late Quaternary record of eolian and fluvial sediment supply to the Arabian Sea and its paleoclimatic significance. In: J. Harbaugh, L. Watney, G. Rankey et al. (Editors), Numerical experiments in stratigraphy: recent advances in stratigraphic and sedimentologic computer simulations. SEPM (Society for Sedimentary Geology) Special Publication 62, pp. 91-111.

Rahmsdorf, S., 2002. Ocean circulation and climate during the past 120,000 years. Nature, 419: 207-214.

Rea, D.K. and Hovan, S.A., 1995. Grain size distribution and depositional processes of the mineral component of abyssal sediments: lessons from the North Pacific. Palaeogeography, 10(2): 251-258.

Reid, J.R., 1996. On the circulation of the South Atlantic Ocean. In: G. Wefer, W.H. Berger, G. Siedler and D.J. Webb (Editors), The South Atlantic: Present and past circulation. Springer, Berlin Heidelberg New York.

Revel, M., Cremer, M., Grousset, F.E. and Labeyrie, L., 1996. Grain-size and Sr-Nd isotopes as tracer of paleo-bottom current strength, Northeast Atlantic Ocean. Marine Geology, 131(3-4): 233-249.

Robinson, S.G. and McCave, I.N., 1994. Orbital forcing of bottom-current enhanced sedimentation on Feni Drift, NE Atlantic, during the mid-Pleistocene. Palaeogeography, 9(6): 943-972.

Roemmich, D. and Wunsch, C., 1985. Two transatlantic sections: meridional circulation and heat flux in the subtropical North Atlantic Ocean. Deep Sea Research, 32(6A): 619-664.

Rühlemann, C., Frank, M., Hale, W., Mangini, A., Mulitza, S., Muller, P.J. and Wefer, G., 1996. Late Quaternary productivity changes in the western equatorial Atlantic: Evidence from 230Th-normalized carbonate and organic carbon accumulation rates. Marine Geology, 135(1-4): 127-152.

Rutberg, R.L., Hemming, S.R. and Goldstein, S.L., 2000. Reduced North Atlantic Deep Water flux to the glacial Southern Ocean inferred from neodymium isotope ratios. Nature, 405: 935-938.

Sarnthein, M., Winn, K., Jung, S.J.A., Duplessy, J.-C., Labeyrie, L., Erlenkeuser, H. and Ganssen, G., 1994. Changes in east Atlantic deepwater circulation over the last 30,000 years: Eight time slice reconstructions. Paleoceanography, 9(2): 209-267.

Saunders, P. and King, B.A., 1995. Oceanic fluxes on the WOCE A11 section. Journal of Physical Oceanigraphy, 25(9): 1942-1958.

Shannon, L.V. and Chapman, P., 1991. Evidence of Antarctic Bottom Water in the Angola Basin at 32°S. Deep-Sea Research, 38(10): 1299-1304.

Singer, J.K., Anderson, J.B., Ledbetter, M.T., McCave, I.N., Jones, K.P.N. and Wright, R., 1988. An assessmet of analytical techniques for the size analysis of fine-grained sediments. Journal of sedimentary petrology, 58(3): 534-543.

Sirocko, F. and Sarnthein, M., 1989. Wind-borne deposits in the northwestern Indian Ocean: record of Holocene sediments versus modern satellite data. In: M. Sarnthein (Editor), Paleoclimatology and paleometeorology: modern and past patterns of global atmospheric transport. Kluwer Academic Publishers, Dortrecht, pp. 401-433.

Speer, K., Zenk, W., Siedler, G., Patzold, J. and Heidland, C., 1992. First resolution of flow through the Hunter Channel in the South Atlantic. Earth and Planetary Science Letters, 113(1-2): 287-292.

Stein, R., 1985. Rapid grain-size analyses of clay and silt fraction by Sedigraph 5000D: comparison with Coulter Counter and Atterberg methods. Journal of Sedimentary Petrology, 55(4): 590-615.

Stein, R., 1986. Late Neogene evolution of paleoclimate and paleoceanic circulation in the Northern and Southern Hemispheres - a comparison. Geologische Rundschau, 75(1): 125-139.

Stein, R. and Robert, C., 1985. Siliciclastic sediments at sites 588, 590, and 591: Neogene and Paleogene evolution in the southwest Pacific and Australian climate. In: C.C. von der Borch (Editor), Initial Reports of the Deep Sea Drilling Program. US Government Printing Office, Washington, DC, pp. 1437-1455.

Stocker, T.F., 1998. A glimpse of the glacial. Nature, 391: 338-339.

Stoll, H.M. and Ziveri, P., 2002. Separation of monospecific and restricted coccolith assemblages from sediments using differential settling velocity. Marine Micropaleontology, 46(1-2): 209-221.

Stommel, H., 1958. The abyssal circulation. Deep Sea Research, 5: 80-82.

Stramma, L. and England, M., 1999. On the water masses and mean circulation of the South Atlantic Ocean. Journal of Geophysical Research, 104(C9): 20863-20883.

Stuut, J.-B.W., Prins, M.A. and Jansen, J.H.F., 2002a. Fast reconnaissance of carbonate dissolution based on the size distribution of calcareous ooze on Walvis Ridge, SE Atlantic Ocean. Marine Geology, 190(3-4): 581-589.

Stuut, J.-B.W., Prins, M.A., Schneider, R.R., Weltje, G.J., Jansen, J.H.F. and Postma, G., 2002b. A 300-kyr record of aridity and wind strength in southwestern Africa: inferences from grain-size distributions of sediments on Walvis Ridge, SE Atlantic. Marine Geology, 180(1-4): 221-233.

Tetzlaff, G. and Peters, M., 1986. Deep-sea sediments in the eastern equatorial Atlantic off the African coast and meteorological flow patterns over the Sahel. Geologische Rundschau, 75(1): 71-79.

Thiede, J., Winkler, A., Wolf-Welling, T., Eldholm, O., Myhre, A.M., Baumann, K.-H., Henrich, R. and Stein, R., 1998. Late Cenozoic history of the Polar North Atlantic: results from ocean drilling. Quaternary Science Reviews, 17(1-3): 185-208.

Thunell, R.C., 1982. Carbonate dissolution and abyssal hydrography in the Atlantic Ocean. Marine Geology, 47: 165-180.

Tiedemann, R. and Franz, S.O., 1997. Deep-water circulation, chemistry, and terrigenous sediment supply in the equatorial Atlantic during the Pliocene, 3.3-2.6 Ma and 5-4.5 Ma. In: N.J. Shackleton, W.B. Curry, C. Richter and T.J. Bralower (Editors), Proceedings of the Ocean Drilling Program, Scientific Results, 154, pp. 299-318.

Tiedemann, R., Sarnthein, M. and Stein, R., 1989. Climatic changes in the western Sahara: Aeolo-marine sediment record of the last 8 million years (sites 657-661). In: W. Ruddiman and M. Sarntheim (Editors), Proceedings of the ODP, Scientific Results, pp. 241-261.

Tucholke, B.E. and Embley, R.W., 1984. Cenozoic regional erosion of the abyssal sea floor off South Africa. In: J.S. Schlee (Editor), Interregional unconformities and hydrocarbon accumulation. AAPG Memoir 36, American Association of Petroleum Geologists, pp. 145- 164.

Van Bennekom, A.J. and Berger, G.W., 1984. Hydrography and silica budget of the Angola Basin. Netherlands Journal of Sea Research, 17: 149-200.

Volbers, A.N.A. and Henrich, R., 2002. Present water mass calcium carbonate corrosiveness in the eastern South Atlantic inferred from ultrastructural breakdown of Globigerina bulloides in surface sediments. Marine Geology, 186(3-4): 471-486.

Volbers, A.N.A. and Henrich, R., submitted. Calcium carbonate corrosiveness in the South Atlantic during the Last Glacial Maximum as inferred from changes in the preservation of *Globigerina bulloides*: A proxy to determine deep water circulation pattern?

Warren, B. and Speer, K.G., 1991. Deep circulation in the eastern South Atlantic ocean. Deep-Sea Research, 38(1): 281-322.

Warren, B.A., 1981. Deep circulation of the World Ocean. In: C. Wunsch (Editor), Evolution of Physical Oceanography. MIT Press, Camebridge, MA, pp. 6-41.

Weltje, G., 1997. End-member modelling of compositional data: Numerical-statistical algorithms for solving the explicit mixing problem. Journal of Mathematical Geology, 29(4): 503-549.

Winkelmolen, A.M., 1982. Critical remarks on grain parameters, with special emphasis on shape. Sedimentology, 29(2): 255-265.

Yasuda, M., Berger, W.H., Wu, G., Burke, S. and Schmidt, H., 1993. Foraminiferal preservation record for the last million years: Site 805, Ontong Java Plateau. In: L.A. Mayer (Editor), Proceedings of the Ocean Drilling Program, Scientific Results, 130, College Station, TX, pp. 491-508.

Yokokawa, M. and Franz, S.-O., 2002. Changes in grain size and magnetic fabric at Blake-Bahama Outer Ridge during the late Pleistocene (marine isotope stages 8-10). Marine Geology, 189(1-2): 123-144.

PART II

PUBLICATIONS

In the duration of this thesis three manuscripts were produced as a major part of this study. The content of these publications is described briefly in the following section.

Manuscript #1 — Surface sediment bulk geochemistry and grain-size composition related to the oceanic circulation along the South American continental margin in the Southwest Atlantic. M. FRENZ, R. HÖPPNER, J.-B. STUUT, T. WAGNER AND R. HENRICH, accepted for: *Mulitza, S., Ratmeyer, V. and Wefer, G. (Eds.): The South Atlantic in the Late Quaternary: Reconstruction of material budget and current systems. Springer, Berlin Heidelberg New York.*

The grain-size distribution of the terrigenous silt fraction was utilised to follow sedimentation processes on the continental margin off Argentina, Uruguay and southern Brazil. With the aid of an end-member modelling algorithm three accumulation patterns were distinguished. Including further support by geochemical bulk parameters ($CaCO_3$, C_{org}) the complex interactions of sediment supply, distribution and modification by oceanographic conditions were traced. In this SW Atlantic "crossroad of the waters" NADW is traced by a band of high carbonate contents at water depths between 2000 and 4000 m as far as 48°S. This continuous band is only interrupted at about 52-54°W by a corridor characterised by high accumulation of C_{org} and medium coarse sediments which is interpreted to be the sedimentary trace of the Malvinas-Brazil-Confluence. The action of the vigorous Malvinas current in combination with the discharge of large rivers leaves very coarse grained sandy sediments at the Argentine outer shelf and continental slope. At the lower southwestern part of the Rio Grande Rise and in the deeper southern Brazil Basin very fine-grained clayey sediments indicate sediments which accumulated under quiet current conditions.

Manuscript #2 — Quantification of foraminifer and coccolith carbonate in South Atlantic surface sediments by means of carbonate grain-size distributions. M. FRENZ, K.-H. BAUMANN, B. BOECKEL, R. HÖPPNER AND R. HENRICH, submitted to *Journal of Sedimentary Research*

In this study the grain-size composition of the carbonate share of pelagic surface sediments from the Mid-Atlantic Ridge was in the focus of interest. The most striking feature of the

carbonate silt grain-size distributions is their general bimodality. In the silt fraction the minimum of about 8 μm divides foraminifer fragments and juvenile tests from coccoliths. Extending this division to the carbonate contents of the sand and clay fractions, foraminifer (and pteropod) carbonate on the one hand and coccolith carbonate on the other are distinguished. Another feature of the carbonate silt grain-size distributions is the regional size-stability of the fine mode. This characteristic was used to distinguish three ecological provinces in the South Atlantic. In the equatorial province foraminifer contribute most of the carbonate (about 70 %). In the central province zooplankton (foraminifers) and phytoplankton (coccoliths) contribute about the same carbonate, while in the southern province coccolith carbonate predominates (about 60 %). Additionally, a close link was found between the equivalent spherical grain size and the mean nominal diameter of distinct coccolith species. This could be the basis for practical enrichment of distinct coccolith species by settling methods, as well as for statistical unravelling of species and their mass quantification by means of fitting Gaussian distributions.

Manuscript #3 — Carbonate dissolution revealed by silt grain-size distribution: comparison of Holocene and last Glacial Maximum sediments from the pelagic South Atlantic. M. FRENZ AND R. HENRICH, submitted to *Sedimentology*

This study revealed the applicability of grain-size variations in calcareous sediments as a proxy for carbonate dissolution. For this purpose the spatial distribution of grain-size characteristics of Holocene sediments were compared to the ones of sediments from the Last Glacial Maximum (LGM). Both sample sets originate from bathymetric highs of the South Atlantic, namely Ceará Rise, Mid-Atlantic Ridge and Walvis Ridge. Ecological differences between mesotrophic equatorial provinces and oligotrophic provinces in the subtropical gyre become obvious from spatial variations in the contribution of foraminifers and coccoliths to the carbonate budget. Within one province a continuous water depth related increase of coccolith on the expense of foraminifer carbonate indicates supralysoclinal calcite dissolution. For the Holocene a certain critical level (sedimentary lysocline) is indicated by strong differences above and below this level. This feature is detected at water depths of about 4100 m for the Brazil and Cape Basins and at about 4600 m in the Angola Basin. Our results suggest that the lysocline was raised to a water depth of about 3000 m during LGM times, lifting the modern asymmetry in water mass distribution and carbonate preservation.

SURFACE SEDIMENT BULK GEOCHEMISTRY AND GRAIN-SIZE COMPOSITION RELATED TO THE OCEANIC CIRCULATION ALONG THE SOUTH AMERICAN CONTINENTAL MARGIN IN THE SOUTHWEST ATLANTIC

M. Frenz *, R. Höppner, J.-B. W. Stuut, T. Wagner and R. Henrich

FB Geowissenschaften, Universität Bremen, Postfach 330440, D-28334 Bremen, Germany

** corresponding author, e-mail: mfrenz@uni-bremen.de*

Abstract

Surface sediments from the South American continental margin surrounding the Argentine Basin were studied with respect to bulk geochemistry ($CaCO_3$ and C_{org}) and grain-size composition (sand/silt/clay relation and terrigenous silt grain-size distribution). The grain-size distributions of the terrigenous silt fraction were unmixed into three end members (EMs), using an end-member modelling algorithm. Three unimodal EMs appear to satisfactorily explain the variations in the data set of the grain-size distributions of terrigenous silt. The EMs are related to sediment supply by rivers, downslope transport, winnowing, dispersal and re-deposition by currents. The bulk geochemical composition was used to trace the distribution of prominent water masses within the vertical profile. The sediments of the eastern South American continental margin are generally divided into a coarse-grained and carbonate-depleted southwestern part, and a finer-grained and carbonate-rich northeastern part. The transition of both environments is located at the position of the Brazil Malvinas Confluence (BMC). The sediments below the confluence mixing zone of the Malvinas and Brazil Currents and its extensions are characterised by high concentrations of organic carbon, low carbonate contents and high proportions of the intermediate grain-size end member. Tracing these properties, the BMC emerges as a distinct North-South striking feature centered at 52-54°W crossing the continental margin diagonally. Adjacent to this prominent feature in the Southwest, the direct detrital sediment discharge of the Rio de la Plata is clearly recognised by a downslope tongue of sand and high proportions of the coarsest EM. A similar coarse grain-size composition extends further south along the continental slope. However, it displays better sorting due to intense winnowing by the vigorous Malvinas Current. Fine-grained sedimentary deposition zones are located at the southwestern deeper part of the Rio Grande Rise and the southern abyssal Brazil Basin, both within the AABW domain. Less conspicuous winnowing/accumulation patterns are indicated north of the La Plata within the NADW level according to the continental margin topography. We demonstrate that combined bulk geochemical and grain-size properties of surface sediments, unmixed with an end-member algorithm, provide a powerful tool to reconstruct the complex interplay of sedimentology and oceanography along a time slice.

---

accepted for: Mulitza, S., Ratmeyer, V. and Wefer, G. (Eds.): The South Atlantic in the Late Quaternary: Reconstruction of material budget and current systems. Springer, Berlin Heidelberg New York.

Key words: surface sediments, terrigenous silt, grain size, Brazil Malvinas Confluence, Rio de la Plata mouth, end-member modelling

1 Introduction

The southwestern part of the South Atlantic Ocean holds a key position in the global ocean circulation, since southern surface, intermediate and deep waters are introduced into the thermohaline cycle (e.g. Gordon 1986). Due to the position at the western boundary of the South Atlantic Ocean, the circulation is focussed to (Deep) Western Boundary (Under-) Currents (Stommel 1958). The increased flow velocities are expected to have a major impact on sedimentary processes, i.e. conducting deposition, winnowing and lateral advection of sedimentary particles.

Modern oceanography differentiates more than eight water masses along the western boundary of the South Atlantic (e.g. Arhan et al. 1999, Larqué et al. 1997, Mémery et al. 2000). Since sedimentological methods are not sensitive enough to distinguish whether the sediments have been in contact to varieties of the same water mass, we apply a model essentially based on Piola and Matano (2001). This model manages the complex vertical stratification structure of the water masses in the western South Atlantic with four main water levels (Fig. 1). Upper and intermediate water levels are occupied by Subantarctic (SAW) and subtropical Thermocline Waters (TW; both < 500 m water depth and admixed with South Atlantic Central Water) and Antarctic Intermediate Water (AAIW, 500-1000 m water depth). As one unit, SAW (branch of the Antarctic Circumpolar Current) and AAIW enter the study area from the South, referred to as the Malvinas (Falkland) Current (MC), flowing NE. Its counterpart in the Northeast is the southwestward flowing Brazil Current (BC). It contains both, TW as well as AAIW and marks the northwestern closure of the subtropical gyre. Both current systems collide in front of the mouth of Rio de la Plata at 38°S, called the Brazil Malvinas Confluence (BMC; Gordon and Greengrove 1986). At the BMC both currents are deflected to the South and experience intense mixing that also affects deeper water levels. The BMC system is further complicated by the discharge from the Rio de la Plata estuary, which releases 470 km^3 a^{-1} of freshwater into the South Atlantic (Milliman and Meade 1983). In comparison, the two deep water levels reveal a much simpler structure. North of the BMC, water depths between 2000 and 4000 m are characterised by the southward flow of North Atlantic Deep Water (NADW). South of the BMC the NADW splits the northward flowing CDW into an upper and lower layer (UCDW and LCDW). Below 4000 m, Antarctic Bottom Water (AABW) flows northward.

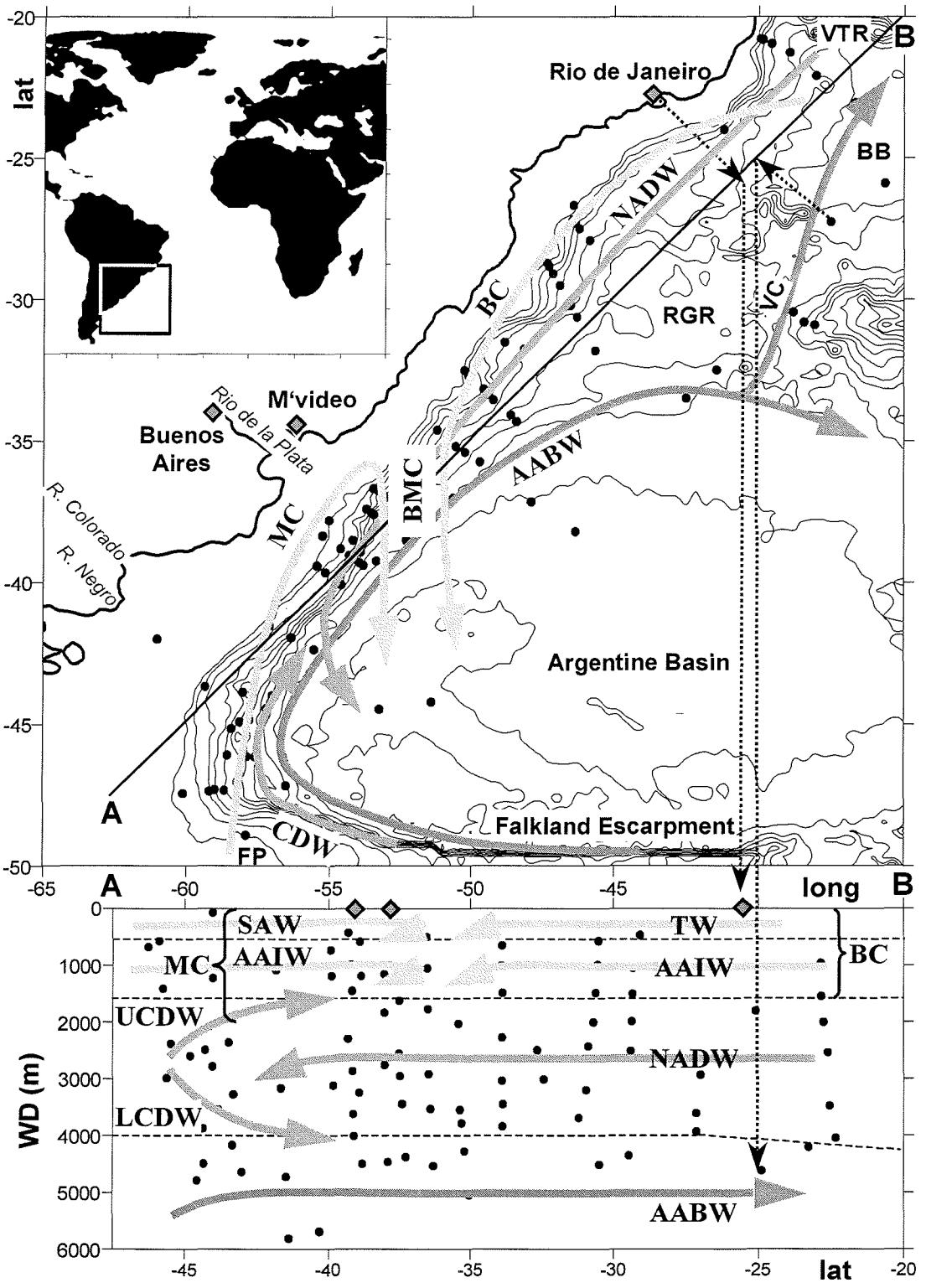

Fig. 1: *Bathymetry according to the ETOPO 2'-grid (top) of the South American continental margin between 20 and 50°S. Main geographic features are indicated (M'video - Montevideo, VTR - Vitória Trindade Ridge, BB - Brazil Basin, RGR - Rio Grande Rise, VC - Vema Channel, FP - Falkland Plateau). Isobaths are 0 m and multiples of 500 m. Arrows show generalised main flow paths of water masses along the western boundary [MC - Malvinas Current, BC - Brazil Current, SAW - Subantarctic Water, TW - Thermocline Water, AAIW - Antarctic Intermediate Water, (U/L)CDW - (Upper/Lower) Circumpolar Deep Water, NADW - North Atlantic Deep Water, AABW - Antarctic Bottom Water]. BMC indicates the Brazil Malvinas Confluence and its extension. Line A-B shows the position of the projection plain of the part below. The dotted arrows indicate the way of projection for two representative locations, Rio de Janeiro and a sample position from the abyssal Brazil Basin.*

Although the oceanographic configuration along the eastern continental margin of South America has been investigated in much detail, our knowledge on the variability of the sedimentary regimes in this area is rather poor and their driving forces not fully understood. Previous studies have elucidated local sediment dispersal mechanisms (e.g. Höppner and Henrich 1997, Benthien and Müller 2000, Hensen et al. 2000, Michaelovitch et al. 2002, Ledbetter 1984). They were based on specific parameters only. In addition, the discrimination of large-scale sediment bodies and their internal structure was investigated by echo sound properties (Mello et al. 1992, Flood and Shor 1988, Ledbetter 1986). Hence, a complementary multiproxy sedimentary study covering the entire region is still lacking.
This study is intended to fill this gap. We present bulk geochemical, bulk sedimentological and terrigenous silt grain-size distribution data from the eastern South American continental margin between 20 and 50°S latitude covering water depths from the outer shelf to the deep sea. This detailed sedimentological data set is unmixed into subpopulations, using an end-member algorithm (Weltje 1997), which are subsequently interpreted in terms of sediment transport mechanisms and depositional processes. In particular, we focus the discussion on the complex interferences of biological and sedimentological processes with variations in physical and chemical properties of the different water masses.

2 Methods

The present study relies on grain-size investigations of 111 surface samples from the southwestern South Atlantic. In addition, 106 bulk geochemical data were consulted [$CaCO_3$ and C_{org} data from this study, Mollenhauer et al. (submitted) and Hease et al. (2000); see www.pangaea.de for accurate references]. The samples were recovered during 6 cruises of RV METEOR between 1993 and 2000. Where available, the uppermost cm (0-1 cm) of multi- and box-core samples was used for analysis. At 16 locations the core tops had already been sampled. For these core positions the second cm (1-2 cm) was used for granulometric analysis (cf. www.pangaea.de).
The freeze-dried bulk samples were split into coarse (sand) and fine fractions by wet sieving using a 63 µm mesh. Subsequently, the fine fraction was split into silt and clay fractions according to their settling velocities after Stokes' Law, assuming a sample density of 2.65 g cm^{-3}. The bulk silt fraction was dried and weighed, decalcified using excess HCl, then washed, dried and weighed again. The grain-size distribution of the carbonate-free silt fraction was analysed using a Micromeritics SediGraph 5100. The measurements were limited to 95 samples, where more than 1 g carbonate-free sample material was left after decalcification. The SediGraph data were converted into fifty size classes from 9-4 Φ (bin width 0.1 Φ each) using the SediMac applet written by G. Kuhn (AWI, Bremerhaven). The statistical parameters [arithmetical mean, modal size (size class containing highest amount), sorting (standard deviation) and skewness] of the size-

frequency distributions are based on momentum calculations according to Krumbein (1936). The terrigenous silt fraction comprises a size window that is highly sensitive for sediment sorting processes (e.g. McCave et al. 1995, Bianchi and McCave 2000, Bianchi et al. 2001, Gröger and Henrich submitted) that are assumed to have a great impact to the investigated sediments (Ledbetter 1984, 1986).

End-member modelling of the carbonate-free silt grain-size distributions was carried out using the algorithm of Weltje (1997). This end-member algorithm has been successfully applied to unravel data sets of rodent palaeocommunity successions (Van Dam & Weltje 1999) and particle-size distributions of deep-sea sediments from the Arabian Sea (Prins and Weltje 1999, Prins et al. 2000), the North Atlantic Ocean (Prins et al 2001, 2002), and the eastern South Atlantic (Stuut et al. 2002). The basic assumption underlying end-member studies is the fact that the data set consists of a number of subpopulations. For each set of end members, the degree to which the composition can be reconstructed is expressed as the coefficient of determination. The appropriate amount of end members is subsequently chosen at the threshold where the best fit is reached with the least amount of end members. The relative proportion of each end member for all samples can then be calculated.

Organic and total carbon were measured in homogenised sub-samples using a Leco CS-300 elemental analyser (precision of measurement ± 3 %). For the determination of organic carbon, calcium carbonate was removed by repeatedly adding aliquots of 0.25 N HCl. The carbonate content was calculated from the difference between total and organic carbon and expressed as calcite [$CaCO_3 = (C_{tot}\text{-}C_{org}) * 8.33$]. To evaluate the reproducibility of carbon data duplicates were measured routinely.

To enable a 3-D impression of the spatial distribution, each parameter is shown as kriging-interpolated isoplots over the ETOPO 2' bathymetric grid and, as a depth-related projection on a vertical plane oriented parallel to the continental slope. As is the nature of any interpolation, areas of higher sample coverage denote higher reliability compared to scarcely covered areas.

Following Benthien and Müller (2000), Holocene ages are assumed for our sample grid that is partly derived from identical stations and from positions in between of those.

3 Results

The bulk geochemical and grain-size composition of surface sediments along the South American continental margin varies from carbonate-rich and fine-grained in the Northeast to carbonate-poor and coarse-grained in the Southwest. The transition zone between these two modes coincides with the position of the BMC and is located at about 52° to 54°W. Overall, grain-sizes generally decrease with increasing water depth. In contrast, the carbon distribution patterns are preferentially related to specific water depths (carbonate) and geographic location (organic carbon).

3.1 Carbonate distribution

One characteristic feature in the bulk carbonate distribution is a continuous level of elevated values all along the continental rise at water depths between 2000 and 4000 m. Typical carbonate contents between 40 and 70 % are observed from 20 to 35°S and from 43 to 48°S, approaching maximum concentrations at about 2500 m water depth. Exceptionally high concentrations are observed at exposed sites, i.e. on top of the Vitória Trindade Ridge (VTR, $CaCO_3 > 90$ %) and on the eastern slope of the Vema Channel (VC, $CaCO_3 > 80$ %). In contrast to these high concentrations, the carbonate contents of the carbonate-rich level is considerably reduced ($CaCO_3 < 20$ %) in a broad sector from about 35 to 42°S (= 50-57°W), which includes the La Plata mouth. Within this sector of depletion the carbonate-rich band is almost interrupted ($CaCO_3 < 10$ %) by a narrow corridor at about 52-54°W. At about 48°S (57°W) the continental margin turns east to build the Falkland Escarpment. Here, and at water depths corresponding to the carbonate-rich level, carbonate contents decrease to concentrations below 20 %.

In the Argentine Basin samples from below 4000 m water depth are almost completely barren in calcium carbonate ($CaCO_3 < 5$ %), whereas in the southwestern Brazil Basin samples down to 4200 m still reveal carbonate contents of 10 to 20 % before they drop to almost zero below 4500 m water depth.

The continental slope (< 2000 m water depth) offshore Uruguay and Argentina is clearly distinguished from corresponding water depth levels in the Northeast offshore Brazil on the basis of carbonate contents. In the Southwest carbonate generally remains below 10 % to decrease to < 5 % above 1200 m water depth. In contrast, sediments from the Northeast contain about 20 % between 2000 and 1000 m water depth to increase to 30 % carbonate at about 600 m water depth.

Fig. 2: Carbonate distribution of surface samples along the eastern South American continental margin (n = 106). NADW is indicated by elevated concentrations down to 48°S. In a broad sector off La Plata mouth the signal is weaker. Sediments under the influence of AABW and Malvinas Current lack carbonate.

Fig. 3: Organic carbon concentrations of surface sediment samples along the eastern South American continental margin (n = 106). Note the high-C_{org} corridor (starting at the outer shelf heading South between 52 and 54°W) tracing the Brazil Malvinas Confluence and its extensions.

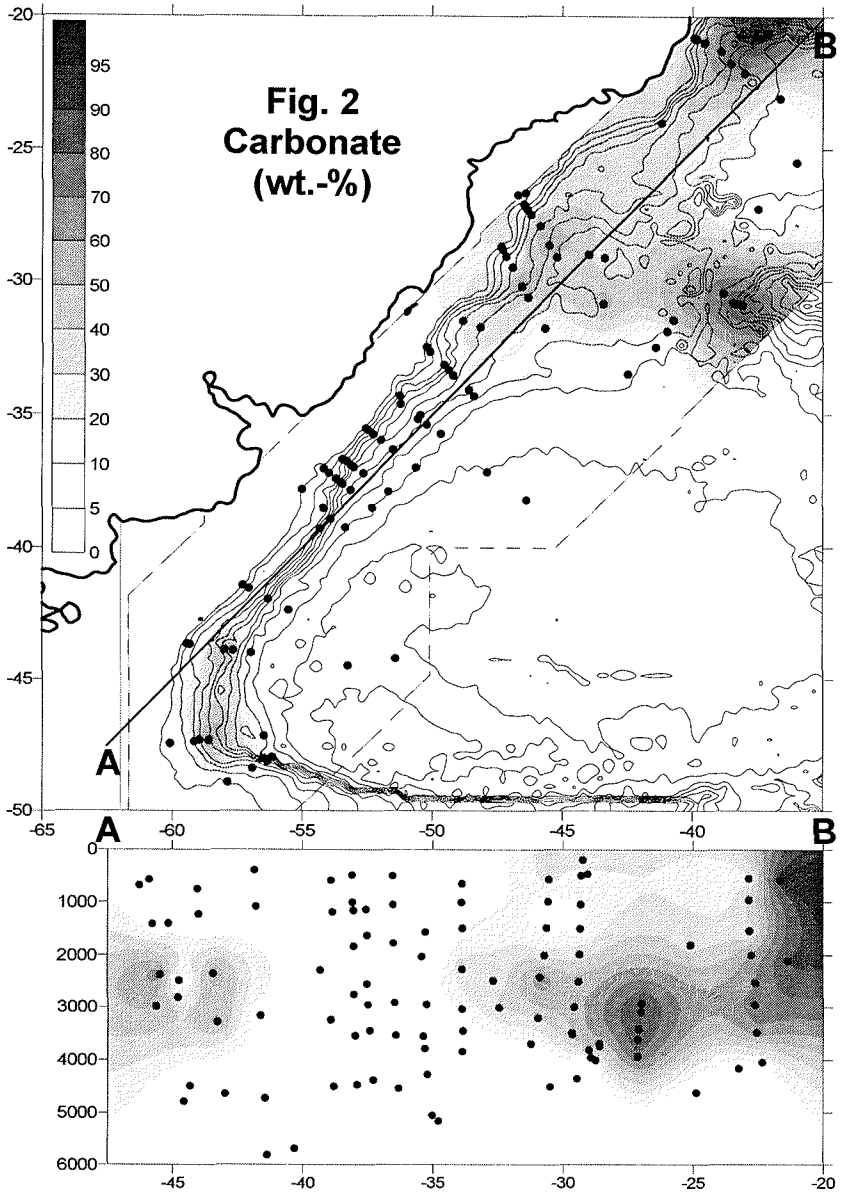
Fig. 2
Carbonate
(wt.-%)
95
90
80
70
60
50
40
30
20
10
5
0
A
B
-20
-25
-30
-35
-40
-45
-50
-65
-60
-55
-50
-45
-40
0
1000
2000
3000
4000
5000
6000

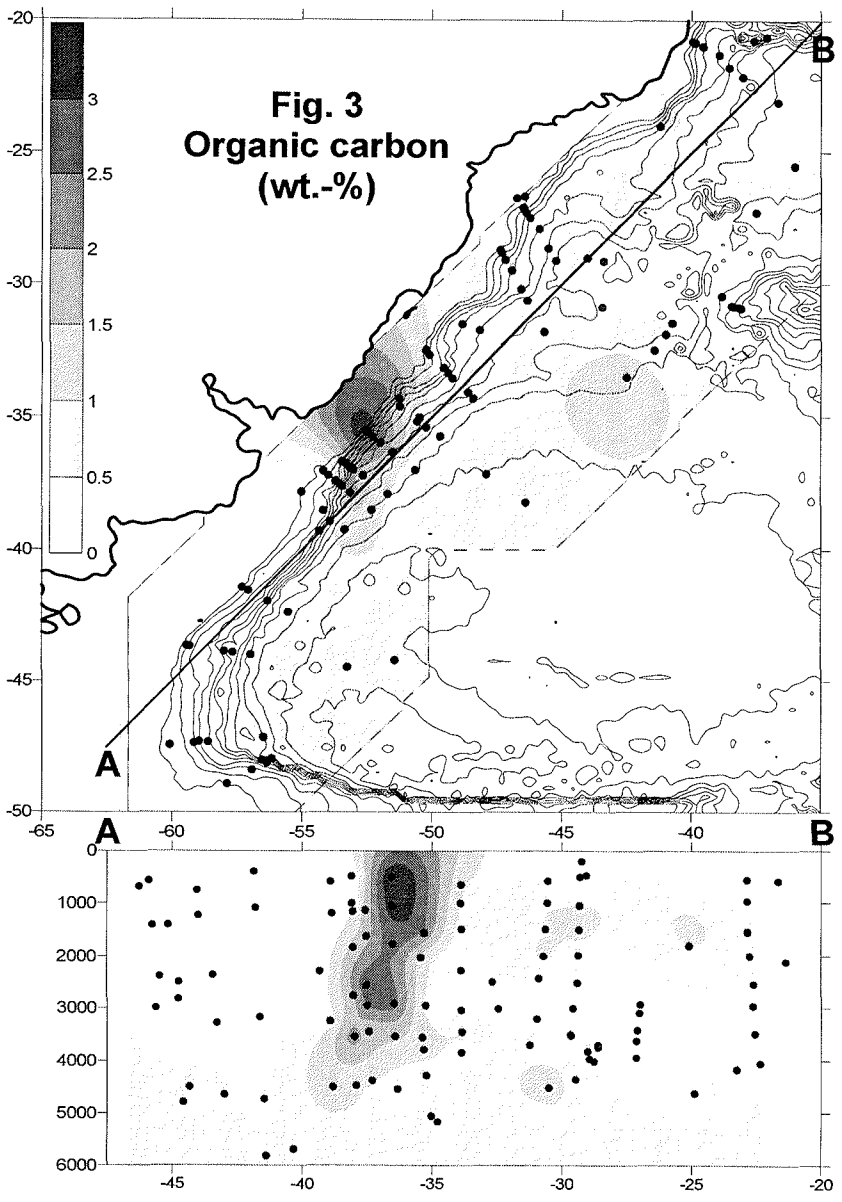
Fig. 3
Organic carbon
(wt.-%)
3
2.5
2
1.5
1
0.5
0
A
B
-20
-25
-30
-35
-40
-45
-50
-65
-60
-55
-50
-45
-40
0
1000
2000
3000
4000
5000
6000

3.2 Organic carbon distribution

The most striking feature of the modern organic carbon distribution along the south-eastern South American continental margin is a narrow N-S striking corridor off the Rio de la Plata mouth at about 52-54°W. Here, the concentrations are up to three times higher as compared to the adjacent areas. In this corridor, organic carbon exceeds 2.5 % at water depths between 500 and 3500 m to gradually decrease to still considerable 1 % at 4500 m water depth. This corridor coincides with the almost carbonate-barren corridor at 52-54°W (Figs. 2, 3). The organic carbon contents remain low southwest of this corridor, in the order of 0.5 % and less, with values being highest below a water depth of 4000 m. The Northeast of the study area indicates a stratification of the organic carbon contents which is related to the water depth. Above 700 m and between 2500-3500 m water depth the sediments hardly contain any organic carbon (C_{org} < 0.5 %). In between and below these two depleted levels the organic carbon contents are elevated in the order of 1.5-0.5 %.

Sediments enriched in organic carbon in front of the La Plata and below the BMC bear a mixed marine and terrigenous organic signature. Supply of riverine organic matter is traced by the presence of higher plant tissue, identified by lignin phenols and organic particles (macerals) of terrigenous origin (vitrinite, inertinite), whereas bodies of marine algae, dinoflagellate cysts and detrital fragments represent organic matter of marine origin (see Wagner et al., this volume and references therein for terrigenous organic matter in South Atlantic sediments). In front of the La Plata and below the BMC, the content of reactive and hydrogen-rich organic matter preserved in surface sediments gradually decreases with increasing distance to the continent. Accordingly, hydrogen indices obtained from Rock-Eval Pyrolysis decreased from 350 mg HC/g C_{org} at shallow sites to slightly above 100 mg HC/g C_{org} at about 4500 m water depth, documenting an enhanced remineralisation of reactive organic matter at greater water depths. First estimates of marine and terrigenous organic fractions based on maceral analysis suggest a 40-50 % contribution from continental sources in front of the La Plata, showing no clear trend over the continental slope.

3.3 Granulometry I: Sand/Silt/Clay relationship of the bulk sediment

Measurements performed by Romero and Hensen (2002) revealed that the contents of biogenic opal in surface sediments of the region of interest are very low (< 1.3 %). Their sample set overlaps to a great extent with the one used in this study. Therefore biogenic opal can be neglected in the sand/silt/clay relations, and the sediments can be regarded to consist of biogenic carbonate and terrigenous components only. Hence, the carbonate contents have to be taken into account when interpreting the relation of these bulk size fractions.

A clear separation of the northeastern and southwestern parts of the continental margin is evident on account of the sand/silt/clay distribution patterns, and projections of these basic granulometric data in a ternary plot (Figs. 4, 5). Accordingly, at approximately 52-54°W,

there is a transition zone that separates relatively coarse-grained, sandy sediments in the Southwest from relatively fine-grained, muddy deposits in the Northeast. Furthermore, higher clay proportions at otherwise comparable sand contents are observed in surface sediments from the Northeast in comparison to the Southwest. In both areas the sand contents consistently decrease with increasing water depth.

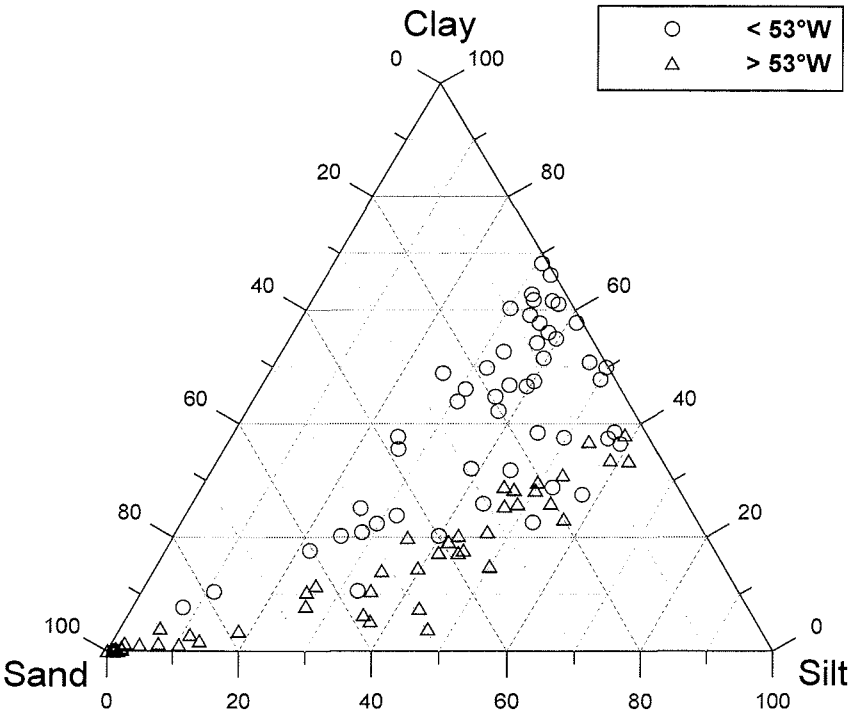

Fig. 4: Ternary bulk sand-silt-clay relations (in wt.-%) of surface sediments from the eastern South American continental margin. Fine grained northeastern samples (< 53°W, circles) can be distinguished from coarse grained southwestern samples (> 53°W, triangles).

In the Southwest, the Argentine shelf and slope sediments contain more than 90 % of sand-sized material at water depths less than 1500 m. This signature persists towards the Falkland Escarpment in the South. The sand contents decrease with increasing water depth across the Argentine continental rise approaching 40 % at 4700 m, and even 20-30 % in the southwesternmost basin exceeding 3500 m water depth. Below a water depth of 3300 m, the fine fraction of all samples from the Southwest is mainly composed of silt (> 40 % silt, < 20 % clay). The silt contents gradually increase across the continental rise towards the continent, most pronounced in front of the La Plata mouth and close to the Falkland Escarpment.

Comparable to the carbonate and organic carbon distribution patterns the sand, silt and clay contents of the sediments of the Northeast show a 4-level structure related to water depth. Sediments from carbonate-rich layers, i.e. shallow (< 700 m water depth) and intermediate (2000-3500 m water depth) water levels are characterised by a very variable size composition (10-60 % sand, 20-50 % silt, 20-50 % clay). Between and below these levels the sand content is reduced to < 10 % at constant silt (30-40 %) and high clay contents (> 50 %). Exceptionally coarse sediment compositions are observed at exposed sites

(eastern slope of VC, VTR and beyond). Here, the sand contents exceed 60 %, whereas silt and clay each approach a relative value of about 20 %.

In the deep sea, below 4000 m water depth, the marked coarse/fine size transition at about 53°W is shifted to the Northeast. Although grain size generally decreases with increasing water depth, abyssal sediments in the Southwest are relatively coarse-grained compared to those in the Northeast. 20-30 % sand and 40-70 % silt are observed as far as 35°S (50°W), indicating that the coarse/fine transition is shifted by about 3° towards the North and the East, respectively, which corresponds to about 400 km.

Fig. 5: *Contribution of bulk size fractions to the surface sediments along the eastern South American continental margin. a) bulk sand (size fraction > 63 µm, n = 111) b) bulk silt (size fraction 63-2 µm, n = 98) c) bulk clay (size fraction < 2 µm, n = 98). Note the sharp break at about 53°W between southwestern coarse (silty and sandy) and northeastern fine sediment mode (mainly clayey). High terrigenous (compare Fig. 2) sand concentrations are observed at the Argentine outer shelf and slope.*

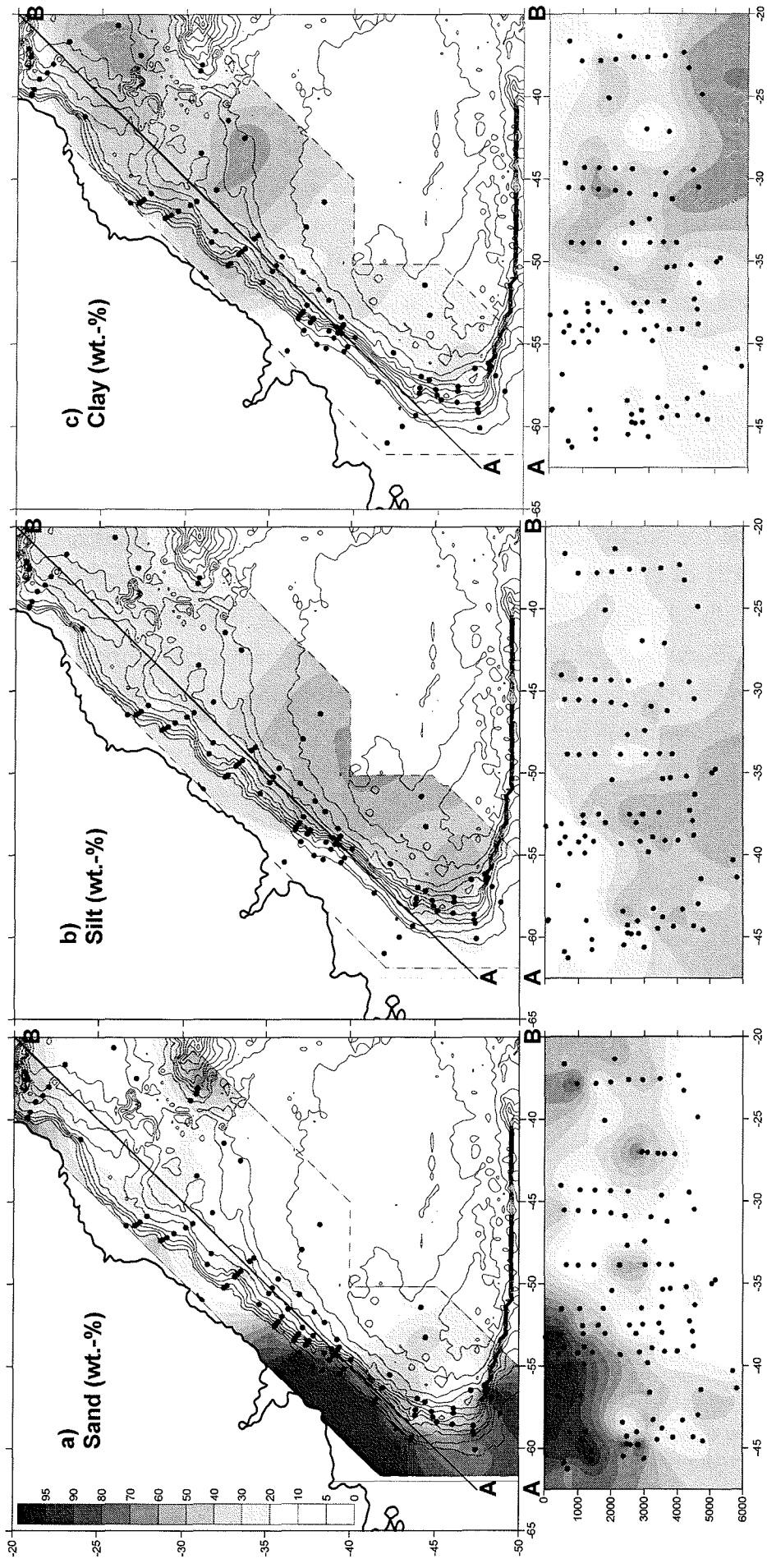
a)
Sand (wt.-%)
b)
Silt (wt.-%)
c)
Clay (wt.-%)
A
B
95
90
80
70
60
50
40
30
20
10
5
0
-20
-25
-30
-35
-40
-45
-50
-65
-60
-55
0
1000
2000
3000
4000
5000
6000

3.4 Granulometry II: Terrigenous silt grain-size distributions

To test if the relative increase of opal contents due to the separation of the carbonate-free silt fraction (removal of sand, clay and carbonate) has a significant effect on its size distribution some additional analyses were carried out. Light microscopy of the sand fraction of samples with elevated opal contents (opal > 1 %, according to Romero and Hensen 2002) revealed some sponge spicules and radiolarians that have, due to their size, evaded the silt fraction. Spot tests of the carbonate-free silt fraction revealed maximum opal concentrations of 13 % in areas vulnerable for elevated opal contents like the southwestern most Argentine Basin and the low-$CaCO_3$/high-C_{org} corridor. Although for two cases this means a tenfold enrichment in the carbonate-free silt, compared to the bulk sample, the biogenic opal content is rather low and its impact on the grain-size distribution of the carbonate-free silt can be neglected. Therefore, the grain-size distributions of the carbonate-free silt fraction are considered to represent terrigenous silt (TS).

The content of TS of the bulk surface sediments (not shown) reveals maximum values of 70 % of the bulk sample. Generally, the TS proportions increase with increasing water depth. At the Argentine shelf and slope its contribution is insignificant because the sediments are predominantly sandy, i.e. they consist of more than 90 % terrigenous sand. On the other hand, the silt deposition is reduced and additionally diluted by high carbonate sand contents at exposed sites.

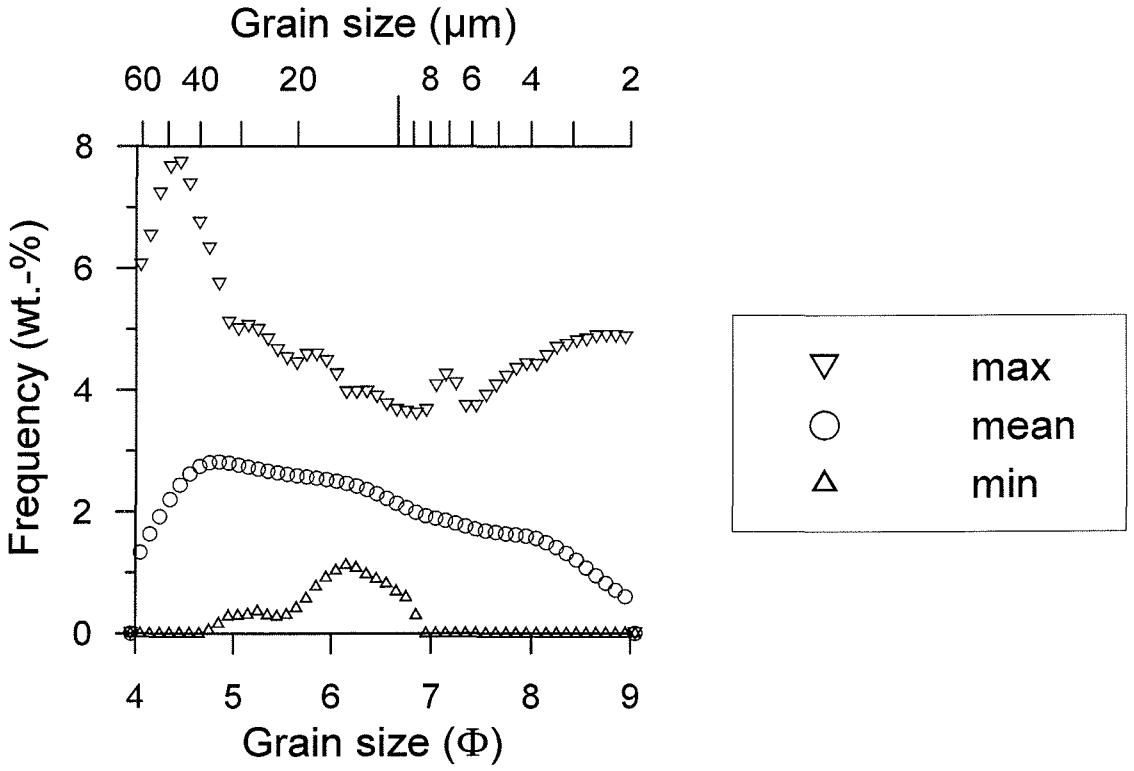

Fig. 6: Brief statistics (maximum, average and minimum) for the 95 measured TS grain-size distributions. The plot reveals the high variability of the terrigenous silt grain size composition along the eastern South American continental margin. Variability is highest coarser than 32 µm (very coarse silt) and finer than 4 µm (very fine silt).

The general statistics for the 96 TS grain-size frequency distributions (minimum, maximum, average) are given in Figure 6. It verifies the inhomogeneous and highly variable grain-size composition of the sediments from the eastern South American continental margin. Maximum size variability is revealed close to the coarse and the fine end of the silt size range.

Although conclusions drawn from the statistical parameters of the TS distributions are restricted by artefacts that are introduced by the empirical size limits of the silt fraction (see Excursion), the general trends can be deduced from their spatial distribution pattern. The spatial variability of the commonly used statistical parameters is illustrated in Figure 7. As expected from bulk granulometry (sand/silt/clay), the grain-size parameters mean, mode and skewness confirm the observed differences between southwestern coarse and northeastern fine-grained sediments. The transition of both modes of sediment composition again coincides with the low-$CaCO_3$/high-C_{org} corridor at about 52-54°W.

In the Southwest, the coarsest TS composition is observed at the continental slope at 1000-1500 m water depth and off the la Plata mouth down to water depths of > 3000 m (mean 20-32 µm, mode > 32 µm). With increasing water depths, the grain size of silt drops to minimum values in the southwestern most rim of the basin below 4000 m water depth (mean and mode 11-16 µm). These sites are also characterised by symmetric distributions (skewness ~ 0) but poor sorting (> 1.3). For TS samples from the remaining area a positive skewness is calculated, most prominent off the La Plata. Sorting is best (< 0.9) at continental slope sites south of La Plata.

In the Northeast, grain size decreases rapidly from shallow (< 1000 m) to intermediate and deep sites. TS mean values vary from 20-15 µm at the continental slope to 7-6 µm at the lower rise and in the southern Brazil Basin. Compared to the mean values, the corresponding modal values generally reveal a similar pattern but a greater variability and contrast, i.e. the water-depth related modal size decrease covers 45-3 µm. In the same way as size decreases, skewness decreases with water depth to negative values, showing minimum values (< -0.7) at the lower rise and southern Brazil Basin. Good sorting (< 1) is observed along a transect slightly north of the La Plata, at the eastern slope of the VC and in the southern Brazil Basin.

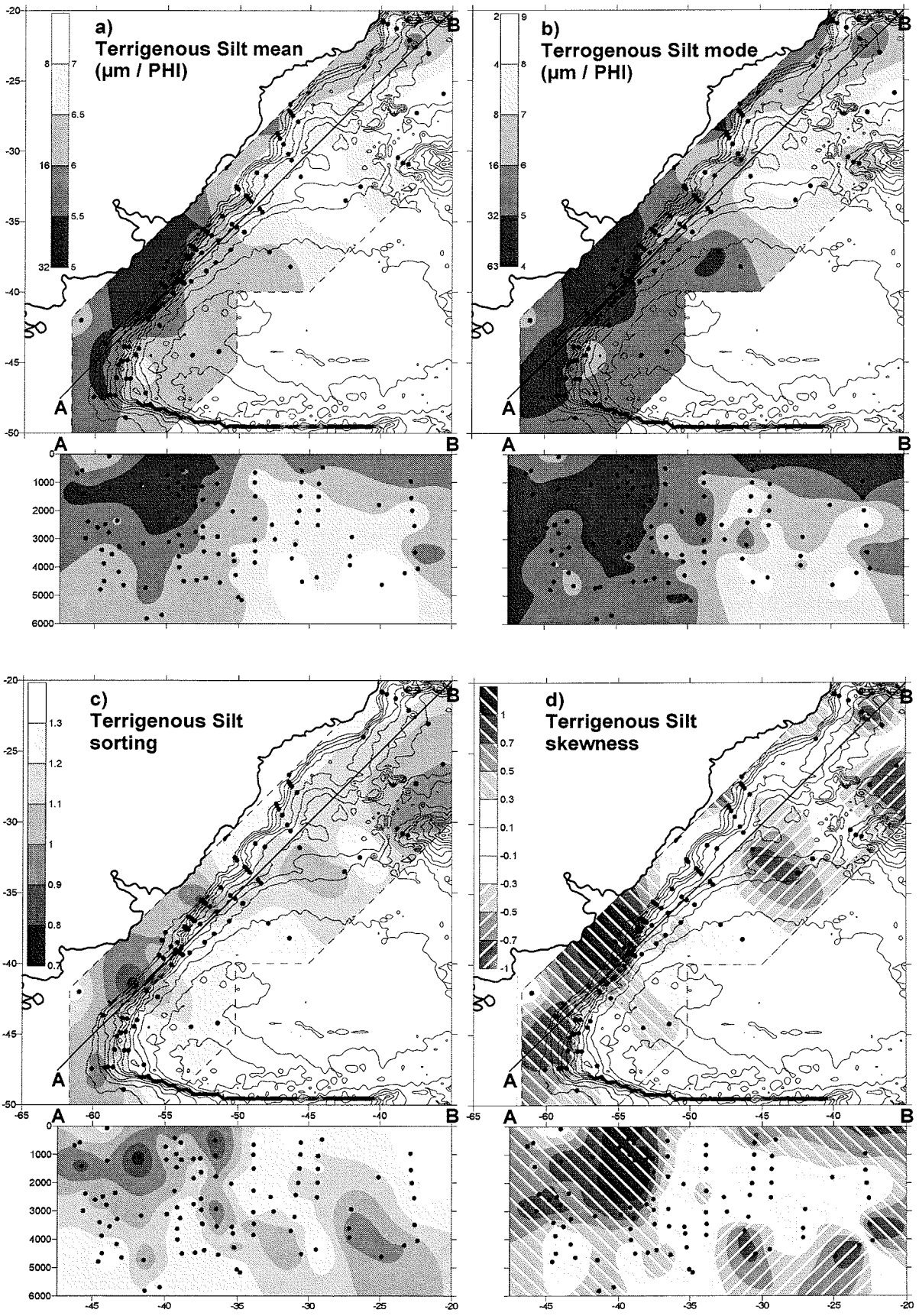
a)
Terrigenous Silt mean
(µm / PHI)
b)
Terrogenous Silt mode
(µm / PHI)
c)
Terrigenous Silt
sorting
d)
Terrigenous Silt
skewness
A
B

3.5 End-member modelling

The silt particle-size data set was unmixed into subpopulations using the end-member algorithm of Weltje (1997). The number of end members (dimensions of mixing space) is determined on the basis of goodness-of-fit statistics (Prins and Weltje 1999), i.e. the maximum fit with the least amount of end members. The end-member algorithm calculates the goodness of fit (coefficient of determination) per size class and per set of end members. For each set of end members, the mean coefficient of determination is used to determine the appropriate amount of end members. The mean coefficient of determination (Fig. 8a) increases with the increasing number of end members. Figure 8b shows the coefficients of determination per size class for models with 2 to 5 and 10 end members. The two-end-member model (mean $r^2 = 0.59$) shows low r^2 values in the size ranges between 32 and 10 µm (~5-6.5 Φ, $r^2 < 0.6$) and < 4 µm (> 8 Φ, $r^2 < 0.6$). The three-end-member model (mean $r^2 = 0.87$) shows low r^2 values in the size range < 2.7 µm (> 8.5 Φ) and relatively low r^2 values ($r^2 = 0.8$-0.9) between 16 and 8 µm (6-7 Φ). The latter size range as well as the fine end of the spectrum is better reproduced by models with four or more EMs (mean $r^2 \geq 0.93$). On average, a three-end-member model reproduces 87 % of the variance in each grain-size class compared to 93 % reproducibility of a four-end-member model. The mean coefficient of determination increases only slightly in models with more than four EMs (e.g. five-end-member model, $r^2 = 0.95$). In conclusion, the goodness-of-fit statistics suggest that a three- or a four-end-member model provides a reasonable choice with respect to contradictory requirements, i.e. reproducibility versus minimal number of EMs. The grain-size frequency distributions of the end members for both, the three- and four-end-member models are shown in Figures 8c and 8d. The statistical parameters of the frequency distributions of the EMs in both models are given in Table 1.

Fig. 7: Spatial distribution of the statistical parameters calculated from the terrigenous silt (TS) grain-size distributions according to Krumbein (1936), n = 95. ***a)*** *TS mean grain size in µm (left of scale bar) and Φ units (right of scale bar).* ***b)*** *TS modal grain size (size class of highest amount) in µm (left of scale bar) and Φ units (right of scale bar). Very coarse TS grain size is indicated along the Argentine continental slope (contourite) and down the slope and rise off the la Plata mouth (turbidite). In contrast, accumulation of very fine sediments are found at deeper sites in the northern Argentine and the southern Brazil Basin.* ***c)*** *TS Sorting (standard deviation of the size frequency distribution). Good sorting (< 1) characterises the alongslope contourites off Argentina whereas the coarse la Plata downslope tongue shows poor sorting. Sediments in the area congruent to the low-$CaCO_3$/high-C_{org}/EM2 corridor (compare Figs. 2 and 9) and in the deeper northeastern parts are well sorted.* ***d)*** *TS skewness. The calculation reveals negative (coarse) skewness for fine grained sediments from the Northeast and positive (fine) skewness for coarse grained sediments from the Southwest. This fake pattern (see Excursion) is the result of the artificial upper and lower size limits of the silt fraction. Most negative values occur at fine accumulation sites, most positive off la Plata mouth.*

Table 1: *Statistical parameters of the size frequency distributions for the three end-member model calculated according to Krumbein (1936).*

	three-end-member model		
	EM1	**EM2**	**EM3**
Mean (Φ)	4.92	6.01	7.44
Mean (µm)	33.14	15.50	5.76
Mode (Φ)	4.55	5.65	8.05
Mode (µm)	42.69	19.92	3.77
Sorting	0.76	0.93	0.95
Skewness	2.10	0.45	-0.75

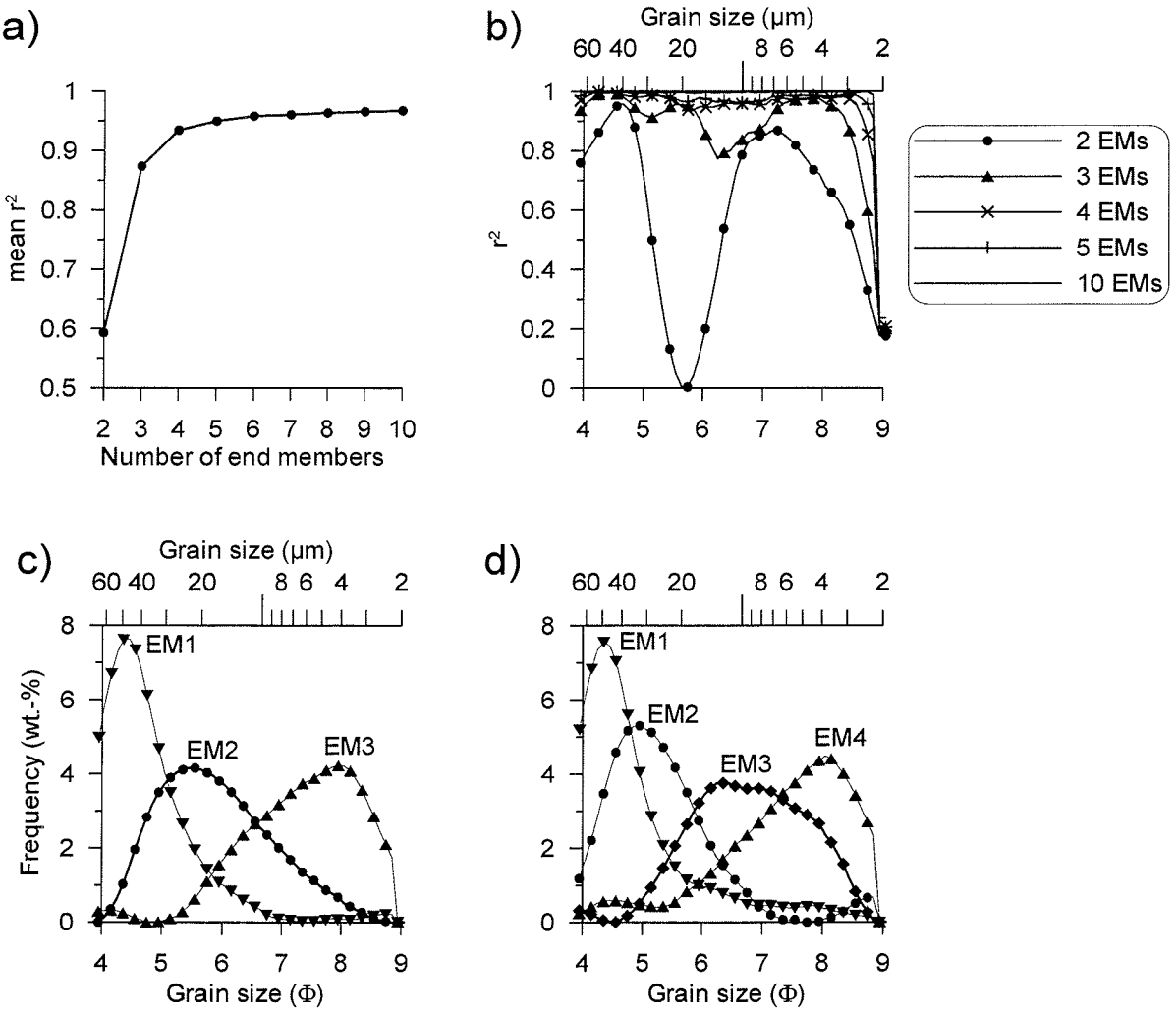

Fig. 8: *Goodness-of-fit statistics to estimate the number of end members.* ***a)*** *Mean coefficient of determination for models with 1 to 10 end members.* ***b)*** *Coefficients of determination for each size class for models with 2-5 and 10 end members.* ***c)*** *and* ***d)*** *Modelled end members of terrigenous silt from the eastern South American continental margin (size frequency distributions of the end members) for the three-end-member model (c) and the four-end-member model (d).*

The coarse and the fine EMs in each model are almost identical, showing prominent modes at approximately 47 µm (4.4 Φ) and 4 µm (8 Φ), respectively. That both models are similar in goodness-of-fit is partly consequential to the similarity of their coarse and fine EMs. Therefore, the two intermediate EMs of the four-end-member model are regarded as the result of the splitting of EM2 of the three-end-member model into EM2 and EM3 in the four-end-member model with minor contributions of the coarse and fine EMs. The marginal improvement in goodness-of-fit from a three-end-member model to a four-end-member model is attributed to one of the EMs of the four- end-member model, namely EM3, that contributes only a minor proportion to the compositional variation (maximum 30 %). Therefore, it is concluded that the TS grain-size composition of the South American continental margin (Atlantic side) can be regarded as a mixture of three end members (Fig. 8c).

The distribution of the three end members in the ternary mixing space (Fig. 9) reveals hardly any concurrence of the coarse and the fine EMs. Samples from the Southwest (> 53°W) are predominantly mixtures of medium and coarse EMs, whereas sediments from the Northeast are mixtures of the medium and fine EMs.

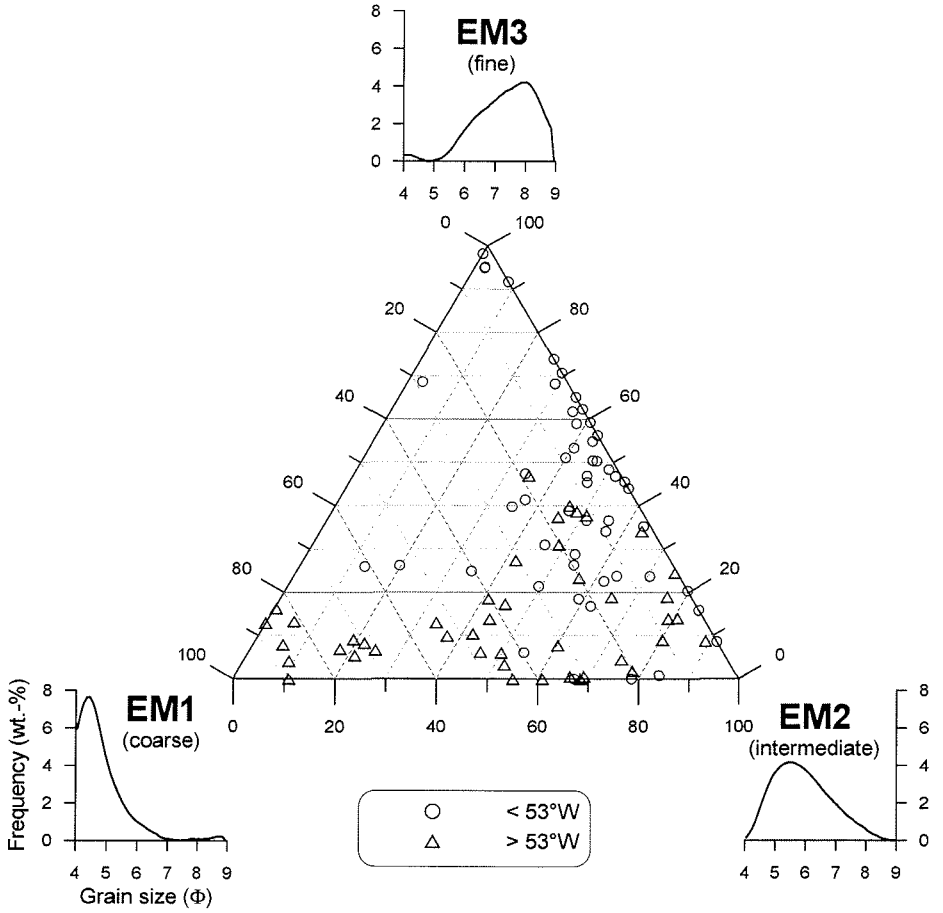

Fig. 9: Ternary mixing diagram for the terrigenous silt of surface sediments from the eastern South American continental margin and the size-frequency distributions of the three end members. Circles represent samples from the northeast (< 53°W) that show mainly binary mixing of the fine and the intermediate end members (EM3-EM2). Triangles denote samples from the Southwest (> 53°W) that reveal predominantly binary mixing of the coarse and the fine end members (EM1-EM2).

The spatial distribution of the relative proportions of the three end members (Fig. 10) reveals that the coarse end member (EM1, Fig. 10a) occurs in highest amounts in sediments at the Argentine continental outer shelf and slope and downslope off the La Plata mouth, as well as at shallow sites in the Northeast (40-90 %). The fine end member (EM3, Fig. 10c) contributes more than 50 % over a wide area of the Northeast. Maximum contributions are observed at the lower rise and in the southern Brazil Basin (> 80 %). 75 of the 95 samples consist by more than 30 % of the intermediate end member (EM2, Fig. 10b). High concentrations of EM2 (> 70 %) are found in the narrow corridor off the La Plata mouth that coincides with the low-$CaCO_3$/high-C_{org} corridor. Another area of higher contributions of EM2 (60-80 %) is located at the southwestern rim of the Argentine Basin.

Fig. 10: *Spatial distribution of the proportion of the three end members (EMs).* ***a)*** *Highest amounts of the coarse EM1 are observed downslope La Plata and along the Argentine continental slope corresponding to coarse TS grain size (Fig. 6a, b). High proportions of this end member indicate winnowing by strong currents and/or direct coarse river sediment discharge.* ***b)*** *Highest amounts of the intermediate EM2 are observed at the area congruent to the high C_{org}/low $CaCO_3$ corridor (Fig. 2) as the imprint of the BMC. Silt sized terrigenous suspended matter picked up by surface currents from rivers is released from the high energetic mixing zone of thermocline and subtropical waters because the energy drops due to increasing water depth along its southward extension at about 52-54°W. High proportions of EM2 at the southwestern most rim of the Argentine Basin are attributed to the release of coarse suspended matter from the MC that was probably eroded on its way across the Falkland Plateau.* ***c)*** *Spatial distribution of the proportion of EM3 once more indicating the contrast between southwestern coarse and northeastern fine sediments. High amounts of this finest end member reveal accumulation processes where current velocities are strongly reduced. Reference areas are the southwestern deep part of the RGR where AABW is dammed up and the abyssal southern Brazil Basin where AABW broadens again behind the jet passage through the Vema Channel.*

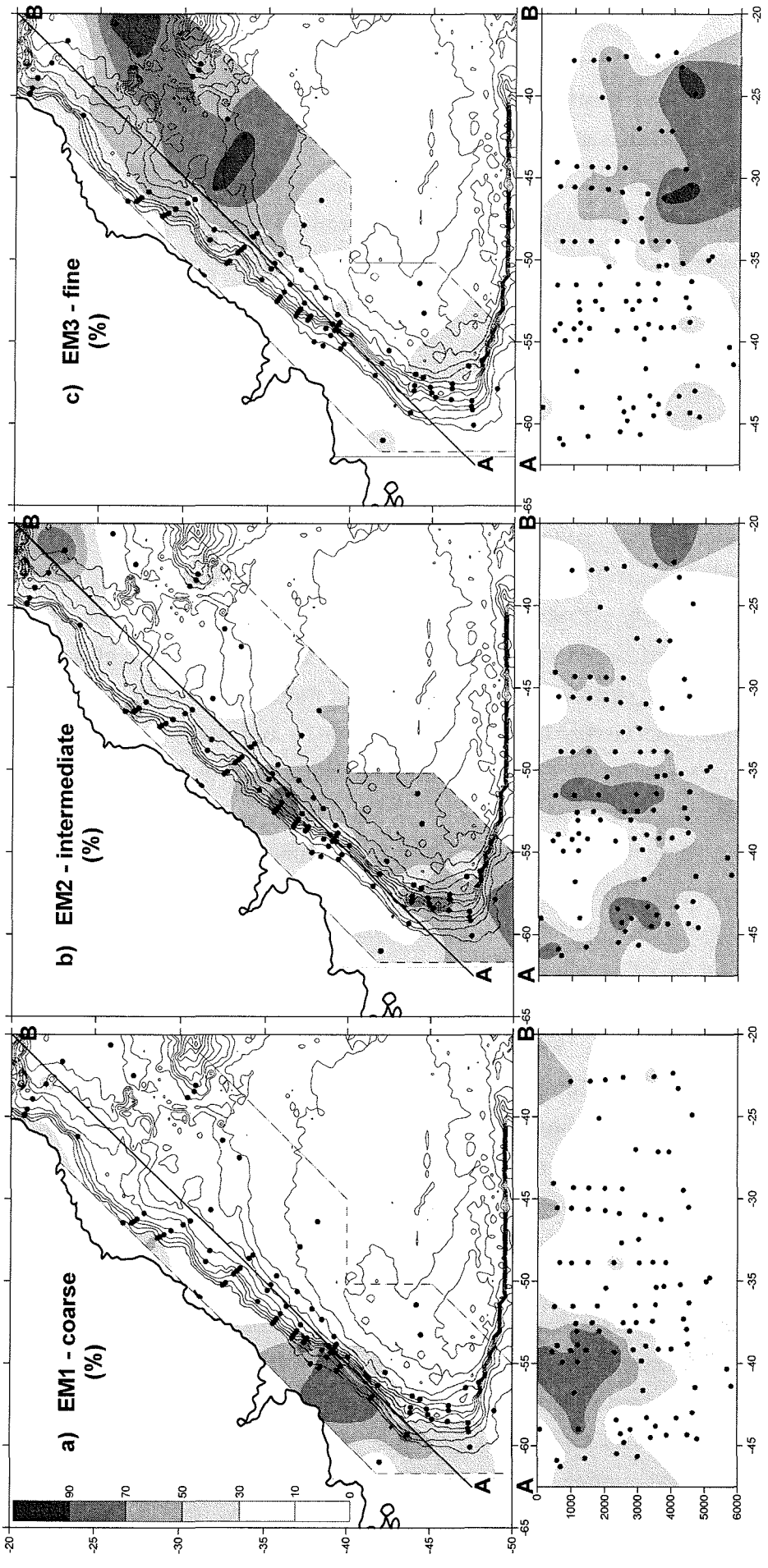
a) EM1 - coarse (%)
b) EM2 - intermediate (%)
c) EM3 - fine (%)
A
B
90
70
50
30
10
0
-20
-25
-30
-35
-40
-45
-50
-55
-60
-65
0
1000
2000
3000
4000
5000
6000

4 Discussion

4.1 Distribution of carbonate and organic carbon as proxies for water masses and main oceanographic features

Apart from the dilution by terrigenous input, the preservation of marine sediment compounds is mainly governed by complex interactions between productivity and the physical and chemical properties of the overlying water mass. The NADW represents a relatively warm and saline water mass, compared to the overlying UCDW and AAIW, and the underlying LCDW and AABW. Most critical for the carbonate preservation is the carbonate-ion saturation level. In the Argentine Basin, the intermediate and deep water masses of southern origin (AAIW, CDW, AABW) display an undersaturation of carbonate ions ($CO_3^{2-} < 90$ µmol kg^{-1}). The NADW, in contrast, is oversaturated with respect to CO_3^{2-} ($CO_3^{2-} > 110$ µmol kg^{-1}, Dittert et al. 1999, Broecker and Peng 1982). Therefore, the dissolution of carbonate is increased in AAIW, CDW and AABW water levels, whereas NADW fosters enhanced carbonate preservation. Following these basic considerations the continuously elevated carbonate contents in surface sediments along the South American continental rise at water depths between 2000 and 4000 m clearly document the flow path of the low corrosive NADW – at least north of the BMC. This is supported by previous studies of Gerhardt and Henrich (2001) and Volbers and Henrich (2002) who used ultrastructures of pteropods and foraminifer tests to trace preservation/dissolution patterns in South Atlantic sediments.

According to the commonly accepted model of recent water mass distribution in the Argentine Basin (e.g. Peterson and Whitworth 1989, Maamaatuaiahutapu et al. 1992, Stramma and England 1999), the NADW travels as a deep western boundary current south as far as 39°S, where it turns away from the continent towards the east. At the continental rise south of the BMC, the NADW is displaced by the upper and lower branch of the CDW (Fig. 1). These modern hydrographic observations are in sharp contrast to the sedimentologic findings. South of the BMC (43-48°S), at a water depth between 2000 and 3500 m, high carbonate contents in the sediments (50-70 %) comparable to those north of the BMC (Fig. 2) are indicative for good carbonate preservation. A considerable decrease in carbonate contents is found only east of 57°W, where the Falkland Escarpment shows an increased steepness, in agreement with the presence of the CDW. The contradiction is based on the contrasting presence of the carbonate undersaturated CDW and good carbonate preservation. The conclusions on the basis of sedimentology are apparent: The NADW extended further south (down to 48°S) during the younger oceanographic history. The disagreement in results of the two scientific disciplines may be caused by the different time windows observed when analysing their specific samples. The set of hydrographic samples comprise the last few decades at the most, i.e. they are snap shots of the most recent oceanographic situation. In contrast to these short-term observations, surface

sediments comprise a mean record over the time represented by the sampled interval, in this case up to several hundred years. Therefore possible variations (production and remote arrival) of northern deep-water flux to the South (Bianchi and McCave 1999) can cause the state of carbonate preservation observed south of the BMC, but is undetectable hydrographically. Consequently, the retroflexion of the CDW occurred already at the Falkland Escarpment near 57°W. From the sedimentological point of view, the whole horizontal band of elevated carbonate contents between 2000 and 3500 m water depth can be related to the presence of NADW along the eastern South American continental margin. The variations of sediment carbonate concentrations within this main NADW flow path, on the other hand, are attributed to different origins. The particularly high carbonate values observed at eastern slope of the VC and shallow sites of VTR relate to a reduced terrigenous supply at exposed and/or distal positions, likely supplemented by good carbonate preservation (Gerhardt and Henrich 2001). Alternatively, reduced carbonate contents off the la Plata mouth may result from two effects, namely terrigenous dilution in response to high river discharges and/or an enhanced supralysoclinal dissolution of carbonate due to high organic-carbon flux rates which are associated with the river-induced high productivity at the Brazil Malvinas Confluence zone. The latter is supported by previous studies that found high nutrient concentrations in surface waters (Benthien and Müller 2000) and sediments (Hensen et al. 2000) off the La Plata.

The presence of hydrogen-enriched organic matter of mixed marine-terrigenous origin at shallow sites in front of the river system and below the BMC, and its general trend to lower contributions in deeper marine settings supports the assumption of an enhanced carbonate dissolution in relation to the remineralisation of settling reactive organic matter. The present data on the origin of sedimentary organic matter from that area, however, are not sufficient to finally rule out a marine or mixed marine-terrigenous source of the reactive organic matter.

The lower boundary of the NADW is the interface to the AABW, which determines the position of the modern calcite lysocline (compare Henrich et al. this volume). According to the carbonate distribution presented here, this boundary is located at about 4000 m water depth in the Argentine Basin and about 200 m deeper in the Brazil Basin. These estimates are in good agreement with Thunell (1982) who reports identical water depths.

Decreasing carbonate contents between 2000 and 1500 m water depth all along the continental margin record the transition from the NADW to the UCDW and AAIW. In the Southwest, three principal processes interact to cause the quasi absence of carbonate along the Argentine continental slope and outer shelf: 1) very low carbonate test production in the cold and turbid surface currents, 2) strong dilution by high terrigenous river discharge, and 3) increased carbonate corrosivity along the outer continental shelf and slope, that are occupied by the UCDW and AAIW.

In the Northeast of the study area, the flow of the UCDW and the AAIW constitutes the western closure of the subtropical gyre, i.e. here the currents flow south-westwards

(Boebel et al. 1997, Stramma and England 1999). In this part the carbonate contents are only depressed at the intermediate water layer (~1500-500 m water depth). This points to the UCDW and the AAIW, although they produce a lower corrosive signal compared to the Southwest. To a certain extent, this is attributed to an advanced alteration of these water masses, after running a complete cycle through the South Atlantic. The main reason for the comparably higher carbonate contents, however, likely relates to Thermocline Water masses, which foster primary production supported by coastal and shelf-break upwelling (Piola et al. 2000). This induces higher carbonate test production that is not completely dissolved by the UCDW and the AAIW. As compared to the Southwest, good preservation and minor terrigenous dilution in the surface water layer, enable higher carbonate contents (compare Gerhardt and Henrich 2001).

The corridor of distinctly elevated organic carbon contents (Fig. 3) marks a narrow zone of preferred deposition of organic matter, which coincides with a key position of upper level (surface and intermediate) circulation: the confluence of the Brazil and the Malvinas Currents in the vicinity of the mouth of Rio la Plata estuary (BMC). The collision of the contrasting MC and BC results in a southward deflection of both currents and a corridor of intense mixing that can affect even the deep water layer (Piola and Matano 2001, Olson et al. 1988, Vivier and Provost 1999). This intense mixing causes an enrichment in nutrients that is also stimulated by a high mean freshwater discharge of the La Plata [14900 $m^3 s^{-1}$ (Milliman and Meade 1983) to 23300 $m^3 s^{-1}$ (Piola et al. 2000)]. The latter carries 7.2 10^{12} g organic carbon annually to the South Atlantic (Depetris and Paolini 1991). These factors result in a high productivity area at the BMC and along its southward extension. The organic matter produced in the BMC drops along its pathway and traces it in the sediments. Therefore, the exact configuration of this specific oceanographic feature is nicely portrayed by the organic-carbon contents of the surface sediments. Even though oceanographers like to define the BMC at 38°S (e.g. Maamaatuaiahutapu et al. 1998, Vivier and Provost 1999, Piola and Matano 2001), the high-C_{org} trace in the sediments has a more North-South alignment at about 52-54°W. This position is in good agreement with oceanographic observations of the MC and BC extensions following the BMC on the shelf (Piola et al. 2000) and over the deep sea (Olson et al. 1988).

The organic-carbon variations observed in the surface sediments northeast and southwest of the BMC corridor provide another tracer for water-mass properties. Below a water depth of 4000 m, the complete dissolution of carbonate leads to a relative enrichment of organic carbon. The preservation of organic carbon in the AABW is supported by low oxidation rates of organic matter due to the low oxygen contents of the AABW.

The core of NADW represented by high carbonate concentrations in the surface sediments at 2000-3500 m water depth in the Northeast is characterised by very low concentrations of organic carbon. These are related to the high oxygen content of the NADW and thus its low preservation potential for organic matter. Elevated contents of organic carbon north of the BMC at 1000-2000 m water depth clearly reflect the presence of the UCDW with its

very low oxygen concentrations. In the upper level in the Northeast, a minor terrigenous dilution and a good carbonate preservation result in a slight decrease in organic carbon. In the Southwest the lack of considerable amounts of organic carbon in the intermediate and upper levels is the result of massive terrigenous dilution as well as of high oxygen concentrations in the formation region of the AAIW (Stramma and England 1999).

4.2 Bulk size composition and its origin

The strong contrasts between southwestern coarse- and northeastern fine-grained deposits, obvious from all parameters related to particle size, are regarded as the product of the combined effects of geological, sedimentological and oceanographic conditions that act on provenance (availability/supply), transport, sorting and accumulation of source components.

Potential source areas for sediments deposited on the eastern South American margin range from the tropics in the North to the subpolar zone in the South. Hence, different weathering regimes act on a large variety of source rocks and soils. Chemical weathering is the most prominent process at low latitudes producing very fine-grained alteration products. In contrast, physical weathering (temperature and frost) becomes increasingly important towards higher latitudes resulting in coarser grained and less chemically altered products.

Physical maps of South America (e.g. GEBCO 1984, chart 5-12) reveal that the central part of the continent is drained by the Rio Paraguay/Rio Paraná system, which is situated in the Paraná Basin that covers a drainage area of 2.83 10^6 km^2. This extensive river system is focussed at the broad river mouth of the Rio de la Plata, which discharges 470 km^3 a^{-1} of freshwater, supplying a sediment load of 92 10^6 t a^{-1} (Milliman and Meade 1983). South of the La Plata mouth other large rivers drain onto the extended Argentinean shelf (e.g. Rio Colorado, Rio Negro, Rio Chubut). In contrast, north of the La Plata mouth the number of rivers draining into the South Atlantic is low and their size is small. According to this general difference in the presence (SW) and absence (NE) of rivers, an overall higher and more variable terrigenous input with a great variety of grain-sizes is expected on the southern shelf.

The Argentine shelf is situated within and beyond the "roaring forties" which are known for their extraordinary high storm potential. During storms, the influence of waves can extend down to a water depth of 200 m (Chamley 1990). Hence, remobilisation processes have a major impact on modern sediments from the continental shelf and slope. Once sediment particles are taken up in suspension, the fine components are likely to be removed and advected downslope or laterally with the Malvinas Current, leaving a coarse residual type of sediment.

Even though we are not able to quantify the contribution of each of these processes, the expected Northeast-Southwest (i.e. fine-coarse) contrast is clearly recognised from the simple sand/silt/clay distribution patterns and their relative proportions (Figs. 4, 5).

4.3 Grain-size composition of the terrigenous silt fraction

The eastern continental margin of South America corresponds to the western boundary of the South Atlantic Ocean. We therefore assume that western boundary currents have a major impact on sedimentary processes. Theoretical considerations on grain-size frequency distribution patterns lead to the assumption that three basic types of current-influenced sediments can be distinguished: 1) low energy depositional (accumulation) sediments, 2) erosional or residual sediments and 3) well-sorted sediments (Michels 2000). According to this model, depositional sediments are characterised by a positive (i.e. fine) skewness due to the lack of coarse grain-size. They occur when current velocities are slowed down enough to allow even fine particles to settle. In contrast, the fine proportion of the residual type sediments is lacking due to the winnowing effect of strong currents. These deposits display a negative (i.e. coarse) skewness. Both accumulation and residual deposits are rather poorly sorted. The third distribution type, which intermediates between the first two, is well-sorted, i.e. it displays a narrow range of grain sizes. Here both, coarse and fine components are absent, due to frequent re-suspension/deposition cycling, which ideally results in a very good sorting and a symmetrical frequency distribution. Hence, for the interpretation of grain-size distributions its symmetry or "shape" matters more than mere "size". On the other hand, size is an indicative parameter to trace energetic regimes and the distance to the source. For example, waves and strong currents leave behind coarser sediments than lower energetic regimes (e.g. McCave et al. 1995; Ledbetter and Ellwood 1980), and the grain size of volcanic ash or atmospheric dust decreases downwind (e.g. Walker 1971, Prins and Weltje 1999).

4.4 Excursion: Some general aspects on the problem of grain-size analyses limited to the silt fraction and characterisation of the EMs

Before discussing the measured grain-size distributions in terms of sedimentary processes, a major problem of analysing the grain sizes of silt has to be addressed: the upper and lower size boundaries of the silt fraction. These artificial borders have a major impact on the character of the silt frequency distributions and hence on the resulting statistical parameters and their interpretation. As demonstrated in Figure 5, the sediments along the South American continental margin show a great variety in general size composition ranging from almost pure sand to almost pure mud. For example, the muddy sediments consist of considerable amounts of clay (30-80 % of bulk sample), besides a major proportion of fine silt. Particularly the carbonate poor sandy sediments on the Argentine shelf and slope (sand > 90 %) contain only a minor proportion of silt (< 10 %) and clay (< 2 %, Fig. 11). These general size relations imply that the terrigenous silt fraction analysed may represent only a minor proportion of the whole size range of the sediment. Hence, conclusions only derived from the TS size frequency distributions and their statistical parameters, may cause misinterpretations of the actual processes governing sediment dispersal and deposition.

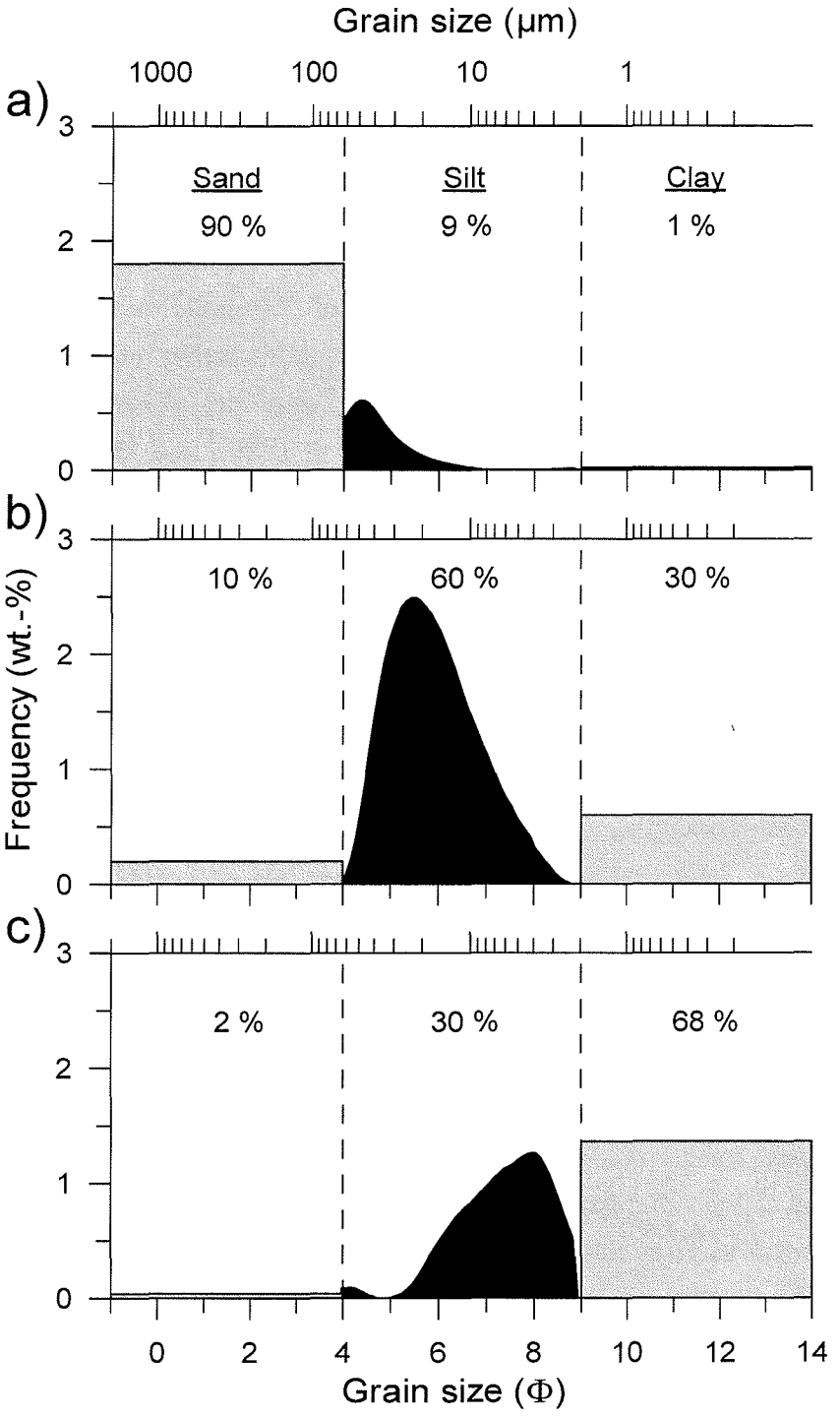

Fig. 11: *Visualisation of the problem of grain-size measurements limited to the silt fraction by means of the three end-member examples (a-c). The terrigenous silt grain-size distributions (black) are rescaled to the relative silt proportion. The sand and clay proportions are divided by 50 size classes and then inserted as one box (grey) because their internal grain-size distribution is unknown. Since the EM examples originate from positions with low carbonate contents (EM1 - Argentine continental slope, EM2 - low-$CaCO_3$/high-C_{org} corridor, EM3 - SW foot of RGR below 4000 m water depth) the sand and clay contents are regarded as terrigenous.* ***a)*** *EM1 represents samples with very high amounts of sand: the silt only is not very representative for such samples, the size cut at the sand border results in a wrongly calculated positive (fine) skewness indicating both, accumulation and winnowing.* ***b)*** *EM2 represents samples with high amounts of silt: interpretation of size distributions are correct, true positive skewness indicates accumulation.* ***c)*** *EM3 represents samples containing high amounts of clay: the fake negative (coarse) skewness suggests that the samples to originate from winnowing processes, however they result from deposition at low current velocities.*

To discuss these potential problems in more detail the end members EM1 and EM3 are used as extreme examples for grain-size distributions in the areas of their preferential occurrence. The coarse EM1 predominantly occurs on the Argentine continental shelf and slope and downslope of the La Plata mouth where the terrigenous sand content exceeds 90 %. In this case any grain size less than 8 μm (~7 Φ) can be neglected [Σ(< 8 μm) < 2 %]. For EM1 the statistical calculations (Table 1) reveal a strong positive (fine) skewness, which is indicative for accumulation processes. On the other hand, very coarse mean and modal grain size and good sorting relate to winnowing by variable albeit strong currents. Considering that these attributes of EM1 are only valid for less than one-tenth of the carbonate-free sediment (Fig. 11a), the rather limited significance of parameters deduced from TS size frequency distributions is obvious. But from the high sand contents we know that the terrigenous bulk spectral mean and modal sizes are actually situated in the sand fraction, i.e. they become even coarser than calculated for TS. The strong positive skewness for TS is attributed to the sharp size cut at 63 μm (4 Φ) that produces a steep slope at the coarse end and therefore a relatively gentle slope towards the fine end of the spectrum. Since the size frequency distribution of the sand fraction is unknown, the question of "true" skewness is open, i.e. it can remain positive or even become negative in the bulk size range. Therefore, EM1 can represent a very coarse accumulation pattern as well as a residual sediment produced due to winnowing and reworking by strong currents. Important evidence allowing to distinguish between theses converse processes represented by EM1 is provided by differences in TS sorting and skewness and by general environmental considerations (current velocities, sediment sources; see also next chapter). At comparable proportions of TS (Figs. 2, 4) and EM1 (Fig. 10a) the TS parameters downslope of the La Plata mouth reveal poorer sorting and even stronger positive skewness compared to alongside the slope further south. Therefore, the sediments downslope of the La Plata are finer grained, making a "true" positive (fine) skewness more reliable. Additionally, the spatial distribution of this pattern as a downslope tongue proximal to the La Plata mouth suggests a direct link to this sediment source. In contrast, the EM1 pattern further south is aligned straight along the Argentine continental slope. The TS from these locations is very well sorted and it can be assumed that the sharp size cut at 63 μm (4 Φ) will be converted into a more gentle slope leaving the slope at the fine end of the size spectrum as the steeper one, i.e. inverting skewness from positive (fake) to negative. That means that here, EM1 experiences a complete reversal in interpretation from a pretended accumulation to an actually erosional deposit. This type of sediment and its rather horizontal distribution is linked to the winnowing processes of relatively strong currents.

In contrast to EM1, for EM3 the size cut at 2 μm (9 Φ) results in a questionable negative (coarse) skewness. Samples with high proportions of EM3 mostly occur below 4000 m water depth (Fig. 10c) where carbonate is almost completely absent (Fig. 2) and the sand

contents can be neglected (Fig. 5a). These sediments display silt/clay ratios which are at about 30/70 (Fig. 5b, c). In these cases it can be assumed that the 70 % clay thin out towards the fine end to reverse the fake negative (coarse) skewness to a positive (fine) one and therefore, reveal an accumulation type of sediment. Additionally, the generally fine grain size of these sediments suggests a low energetic deposition rather than current sorting or even winnowing.

In contrast to the two other complementary end-members, in areas of its frequent occurrence EM2 represents a high proportion of the complete size spectrum (Fig. 11b) exceeding 60 % of the carbonate-free sample. Therefore, its character can be derived directly from its frequency distribution in the silt-size spectrum. According to its positive (fine) skewed distribution we infer accumulation as the main sedimentation process. In contrast to EM3, the relative coarse grain size indicates a higher energetic regime within the seawater suspensions from where the particles settle.

In summary: all three end members indicate sediment accumulation attributed to different energetic regimes or proximity to source, except EM1, which can indicate residual sediments as well.

4.5 Spatial distribution of end-member proportions complemented by parameter distribution – the relation to sedimentary processes

4.5.1 EM1 – very coarse, accumulation and/or residual deposit

In the Northeast only few locations along the shelf break and slope off southern Brazil show considerable proportions of the coarse EM1 (> 50 %). The two other EMs at these positions provide about 25 % each. The relative high proportion of EM1 in this area is related to current sorting (winnowing) under the influence of the Brazil Current. The resulting relative coarse composition is supplemented by the relative proximity to the rare terrestrial sources due to a narrow shelf, which enables a distinct contribution of accumulative EM1 and EM2. However, compared to the Southwest, the winnowing signal is rather weak indicating the BC to be less strong than its southern counterpart. Current measurements revealed mean speeds of 10-20 cm s^{-1} close to the slope in the intermediate water level (Boebel et al. 1999, Hogg et al. 1999). This velocity range is apparently sufficient to produce a winnowing pattern, since the clay contents (< 30 %) and therefore the cohesive behaviour of these sediments is reduced.

Even though variations are subtle, slightly elevated proportions of EM1 occur along a transect at about 34°S between 2000 and 3000 m water depth and at the lower part of the next northern transect at about 3000 m water depth (Fig. 10a). This pattern is likely to be caused by the flow of the NADW, which is focused at two topographic ledges, whereas samples from other water depths of these transects and the same water depths of neighbouring transects lack this feature. There, the samples are situated at topographic

inlets where current speeds drop again at lee sides. Elevated sand contents, and the resulting fake fine skewness (see above) at these sites support these assumptions.
In the Southwest, there are two major axes of high EM1 concentrations (> 70 %), one along the continental slope and outer shelf, and one downslope off the La Plata mouth. The continental slope axis is clearly related to the strong Malvinas Current, leaving a residual type of sediment. Contourites have been detected in this area by means of parasound patterns (Segl et al. 1994, Bleil et al. 2001) confirming our conclusions. The downslope axis shows a weakening trend towards the South but an abrupt break to the east. Notably, this La Plata tongue is situated west of the low-$CaCO_3$/high-C_{org}/EM2 corridor (see below). It is assumed that the coarse La Plata tongue is superimposed by this adjacent EM2 corridor and therefore capped in the east to finally display an oblique downslope orientation. The equally high proportions of EM1 in the axes alongside the slope and downslope are divided into 1) residual sediments left by winnowing of vigorous MC (contourite) and 2) direct sandy la Plata discharge prograding downslope mainly as bed load, by differences in TS skewness and sorting (see above). Additionally, oceanographic current velocity data (Boebel et al. 1999, Peterson 1992, Maamaatuaiahutapu et al. 1998, Weatherly 1993 and Vivier and Provost 1999) reveal high near-bottom current speeds of > 30 cm s^{-1} for the MC along the continental slope (800-1500 m water depth) which drop to < 5 cm s^{-1} directly off the la Plata mouth. The low current velocity off the La Plata is continued downslope towards the deep sea allowing finer-grained sediment particles to settle. This increases an admixture of fine grain sizes and consequently results in the observed poorer sorting of the sediments downslope of the La Plata mouth.

4.5.2 EM3 – very fine, accumulation deposits

To emphasise the contrast to the other two end members we continue with the discussion of the fine EM3. Wide areas of the northeastern part are covered with sediments containing proportions of EM3 above 50 %. There are two areas where this EM3 signature occurs as a quasi-single feature (both other EMs < 5 %), these are situated at the deeper parts of the southern Rio Grande Rise (RGR) and in the southern Brazil Basin. The southern part of the RGR, below 4000 m water depth is situated where the AABW flows north-eastwards. Since the RGR represents a natural obstacle for the AABW, this results in a stowage effect that causes the current velocity to drop considerably, upon which even the finest sediment load is released.
After the jet passage of the Vema Channel (VC, no data, but compare e.g. Ledbetter 1984) the AABW enters the southern Brazil Basin where there is plenty lateral space to spread. This again results in a rapid drop of current speed and release of fine load picked up further south. Low TS mean and modal grain sizes, as well as the (fake) negative skewness and poor sorting of about 1 for both EM3 reference areas support this assumption.
Another area of high proportions of EM3 occurs on the eastern slope of the VC at water depths between 3000 and 4000 m. Therefore, relatively low current velocities of the

NADW are suggested to prevail at this site. This assumption is explained by the position at the eastern flank of the VC where minor current focussing occurs. Additionally, lower primary velocities are assumed for the NADW offshore compared to surface currents and the AABW in the deepest parts of the VC (Ledbetter 1984).
Other high EM3 contributions in the Northeast are found at downslope transects that are situated within or across topographic inlets. They represent the leeward side of current focussing ledges, and are therefore places of accumulation as indicated by a negative (fake) skewness. The WOCE current metre velocities (Hogg et al. 1999) within one inlet at 2000 to 4000 m water depth (100 m above seafloor) revealed velocities of 6-7 cm s^{-1}, which is obviously low enough to allow fine grain sizes to settle, taking into account an even lower near-bottom speed and assuming a decreasing current profile towards the bottom.
In the Southwest, there is only one area with a considerable concentration of the fine EM3 (30-50 %). This is in the deepest southwestern most part of the Argentine Basin in the domain of the AABW (> 4000 m water depth). Here the AABW flows along the Falkland Escarpment from the east and collides with the lower continental rise before it turns northeastwards. Similar to the southern RGR, the rise represents an obstacle, causing obstruction, drop of flow velocity, and finally the settling of suspended matter. Complicating this view, intermediate amounts of EM2 (30-60 %) are also observed here, causing a symmetric to slight positive skewness and very poor sorting altogether.

4.5.3 EM2 – intermediate, coarse accumulation deposits

EM2 reveals medium proportions in a large part of the study area (Fig. 10b). One area of highest EM2 concentrations is congruent to the low-$CaCO_3$/high-C_{org} corridor. The coincidence of organic carbon and EM2 reveals that both, organic matter and terrigenous medium to coarse silt have settled together along this corridor. The organic matter originates from the La Plata river input and marine high production along the BMC mixing zone. First estimates based on optical investigation (maceral analysis) suggest a dominance of the marine organic fraction, although with considerable contribution (about 40-50 %) from non-woody angiosperm terrigenous plant tissue. The supply of both oxidised and non-oxidised terrigenous organic matter (inertinite, vitrinite) presumably indicates erosion and subsequent riverine transport of differentially altered plant matter, either from peat deposits along the adjacent lowlands of the La Plata and/or from fossil, C_{org}-bearing strata in the hinterland (Wagner et al., this volume).
Our data suggest that the Malvinas Current on the shelf flowing north-eastwards picks up the suspended river discharge from the La Plata containing amounts of terrigenous detritic constituents and terrigenous organic material. Immediately after the passage across the river mouth the MC collides with the BC to form the BMC. The MC including its suspension load is deflected to the South, building the MC Return Flow that is intensely mixed with the thermocline water of the BC. Downstream, the velocity and energy regimes decrease due to the increasing water depth, which allows the particles of the suspension to

settle, starting with the coarse proportion (coarse silt). Scavenging of autochthonous marine organic matter (settling of algae blooms) might support this hemipelagic mechanism and include finer particle sizes.

The location of the low-$CaCO_3$/high-C_{org}/EM2 corridor between 52 and 54°W coincides almost exactly with the recent modal positions of the extension of the Brazil (53.5°W) and Malvinas Currents (54.5°W) of Olson et al. (1988). The subtropical and subantarctic fronts, respectively, are situated east and west of these extensions. The high energetic mixing zone of the BMC extension occupies the space in between. The slight shift of the position of the BMC (about 1° towards the east) is attributed to differences in spatial and temporal resolution between oceanographical and sedimentological methods. As discussed before, oceanographic studies display high spatial but low temporal resolution, i.e. they are snapshots of the modern situation. Surface sediments, in contrast, may have a lower spatial resolution but represent mean values of corresponding parameters over a longer period of time (decadal to centurial timescales). The sedimentologically traced BMC therefore, represents the mean position of a highly variable oceanographic feature that shifts to the Northeast in winter and to the Southwest in summer. South of 40°S the organic carbon corridor is below the detection limit of the surrounding background of C_{org} = 0.5-1 %. This indicates that the highest proportion of organic matter introduced by the La Plata, or produced at the confluence, has been deposited.

The second area of high EM2 concentration extends North-South at an intermediate water depth (2000-4000 m) along the southwestern rim of the Argentine Basin. A combination of processes is suggested to be responsible, i.e. 1) drop of sediment load eroded from the Falkland Plateau within the MC, 2) drop of load picked up by NADW from downslope processes and/or 3) graded succession from erosion (EM1, slope) via coarse accumulation (EM2, upper rise) to fine accumulation (EM3, lower rise/abyss) according to decreasing current velocity.

Data of Peterson (1992) and Boebel et al. (1999) indicate high near-bottom speeds (> 30 cm s^{-1}) of the MC along the continental slope off southern Argentina that is strong enough to cause erosion on and along the Falkland Plateau. When flowing north/northeast, the MC faces deeper waters and therefore slows down to release the coarsest load first. Due to the similarity to the EM2 corridor at the BMC, we favour coarse silt deposition from the MC to be the important mechanism to produce this pattern that is supplemented by the downslope decreasing sediment grain size.

In the previous paragraphs we have discussed characteristic examples of end-member occurrence and accompanying parameters in terms of sedimentation processes. South of the VTR a downslope transect of samples shows no apparent affinity to sorting processes. Grain-size related parameters as well as the distribution of end-member proportions show an irregular pattern. According to studies of Mello et al. (1992) this transect is situated across a system of turbidite channels that feed the Columbia and Carioca Channels in the

deep sea. The observed irregularity of the distribution pattern of the sediment grain-size properties, therefore, is strongly attributed to mixing with turbidites.

5 Summary and Conclusions

This study presents a synthesis of the results of geochemical ($CaCO_3$ and C_{org}) and grain-size investigations (sand/silt/clay proportions and terrigenous silt grain-size distributions) on a set of surface sediment samples from the western South Atlantic that covers the South American continental margin from 20 to 50°S, and from the outer shelf to abyssal water depths. Bulk geochemical and grain-size distribution patterns reveal a multifarious composition of the sediments along the eastern South American continental margin. These patterns are primarily attributable to differences in climatic conditions (weathering), geographic settings (presence of rivers) and marine production, and are secondary strongly modified by the modern ocean circulation.

The bulk geochemical parameters mainly serve as tracers for water masses. Over the mean of time represented by the surface sediment samples (100s of years?), elevated carbonate contents between 2000 and 4000 m water depth prove NADW in this level down to 48°S before it leaves the continental margin. The almost complete absence of carbonate in sediments from below 4000 m water depth in the Argentine Basin and below 4200 m water depth in the southern Brazil Basin indicates the position of the NADW/AABW interface that simultaneously marks the modern calcite lysocline in these areas. Weaker differences in carbonate and organic carbon contents enable us to distinguish Subantarctic/ Thermocline Waters, AAIW and UCDW .

In general, the grain-size investigations reveal sharp contrasts between northeastern fine-grained and southwestern coarse-grained sediments. The transition between both modes is situated at about 53°W. Sediment accumulation occurs in three different manifestations which are proven with the three end members from the application of an end-member algorithm to the terrigenous silt grain-size distributions. The coarsest depositional pattern is observed in front of the mouth of the Rio de la Plata. This direct river discharge is traced as a straight downslope tongue of moderately sorted sandy terrigenous sediments down to 4000 m water depth (EM1).

Deposition of mainly silty sediments (EM2) occurs along a corridor striking North-South between 52 and 54°W, in combination with high accumulation rates of organic carbon and low accumulation rates of carbonate. We propose the following model for the hemipelagic sedimentation within this corridor: 1) incorporation of suspended Rio de la Plata discharges (mainly silt and clay sized terrigenous detritus and organic matter) by the MC in front of the La Plata mouth, 2) distribution of the suspended matter along the pathway of the MC that collides with the BC at the BMC and experiences intense mixing along the BMC extension to the South, 3) decrease in energy regime along the BMC extension due to increasing water depth and release of the suspended matter starting with the coarsest material (coarse silt). As a result the low-$CaCO_3$/high-C_{org}/EM2 corridor is the direct

sedimentological imprint of the prominent oceanographic feature of the BMC and its southward extension.

Accumulation of fine-grained sediments (EM3) occurs at the southwestern Rio Grande Rise, at the southwestern most rim of the Argentine Basin and in the southern Brazil Basin, all in the AABW domain. The deposition of silty clay at these locations is attributed to a decrease in current velocity of the AABW in the course of stowage effects at bathymetric obstacles (RGR, lower Argentine continental rise) or due to re-spreading of this water mass following the jet passage of the Vema Channel (southern Brazil Basin).

The sediments along the Argentine continental outer shelf and slope reveal a similar coarse size composition compared to that of the sandy downslope tongue off the La Plata mouth (high sand contents, high proportions of EM1). In contrast to the La Plata tongue, however, the Argentine slope sediments show a less strong fine (fake) skewness and an extremely good sorting. From these differences a strong winnowing effect of the MC with its high near-bottom current velocities is inferred to be responsible for the contourite sediments at the Argentine outer shelf and slope. In this case the end-member modelling and sedimentological considerations revealed one EM (here EM1) to indicate two different deposits: contourites (winnowing) and continuous bed load sediments (downslope accumulation).

South of VTR a sample transect crosses a system of turbidity channels, clearly documented by a completely unordered shallow-deep sedimentological sequence. As the conclusions from sedimentological data are in good agreement with oceanographic observations, except for this transect south of VTR, we assume that downslope mass wasting processes have a minor impact on sediment grain-size composition of surface sediments.

Methodically, this study tackled two basic aspects: We have demonstrated that the combination of bulk geochemical data and grain-size properties of surface sediments, unmixed with an end-member algorithm forms a powerful tool to reconstruct oceanographic conditions along a time slice. The use of discrete size fractions (i.e. separation of sand and/or clay) will affect the results concerning grain-size frequency distributions. It is recommended to have a look beyond these size limits in order to reveal the proper characteristics of a deposit and hence, to deduce appropriate interpretation.

Acknowledgements

We thank the members of the shipboard and scientific crews of the RV METEOR. G. J. Weltje kindly provided the end-member algorithm applet. M. Klann is acknowledged for carrying out the opal measurements. We like to thank M. A. Prins and an anonymous reviewer whose critical remarks improved the manuscript. This research was funded by the Deutsche Forschungsgemeinschaft (Sonderforschungsbereich 261 at the University of Bremen). This is SFB contribution no. 352. All data presented in this publication are archived in the PANGAEA database at www.pangaea.de (search string: FrenzM).

6 References

Arhan M, Heywood KJ, King BA (1999) The deep waters from the Southern Ocean at the entry to the Argentine Basin. Deep Sea Res II 46:475-499

Benthien A, Müller PJ (2000) Anomalously low alkenone temperatures caused by lateral particle and sediment transport in the Malvinas Current region, western Argentine Basin. Deep Sea Res I 47:2369-2393

Bianchi GG, McCave IN (1999) Holocene periodicity in North Atlantic climate and deep-ocean flow south of Iceland. Nature 397:515-517

Bianchi GG, McCave IN (2000) Hydrography and sedimentation under the deep western boundary current on Björn and Gardar Drifts, Iceland Basin. Mar Geol 165: 137-169

Bianchi GG, Vautravers M, Shackleton NJ (2001) Deep flow variability under apparently stable North Atlantic Deep Water production during the last interglacial of the subtropical NW Atlantic. Paleoceanogr 16 (3):306-316

Bleil U, cruise participants (2001) Report and preliminary results of Meteor-cruise M46/3. Berichte aus dem Fachbereich Geowissenschaften der Universität Bremen 172: 161pp, Bremen.Boebel O, Schmid C, Zenk W (1997) Flow and recirculation of Antarctic Intermediate Water across the Rio Grande Rise. J Geophys Res 102 (C9):20967-20986

Boebel O, Schmid C, Zenk W (1999) Kinematic elements of Antarctic Intermediate Water in the western South Atlantic. Deep Sea Res II 46:355-392

Broecker WS, Peng TH (1982) Tracers in the sea. Lamont Doherty Geol Obs Publ. Columbia University, New York, 690pp.

Chamley H (1990): Sedimentology. Springer, Berlin, 628pp.

Depetris PJ, Paolini JE (1991) Beiogeochemical aspects of South American rivers: the Parana and the Orinoco. In: Degens ET, Kempe S, Richey JE (eds) Biogeochemistry of major world rivers. Wiley, Chichester, pp 323-348

Dittert N, Baumann KH, Bickert T, Henrich R, Huber R, Kinkel H, Meggers H (1999) Carbonate dissolution in the deep-sea: Methods, quantification and paleoceanographic application. In Fischer G, Wefer G (eds.) Use of proxies in paleoceanography: Examples from the South Atlantic. Pp 255-284, Springer, Berlin Heidelberg

Flood RD, Shor AN (1988) Mud waves in the Argentine Basin and their relationship to regional bottom circulation patterns. Deep Sea Res A 35 (6):943-971

GEBCO (1984) General bathymetric chart of the Oceans. Department of Fisheries and Oceans, Ottawa, Canada

Gerhardt S, Henrich R (2001) Shell preservation of Limacina inflata (pteropoda) in surface sediments from the Central and South Atlantic Ocean: a new proxy to determine the aragonite saturation state of water masses. Deep Sea Res I 48:2051-2071

Gröger M, Henrich H (2002) Deep-water circulation during the Pleistocene (0.8-0.25 Ma): inferences from near-bottom-current flow variability and deep-water chemistry in the western equatorial atlantic. Submitted to Paleoceanography

Gordon AL (1986) Interocean exchange of thermocline water. J Geophys Res 91 (C4):5037:5046

Gordon AL and Greengrove C (1986) Geostrophic circulation of the Brazil-Falkland Confluence. Deep Sea Res. 36:359-384

Haese RR, Schramm J, Rutgers van der Loeff MM, Schulz HD (2000) A comparative study of iron and manganese diagenesis in continental slope and deep sea basin sediments off Uruguay (SW Atlantic). Int. J Earth Sci 88:619-629

Hensen C, Zabel M, Schulz H (2000) A comparison of benthic nutrient fluxes from deep-sea sediments off Namibia and Argentina. Deep Sea Res II 47:2029-2050

Höppner R, Henrich R (1997): Kornsortierungsprozesse am Argentinschen Kontinentalhang anhand von Siltkorn-Analysen. Zentralblatt Geol Pal I 7-9:897-905

Hogg N, Siedler G, Zenk W (1999) Circulation and variability at the southern boundary of the Brazil Basin. J Phys Oce 29:145-157

Krumbein WC (1936) Application of logarithmic moments to size frequency distributions of sediments. J Sed Pet 6:35-47

Larqué L, Maamaatuaiahutapu K, Garçon V (1997) On the intermediate and deep water flows in the South Atlantic Ocean. J Geophys Res 102 (C6):12425-12440

Ledbetter MT (1984) Bottom-current speed in the Vema Channel recorded by particle size of sediment fine-fraction. Mar Geol 58 (1/2):137-149

Ledbetter MT (1986) Bottom-current pathways in the Argentine Basin revealed by mean particle size. Nature 321:423-425

Ledbetter MT, Ellwood BB (1980) Spatial and temporal changes in bottom water velocity and direction from analysis of particle size and alignment in deep-sea sediment. Mar Geol 38 (1/3):245-261

Maamaatuaiahutapu K, Garcon VC, Provost C, Boulahdid M, Osiroff AP (1992) Brazil-Malvinas Confluence: water mass composition. J Geophys Res 97 (C6):9493-9505

Maamaatuaiahutapu K, Garçon VC, Provost C, Mercier H (1998) Transports of the Brazil and Malvinas Currents at their confluence. J Mar Res 56:417-438

McCave IN, Manighetti B, Beveridge NAS (1995) Circulation in the glacial North Atlantic inferred from grain-size measurements. Nature 374:149-152

Mello GA, Flood RD, Orsi TH, Lowrie A (1992) Southern Brazil Basin: Sedimentary processes and features and implications for continental-rise evolution. In: Poag CW, de Graciansky PC (eds) Geologic evolution of Atlantic continental rises. Van Nostrand Reinhold, New York, pp 189-213

Mémery L, Arhan M, Alvarez-Salgado XA, Messias M-J, Mercier H, Castro CG, Rios AF (2000) The water masses along the western boundary of the south and equatorial Atlantic. Prog in Oce 47:69-98

Michaelovitch de Mahiques M, Almeida da Silveira IC, de Mello e Sousa SH, Rodrigues M (2002) Post-LGM sedimentation on the outer shelf-upper slope of the northernmost part of the São Paulo Bight, southeastern Brazil. Mar Geol 181 (4):387-400

Michels KH (2000) Inferring maximum current velocities in the Norwegian-Greenland Sea from settling-velocity measurements of sediment surface samples: methods, application, and results. J Sed Res 70 (5):1036-1050

Milliman JD, Meade RH (1983) World-delivery of river sediment to the oceans. J Geol 91:1-21

Mollenhauer G, Jennerjahn T, Müller PJ, Schneider RR, Wefer G (submitted) Spatial distribution and accumulation of organic carbon in the South Atlantic Ocean: Its modern and glacial contribution to the carbon cycle. submitted to Global and Planetary Change

Olson DB, Podestá GP, Evans RH, Brown OB (1988) Temporal variations in the separation of Brazil and Malvinas Currents. Deep Sea Res A 35 (12):1971-1990

Peterson RG (1992) The boundary currents in the western Argentine Basin. Deep Sea Res 39 (3/4) 623-644

Peterson RG, Whitworth III T (1989): The subantarctic and polar fronts in relation to deep

water masses through the southwestern Atlantic. J Geophys Res 94:10817-10838
Piola AR, Campos EJD, Möller OO Jr, Charo M, Martinez C (2000) Subtropical shelf front off eastern South America. J Geophys Res 105 (C3):6565-6578
Piola AR, Matano RP (2001): Brazil and Falklands (Malvinas) Currents. In: Steele JH, Thorpe SA, Turekian KK (eds): Encyclopedia of Ocean Sciences. Academic Press, San Diego, pp 340-349
Prins MA, Bouwer LM, Beets CJ, Troelstra SR, Weltje GJ, Kruk RW, Kuijpers A, Vroon PZ. (2002) Ocean circulation and iceberg discharge in the glacial North Atlantic: inferences from unmixing of sediment size distribution. Geology 30: 555-558
Prins MA, Postma G, Weltje GJ (2000) Controls on terrigenous sediment supply to the Arabian Sea during the late Quaternary: the Makran continental slope. Mar Geol 169:351-371
Prins MA, Troelstra SR, Kruk RW, Borg van der K, Jong de AJ, Weltje GJ (2001) The Late Quaternary sediment record from Reykjanes Ridge, North Atlantic. Radiocarbon 43: 939-947
Prins M, Weltje G (1999): End-member modelling of siliciclastic grain-size distributions: The late Quaternary record of eolian and fluvial sediment supply to the Arabian Sea and its paleoclimatic significance. SEPM Spec Publ 62:91-111
Romero O, Hensen C (2002) Oceanographic control of biogenic opal and diatoms in surface sediments of the Southwestern Atlantic. Mar Geol 186 (3-4):263-280
Segl M, cruise participants (1994) Report and preliminary results of Meteor-cruise M29/1. Berichte aus dem Fachbereich Geowissenschaften der Universität Bremen 58: 94pp, Bremen.
Stramma L, England M (1999) On the water masses and mean circulation of the South Atlantic Ocean. J Geophys Res 104 (C9):20863-20883
Stommel H (1958) The abyssal circulation. Deep Sea Res 5:80-82
Stuut JB, Prins MA, Schneider RR, Weltje GJ, Jansen JHF, Postma G. (2002) A 300 kyr record of aridity and wind strength in southwestern Africa: inferences from grain-size distributions of sediments on Walvis Ridge, SE Atlantic. Mar Geol 180:221-233
Thunell RC (1982) Carbonate dissolution and abyssal hydrography in the Atlantic Ocean. Mar Geol 47:165-180
Van Dam JA, Weltje GJ (1999) Reconstruction of the Late Miocene climate of Spain using rodent palaeocommunity successions: an application of end-member modelling. Palaeogeogr Palaeoclimat Palaeoeco 151: 267-305
Vivier F, Provost C (1999) Direct velocity measurements in the Malvinas Current. J Geophys Res 104 (C9):21083-21103
Volbers A, Henrich R (2002) Present water mass calcium carbonate corrosiveness in the eastern South Atlantic inferred from ultrastructural breakdown of Globigerina bulloides in surface sediments. Mar Geol 186 (3-4):471-486
Walker GPL (1971) Grain-size characteristics of pyroclastic deposits. J Geol 79:696-741
Weatherly GL (1993) On deep-current and hydrographic observations from a mudwave region and elsewhere in the Argentine Basin. Deep Sea Res II 40 (4/5):939-961
Weltje G (1997) End-member modelling of compositional data: Numerical-statistical algorithms for solving the explicit mixing problem. J Mat Geol 29:503-549

QUANTIFICATION OF FORAMINIFER AND COCCOLITH CARBONATE IN SOUTH ATLANTIC SURFACE SEDIMENTS BY MEANS OF CARBONATE GRAIN-SIZE DISTRIBUTIONS

M. Frenz*, K.-H. Baumann, B. Boeckel, R. Höppner and R. Henrich

FB Geowissenschaften, Universität Bremen, Postfach 330440, D-28334 Bremen, Germany

** corresponding author, e-mail: mfrenz@uni-bremen.de*

Abstract

Surface sediments from the Mid-Atlantic Ridge of the South Atlantic were investigated with respect to the carbonate grain-size composition. Upon a separation into sand, silt and clay sub-fractions the silt grain-size distribution was measured using a SediGraph 5100. By means of SEM observations of the sub-fractions the results indicate that carbonate particles with equivalent spherical diameters larger than 8 μm mainly consist of planktic foraminifers and their fragments. Calcareous particles smaller than this are coccoliths and occasionally dinoflagellate cysts. On the basis of this division the regional variation of the contribution of foraminifers and coccoliths to the carbonate budget of the sediments are calculated. The carbonate silt (CS) grain-size distributions < 8 μm revealed three outstanding provinces with characteristic coccolith assemblages independent from water depth. In contrast, the coarse CS decreases with increasing water depth, indicating a higher susceptibility to carbonate dissolution of foraminifers relative to coccoliths. The coccoliths present in the silt fraction are predominantly large species (> 4 μm). By means of Gaussian distributions the fine CS was unravelled into species including simple and complex composed coccolith assemblages.

Keywords: South Atlantic, surface sediments, calcareous ooze, silt grain size, coccoliths, foraminifers

1 Introduction

Biogenic calcium carbonate is one of the important components of deep-sea sediments. About 55 % of the sea floor is covered by carbonate-rich sediments (Milliman, 1993). Three factors control the carbonate sedimentation: primary carbonate production, dilution by terrigenous or opaline compounds and carbonate dissolution. The sedimentary record serves as an archive summarising the results of these interfering processes with the uppermost part of the sediment column (core top) having a close connection to the modern situation (calibration).

submitted to Journal of Sedimentary Research

A number of organisms contribute to the bulk carbonate budget in marine sediments. In pelagic open-ocean conditions this number is reduced to coccolithophores and planktic foraminifers, with minor contributions of pteropods, calcareous dinoflagellate cysts and benthic foraminifers. Several efforts have been made to separate and quantify the respective contribution of foraminifers and coccoliths and/or use the separates for further investigations. However, in all these studies the approximations were deduced only from distinct sieve size fractions that vary from 200 to 25 µm. Investigations of the faunal assemblages usually focus on very coarse fractions varying between > 200 µm (Beiersdorf et al., 1995), > 150 µm (Pflaumann et al., 1996), > 125 µm (Henderiks et al., 2002) and > 100 µm (Peeters et al., 1999; Conan and Brummer, 2000; Conan et al., 2002). The bulk foraminifer carbonate, as an approximation is usually based on the sand fraction (Henrich et al., 1989; Henrich et al., 1995; Bickert and Wefer, 1996; Henrich, 1998; Giraudeau et al., 2000; Baumann et al., in press). Knowing to miss an unknown amount of juvenile foraminifers and foraminifer fragments the foraminifera limit moved to smaller sizes of > 32 µm (van Kreveld et al., 1996; Ziveri et al., 2000) and > 25 µm (Divakar Naidu and Malmgren, 1999). Similarly, coccolith carbonate estimates are based on the size fractions < 63 µm (Henrich et al., 1989; Henrich et al., 1995; Henrich, 1998; Ennyu et al., 2002; Baumann et al., in press), < 38 µm (Paull and Thierstein, 1987; Paull et al., 1988; Haidar et al., 2000; Henderiks et al., 2002), < 32 µm (van Kreveld et al., 1996; Broerse et al., 2000a; Broerse et al., 2000b; Broerse et al., 2000c; Ziveri et al., 2000; Stoll and Ziveri, 2002) down to < 25 µm (Divakar Naidu and Malmgren, 1999).

In general, the above mentioned approaches to quantify genetically different carbonate portions are rather surprising since already Robinson and McCave (1994) and McCave et al. (1995) delivered very precise results based on grain-size investigations – thematically very close to the present study. Theses authors investigated Pleistocene drift sediments in the northeast Atlantic and they found prominent minima in the silt grain-size distributions of both, the terrigenous and the biogenic (calcareous) share at about 8-10 µm. Their findings for the terrigenous fraction resulted in the concept of "sortable silt" (McCave et al., 1995). Additionally, together with microscopic observations (smear slides) the mentioned authors attributed the coarse silt of the calcareous fraction to foraminifer fragments and the fine silt and clay to coccoliths.

However, relative variations in the carbonate content of distinct size fractions may reflect spatial and temporal changes in primary production, dilution or dissolution. The question arises what the size fractions actually represent then, and to what account over-, underestimations or contaminations by other carbonate compounds have to be considered. As we will show, the estimations for the carbonate contribution described above can be optimised at least for calcareous zoo- and phytoplankton in pelagic sediments by means of silt grain-size distributions.

Besides the differentiation of bulk foraminifer and coccolith carbonate the contribution of different species to the carbonate budget is of interest. For foraminifers Michels (2000) has

shown that it is possible to distinguish even single foraminifer species from grain-size spectra using a sedimentation balance. Because the size window used in the present study (silt = 63-2 μm) hardly comprises whole adult foraminifer tests we focus on the coccolith share to detect single species and, if possible, to quantify it analogue to Michels (2000). Hitherto, the coccolith composition of a given sample usually base on the number of individuals. Thereby, large and small individuals are traded equally, which does not display the carbonate contribution of the species involved. Young and Ziveri (2000) suggested to quantify species via volume estimates of coccoliths based on biometrical studies. The same authors admit that errors of up to 50 % for the resulting weight occur. Applying these volume estimates to trap samples the sum of all coccolith and calcareous dinoflagellate species amounted to 55 % of the calcareous < 32 μm fraction only (Broerse et al., 2000c), which is an expression of the contamination by larger calcareous particles. In a further step Stoll and Ziveri (2002) tried to separate, or at least enrich, single coccolith species with a settling technique to use the separates for isotope studies. In the present study following Michels (2000) the calcareous silt (CS) grain-size spectra are used to identify single peaks and attribute them to individual species by means of countings and biometrical measurements. We will show that in some cases it is possible to quantify the carbonate contribution of these species. Our results provide useful evidence where and how to separate samples with the goal to enrich species for further investigations. In addition, the achieved accuracy in the differentiation of the weight-balanced contribution of calcareous phyto- and zooplankton carbonate enables reliable paleo-flux calculations that have been demanded by climate modellers for a long time.

2 Methods

This study relies on the grain-size investigations of 72 surface sediment samples from the Mid-Atlantic Ridge (MAR) in the South Atlantic. The samples were recovered during 9 different cruises of the RV METEOR between 1988 and 2000 using multi- and box-corers. The sample distribution covers the MAR from the equator to about 45°S and the ridge crest and flanks towards the Angola, Brazil and Argentine Basins (0-25°W, Fig. 1).

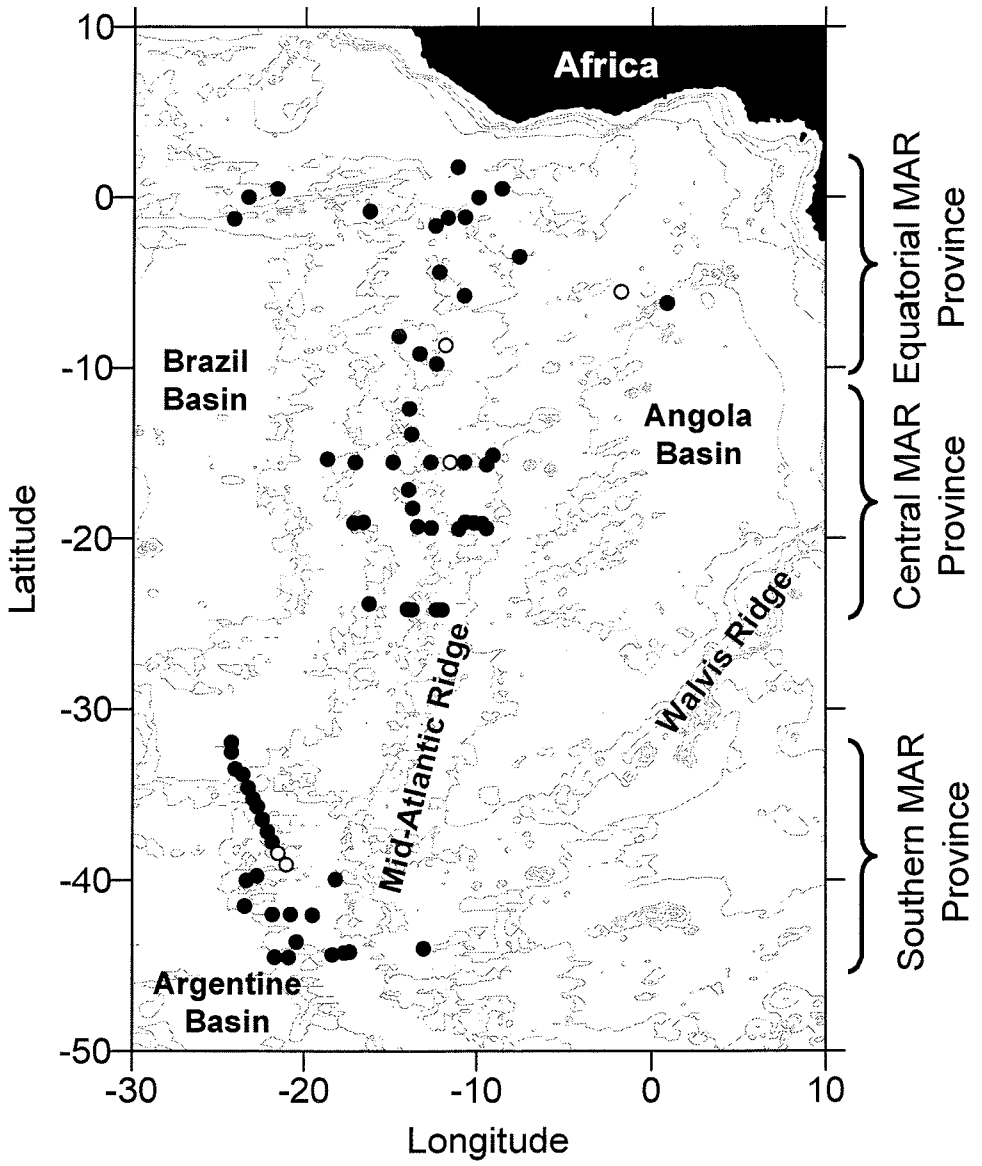

Fig. 1: Bathymetric map of the South Atlantic showing the sample distribution and their regional arrangement into the Equatorial, Central and Southern provinces. The open symbols indicate samples that were used for SEM investigations. Isopleths are 0 m and multiples of 1000 m.

2.1 Grain-size analyses

The freeze-dried samples (0-1 cm bsf, net weight 6 to 54 g) were first wet-split into coarse (i.e. sand, > 63 µm) and fine (< 63 µm) fractions using a 63 µm sieve. Subsequently the fine fraction was separated into silt (63-2 µm) and clay (< 2 µm equivalent spherical diameter - ESD) fractions in settling tubes. All three sub-fractions were dried and weighed. At this point a representative split (50-80 mg) of the bulk silt (BS) was removed to enable SEM investigations in this size fraction (see below). Another representative 2 to 3 g of BS were dispersed in 0.05 % calgon solution by shaking for 24 h and analysed for the grain-size distribution using a Micromeritics SediGraph 5100. Afterwards, the remaining BS was remerged with the measured portion, dried and weighed. Then the carbonate content was completely removed by the stepwise addition of hydrochloric acid. Subsequently, the carbonate-free silt (S_{cf}) samples were washed to neutral pH, dried and weighed. The

relative loss of weight during this procedure is considered to be the (still uncorrected) carbonate content of the silt fraction. All samples, where more than 1 g of S_{cf} remained after decalcification (24 of 72) were measured a second time with the SediGraph, prepared in the same way as described above. To our experience at least 1 g of silt is necessary to guarantee an appropriate sample concentration and therefore to obtain reliable results from the SediGraph. The unreduced SediGraph data were converted into 50 equally Φ-spaced size classes from 4-9 Φ (about 62.5 to 2 µm). A sub-sample of the clay fraction was quantitatively decarbonised as well using acetic acid to enable clay mineral analysis (e.g. Diekmann et al., 2003). All proportions (sand, silt, clay, carbonate contents) are related to the corrected weights, respectively. These corrections comprised the rescaling to 100 % of the sum of the sub-fraction weights, and the transfer of the clay percentage detected in the silt fractions during the SediGraph analyses from the silt to the clay fraction.

From the two grain-size distributions analysed (BS and S_{cf}) and the known bulk silt carbonate content it is possible to calculate the grain-size distribution of the carbonate silt (CS) (Paull et al., 1988; Robinson and McCave, 1994; McCave et al., 1995). The relative CS size distribution is the difference between the absolute BS and the relative S_{cf} size distribution (rel. CS = %tot. BS – %rel. S_{cf} in each size class, respectively (Fig. 2). The resulting relative CS grain-size distribution is rescaled to 100 % to derive the statistical parameters according to Krumbein (1936). The higher the carbonate contents of the silt fraction, the lower are the differences between the BS and the calculated CS distributions (Fig. 2). Therefore the calculation of the CS in samples with carbonate contents of > 90 % is a more or less cosmetic correction. The 48 samples of our sample set that failed the S_{cf} grain-size analysis due to low amount of non-carbonate silt (S_{cf} < 1 g) contained generally more than 90 %, in most of these samples more than 95 % carbonate in the silt fraction. In these cases the BS grain-size distribution is considered to represent the CS grain-size distribution adequately.

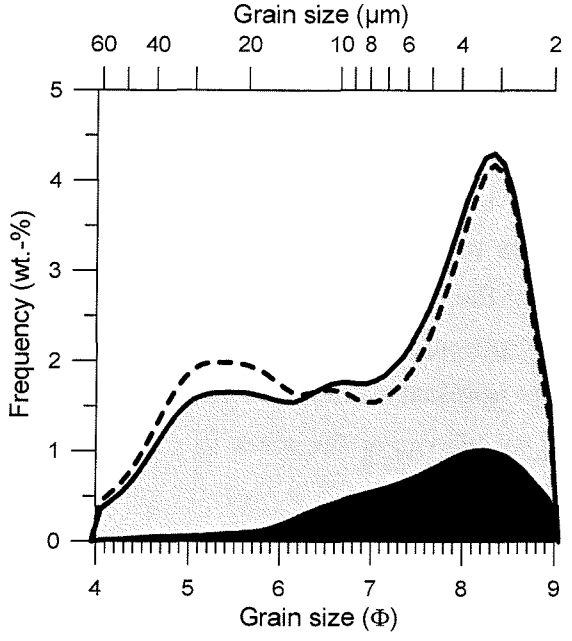

Fig. 2: Example (GeoB 6410-1) to illustrate the calculation of the CS grain-size distribution from the given BS and S_{cf} distributions and the known carbonate content of the silt fraction (here about 79 %). The bold black line is the total BS distribution (sum of all classes 100 %). The black area is the relative S_{cf} distribution [sum of all classes = (100 % – 79 %)]. The grey area is the relative CS distribution that is given by the difference of both lines in each size class (here 50 as indicated by the numerous minor tick marks of the lower abscissae). The dashed line is the CS rescaled to 100 %. Even though the non-carbonate fraction contributes considerable 21 % to the bulk silt both, the BS and the CS grain-size distributions are closely related. This effect increases with decreasing non-carbonate content.

2.2 Coccolith assemblages and biometry in silt and clay fractions

From the results of the CS grain-size analyses three provinces with characteristic size distributions appeared to be conspicuous (Figs. 1, 4). From each of these provinces one or two representative BS sample were selected for SEM studies (Fig. 1, 4), in order to compare composition and size distribution. To test if the conclusions (relative enrichment, depletion of species) blamed on the silt/clay size separation are correct, the bulk clay sample appropriate to Equatorial reference BS sample underwent the same procedure. For the preparation of the selected samples for the SEM investigations a combined dilution/filtering technique as described by Andruleit (1996) was used. 50 to 80 mg of dry silt or clay were brought into suspension using tap water and treated with ultrasonic for 30 seconds. After dilution with a rotary splitter $1/100^{th}$ split of the suspension was filtered onto polycarbonate membrane filters (Schleicher & Schuell™, 50 mm diameter, 0.4 µm pore size). The filters were dried in an oven at 40°C for 24 h before a small piece of the filter (about 10x10 mm) was cut out and mounted on an aluminium stub. At least 500 coccoliths of a representative area were counted in each sample by means of a scanning electron microscope at a magnification of 3000x or 5000x. Comparative coccolith data for corresponding bulk samples were taken from Boeckel et al. (submitted). Species that comprise less than 5 % in the silt fraction generally were combined to "others". Biometrically acquired in the silt and clay samples was the coccolith size (maximum "diameter" or length of spine) now referred to as the Nominal Diameter (ND) of the frequent species. These are:

Calcidiscus leptoporus large (B)
Calcidiscus leptoporus intermediate and small (A+C)
Rhabdosphera clavigera
Helicosphera carteri
Umbilicosphera sibogae
Emiliania huxleyi
Florisphera profunda.

To give full significance to both, relatively large and small size classes, grain size usually is dealt logarithmically. "Differences of 1 µm in the diameters of large particles are negligible, whereas the difference between particles of 1.0 and 2.0 µm diameter may be significant" (Krumbein and Pettijohn, 1938). Out of the different grade scales the Φ-scale (Krumbein, 1936) is wide spread. To meet these requirements, all calculations concerning size, i.e. the mean grain-size, as well as the average nominal diameter of coccolith species, are based on Φ-units. However, for comparison we also give the sizes in µm. For both purposes these units were converted according to:

$$[size(\Phi)] = -\log_2[size(mm)] \quad \leftrightarrow \quad [size(mm)] = 2^{-[size(\Phi)]}$$

3 Results

3.1 Grain-size distribution of South Atlantic MAR sediments

The sand and clay contents of the MAR surface sediments in the South Atlantic are distinctly anti-correlated. Generally, the sand content decreases with increasing water depth, whereas the clay content increases vice versa. Regionally, the strongest increase/decrease is observed in the Central and Southern provinces at water depths between 3500 and 4500 m, and in the Equatorial province between 4500 and 5500 m which is about 1000 m deeper (Fig. 3a, 3c). In contrast, surprisingly for the bulk silt contents no water-depth dependence is indicated (Fig. 3b). The investigated sediments generally contain 20-50 % silt. The values tend to increase from the Equatorial to the Southern provinces.

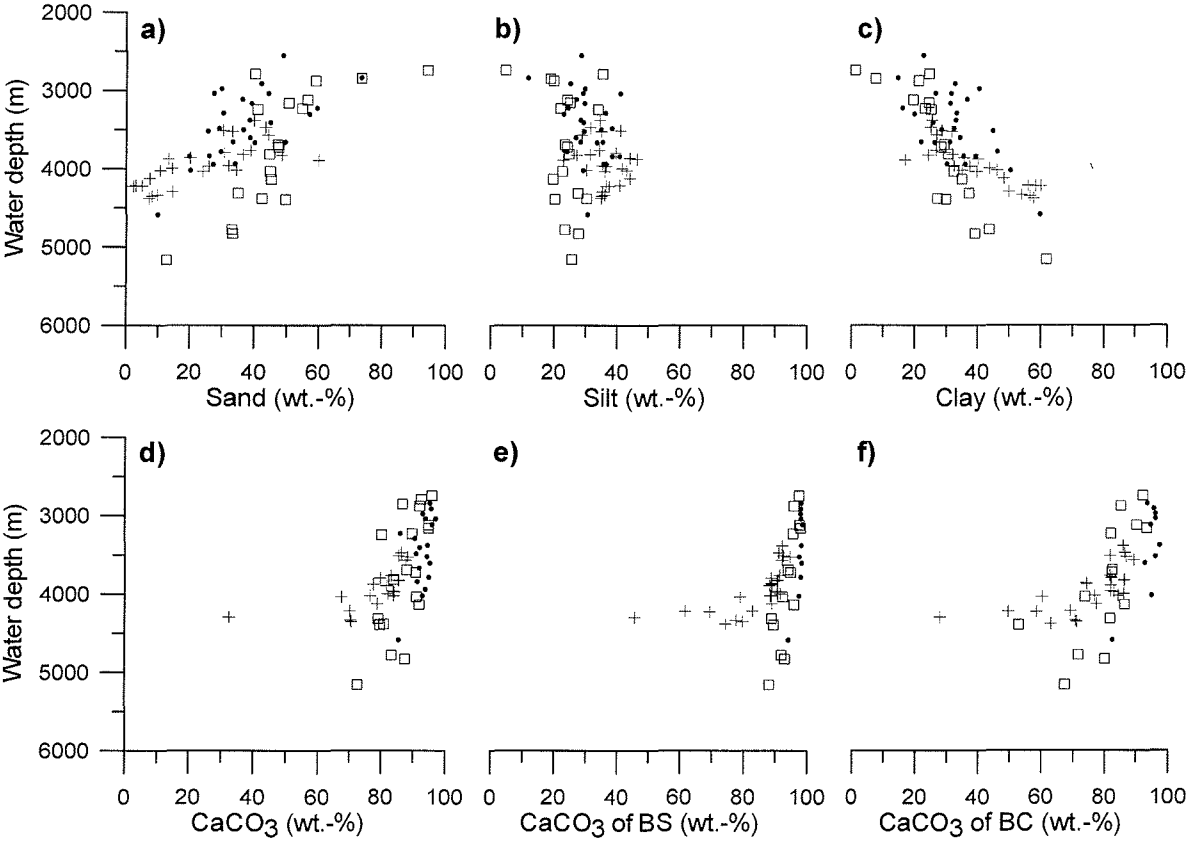

Fig. 3: Relative proportions of a) bulk sand, b) silt and c) clay and the relative carbonate contents of the d) bulk samples, e) silt and f) clay fractions for the Equatorial (squares), Central (dots) and Southern MAR provinces (crosses). Bulk carbonate contents (d) according to Mollenhauer et al. (submitted).

Both, the carbonate content of the bulk samples (Mollenhauer et al., submitted), and the relative carbonate content in the silt and clay fractions generally decrease with increasing water depth (Fig. 3d-f). Despite this overall trend, there is a considerable regional variation in carbonate values. In the Southern province the bulk carbonate contents at water depths shallower than 4000 m vary between 80% and 90 %, whereas in the Equatorial and Central Atlantic province carbonate contents generally exceed 90% in the same depth interval. In the Southern province the carbonate content decreases rapidly (< 70 %) below 4000 m

water depth, whereas in the Central and Equatorial provinces carbonate values hardly decrease to < 80 % even at deepest sites of more than 4500 m water depth. For the two fine fractions these patterns are even more differentiated (Fig. 3e, f).

A general feature, recognised for all South Atlantic MAR surface sediments investigated, is a more or less distinct bimodal distribution in their CS grain-size distributions (Fig. 4). In all three MAR provinces the grain size varies in the coarse mode between 43 and 10 µm (4.5-6.7 Φ), and in the fine mode between 4.3 and 2.5 µm (7.8-8.7 Φ). In addition, the two modes are separated by a persistent minimum at about 8 µm (7 Φ) which divides the CS into two populations: coarse and fine CS. However, in detail, distinctly different CS grain-size distributions are recognised in the three MAR provinces; characteristics for the distinction include the position (size) of the modes as well as the shape of the distributions.

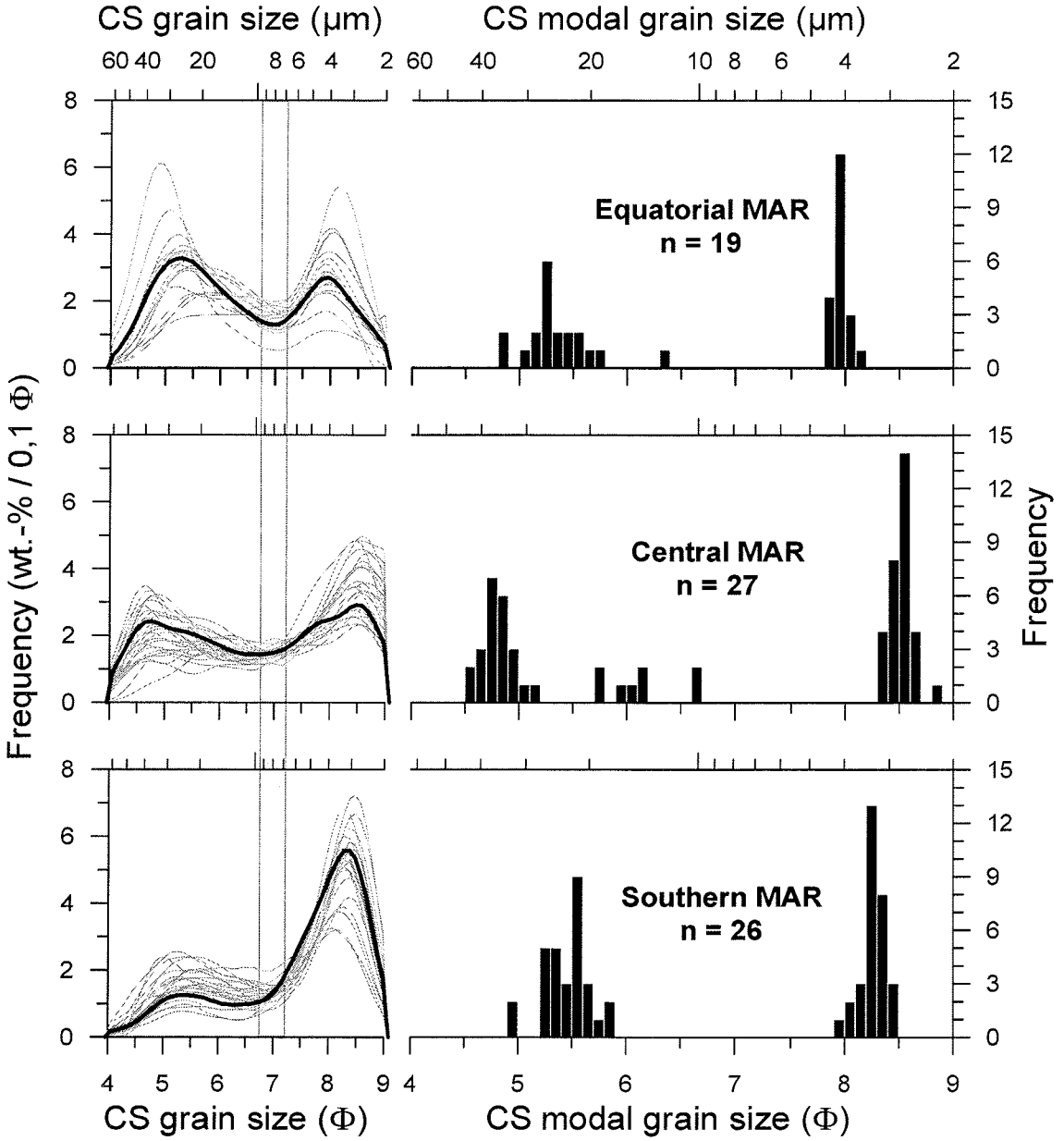

Fig. 4: Carbonate silt grain size distributions and coarse and fine modal grain size of the Equatorial, Central and Southern MAR provinces. The bold lined size distributions indicate samples that were selected for SEM investigations.

For comparison these characteristics are summarised as statistical parameters of the coarse and fine CS in Table 1.

Table 1: *Statistical parameters for the coarse (63-8 µm) and fine carbonate silt (8-2 µm) calculated according to (Krumbein, 1936)*

MAR province	Equatorial			Central			Southern		
Latitude	5°N – 10°S			10 – 25°S			30 – 45°S		
CS coarse (63-8 µm)									
mean size in Φ (min / av. / max)	5.72	5.50	5.09	5.75	5.37	5.15	5.70	5.56	5.44
in µm (min / av. / max)	19.04	22.10	29.39	18.62	24.22	28.14	19.21	21.13	22.97
modal size in Φ (min / av. / max)	6.35	5.38	4.85	6.65	5.12	4.55	5.85	5.45	4.95
in µm (min / av. / max)	12.26	24.03	34.67	9.96	28.75	42.69	17.34	22.88	32.35
sorting (min / av. / max)	0.58	0.63	0.67	0.61	0.70	0.76	0.58	0.64	0.69
skewness (min / av. / max)	-0.35	-0.01	0.58	-0.43	0.10	0.48	-0.32	-0.12	0.00
CS fine (8-2 µm)									
mean size in Φ (min / av. / max)	7.97	7.84	7.66	8.15	8.02	7.91	8.20	8.04	7.82
in µm (min / av. / max)	3.98	4.37	4.96	3.52	3.84	4.15	3.41	3.81	4.43
modal size in Φ (min / av. / max)	8.15	7.96	7.85	8.65	8.51	8.35	8.45	8.28	8.05
in µm (min / av. / max)	3.52	4.01	4.33	2.49	2.74	3.06	2.86	3.22	3.77
sorting (min / av. / max)	0.53	0.57	0.61	0.57	0.62	0.65	0.51	0.54	0.59
skewness (min / av. / max)	-0.46	-0.13	0.01	-0.68	-0.39	-0.17	-0.76	-0.48	-0.08

CS grain-size characteristic of the Equatorial MAR province

In the Equatorial province the CS grain-size distributions preliminarily seem to consists of two unimodal distributions that both are well sorted and almost symmetrically distributed (skewness ≈ 0). The mean grain size of the coarse CS is between 19 and 29 µm (5.7-5.1 Φ) with an average mean of about 22 µm (5.5 Φ). The coarse CS modal grain size, apart from two exceptions, is within the range of 31 to 18 µm comprising 8 size classes (5.0-5.8 Φ). In contrast, the fine CS mode spans 4 size classes only (7.8-8.2 Φ) which correspond to the narrow size range of 4.5 to 3.8 µm. Twelve out of nineteen samples (63 %) from this province have a fine CS mode at 4 µm (7.95 Φ, Fig. 5).

CS grain-size characteristics of Central MAR sediments

The CS grain-size distributions of the Central MAR province show a more complex pattern. Both, the fine and the coarse modes seem to be composed of two peaks respectively, which finds expression in the poor sorting. The skewness is positive for the coarse and negative for the fine CS sub-fractions. This is because of the proximity of both modes to the upper and lower end of the silt size range, respectively, which cut the more or less gentle slopes down (Frenz et al., in press). The coarse CS mean values are similar to those of the Equatorial province (19-28 µm, 5.1-5.8 Φ) but the modal grain sizes are much coarser and more variable, ranging from 43 to 10 µm (4.5-6.7 Φ). In most samples the modes vary between 43 and 29 µm (4.5-5.1 Φ). The fine CS mean size spans from 4.2 to 3.5 µm (8.1-7.9 Φ) and is about 0.5 µm smaller than in the equatorial province (i.e. about 1/8 of the diameter). The fine CS modal size, in contrast, is about 1.25 µm smaller than in

the Equatorial province (i.e. about 1/3 of the diameter). In the Central province the fine CS mode is about 2.75 µm (8.5 Φ), ranging from 3.1 to 2.5 µm (8.3-8.7 Φ). This is a very narrow range, with 13 out of 27 samples (about 50 %) having a fine CS mode at 2.7 µm (8.55 Φ, Fig. 5).

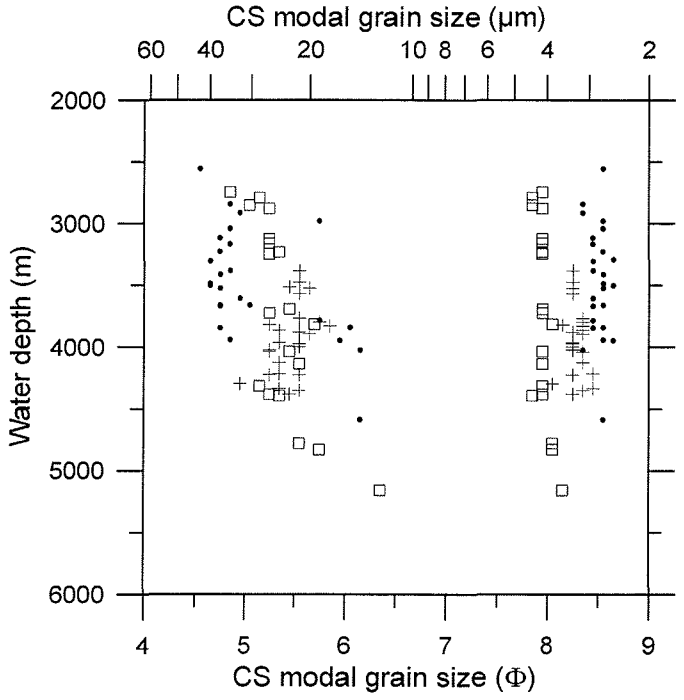

Fig. 5: Coarse and fine CS modal grain size of the Equatorial, Central and Southern MAR Provinces versus water depth. Symbols as indicated in Figures 1 and 3. Note the size stability of the fine modal size in contrast to the coarse modal size that tends to decrease with increasing water depth.

CS grain-size characteristics of Southern MAR sediments

The most striking feature of the CS grain-size distributions of the Southern MAR province is the dominance of the fine CS with an average coarse/fine CS ratio of about 30/70. The coarse share shows an intermediate sorting and a symmetric distribution. The coarse CS mean size varies between 19 and 23 µm only (5.7-5.4 Φ). The coarse CS modal size, in contrast, reveals a higher variability (17-32 µm, 5.9-4.9 Φ) and an overall finer grain size compared to the other two provinces. The fine CS proportion is obviously unimodal distributed and shows a good sorting and only a slight negative skewness. The size range of the fine CS mean is 4.4-3.4 µm (7.8-8.2 Φ) which is slightly coarser than in the Central province. The fine CS mode spreads from 3.8-2.9 µm (8.0-8.5 Φ) only, with 13 of 26 samples (50 %) having it at 3.3 µm (8.25 Φ, Fig. 5).

3.2 Coccolith assemblages in South Atlantic MAR surface sediments

Coccolith assemblages in South Atlantic MAR surface sediments also clearly display the three provinces with account to relative numerical abundance of species (Fig. 6). In the bulk samples from all three provinces *E. huxleyi* and *F. profunda* predominate, with these two species already contributing between 45 and 61 % of the entire coccolith assemblage. In the Equatorial and Central MAR provinces these two species are accompanied by *C. leptoporus* (A+C), *R. clavigera* and *U. sibogae* (< 10 % each). In the Central province the "others" comprise 26 % *Gl. flabellatus*, a species uncommon in all other samples. In

addition, in the bulk sample of the Southern province *C. leptoporus* (A+C) becomes prominent (29 %) instead of *F. profunda*.

The coccolith assemblage of the separated silt fractions in contrast reveals a completely different composition (Fig. 6). Here, *E. huxleyi* and *F. profunda* only amount to 22-30 % in the Equatorial and the Central province, and only less than 3 % in the Southern province. Instead *C. leptoporus* becomes most dominant (about 80 % in the Southern province, and about 30 % in the Equatorial and Central provinces). In addition, in the Equatorial and in the Central province other else rare species become more frequent.

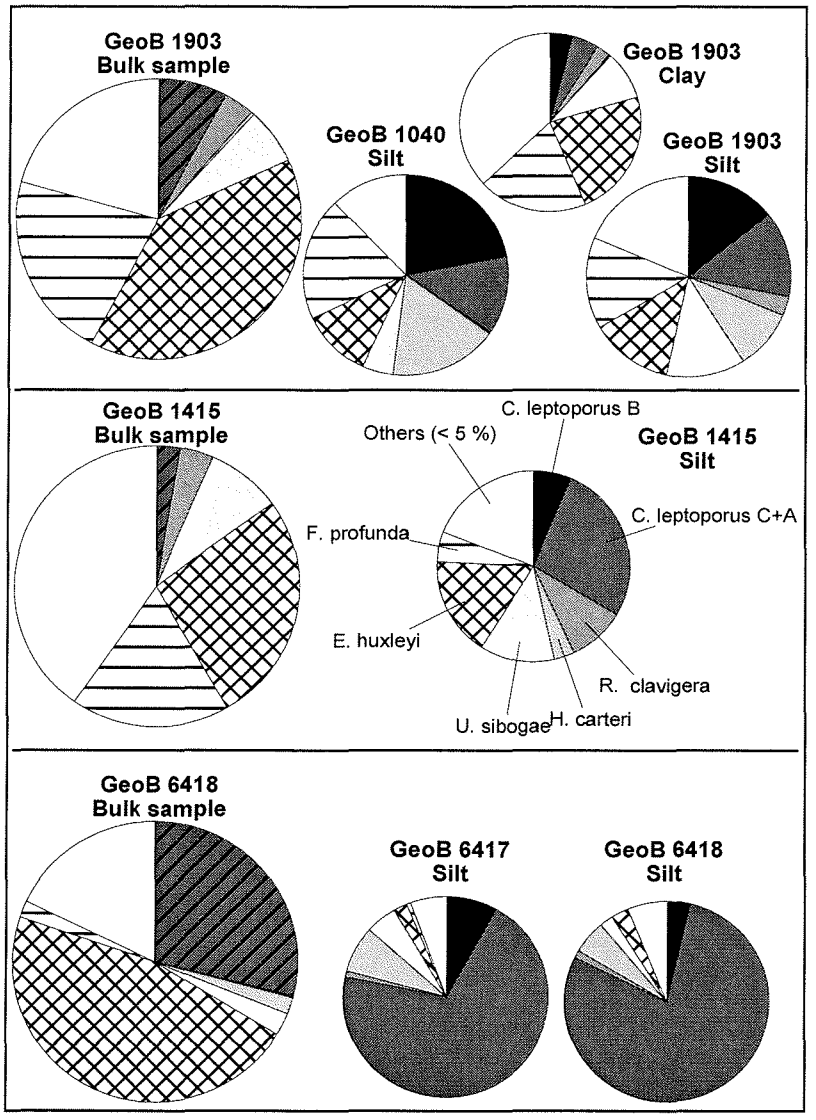

Fig. 6: *Relative abundances of coccolith species according to the number of individuals in representative samples from the Equatorial (upper), Central (middle) and Southern provinces (lower panel). Large pie-charts represent bulk samples (Boeckel et al., submitted). In these* C. leptoporus *is not differentiated in morphotypes (dark hatched). Small pies are silt samples. Note the strong depletion of the relatively small species* E. huxleyi *and* F. profunda *whereas large species especially* C. leptoporus *become abundant.*

Coccolith species in the representative silt samples display clear shifts in their measured nominal diameters (Fig. 7). It emanates that the methodically depleted species (*E. huxleyi*, *F. profunda*) have small nominal diameters of 4-2.5 µm (8-8.8 Φ). The most important species (*C. leptoporus* A+C) on average becomes successively larger from the Equatorial province (5.25 µm, 7.6 Φ) towards the Southern province (6.4 µm, 7.3 Φ). In the Equatorial and in the Central province larger species (11-6.8 µm, 6.5-7.2 Φ) are more frequent, e.g. *C. leptoporus* (B), *R. clavigera* and *H. carteri* (Fig. 7).

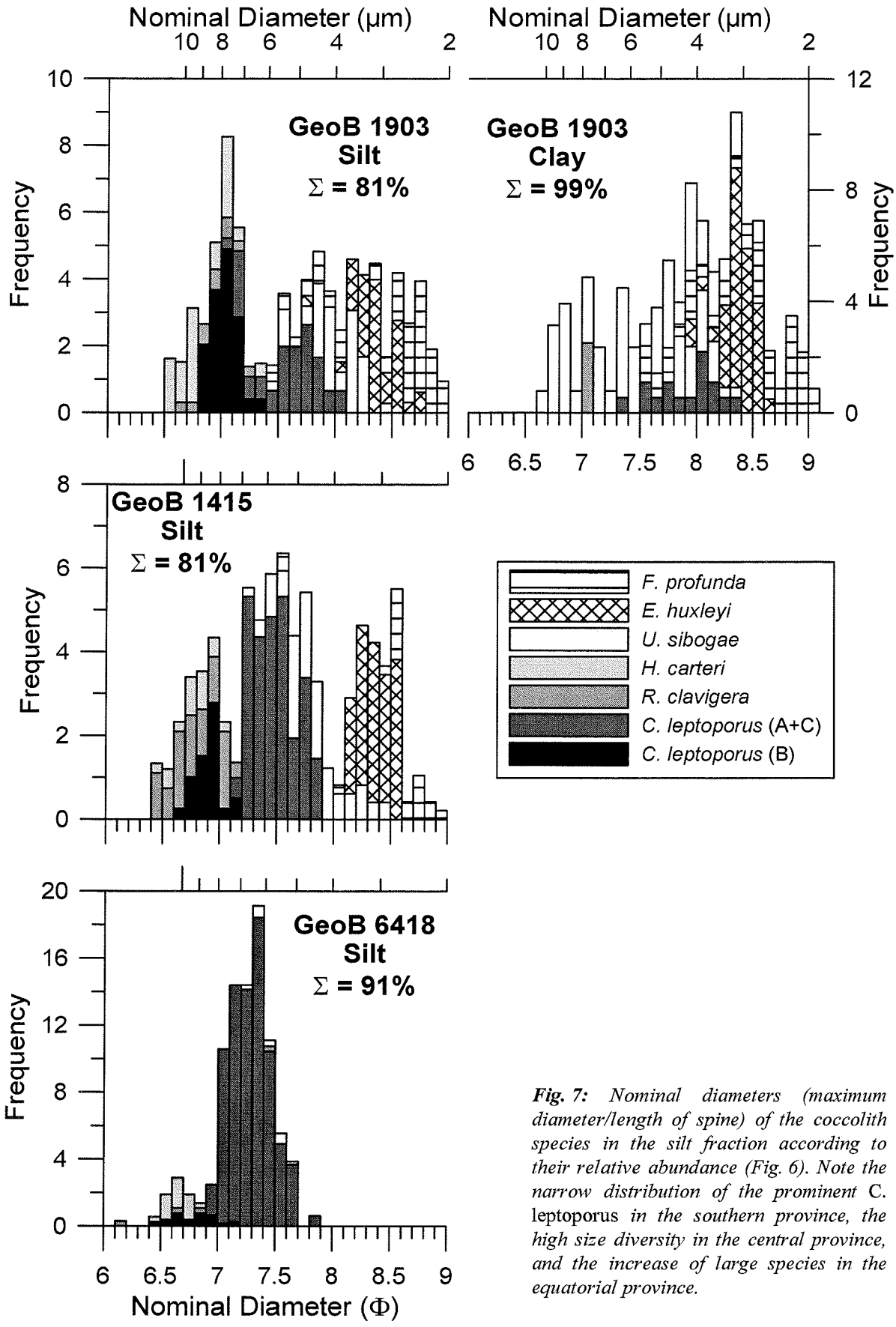

Fig. 7: *Nominal diameters (maximum diameter/length of spine) of the coccolith species in the silt fraction according to their relative abundance (Fig. 6). Note the narrow distribution of the prominent* C. leptoporus *in the southern province, the high size diversity in the central province, and the increase of large species in the equatorial province.*

4 Discussion

4.1 Evaluation of methodical aspects for the application of CS proxies

The carbonate grain-size distributions and the calcareous particle assemblage of a given sample are causally linked. This is apparent from the relative regional stability of the characteristic CS grain-size distributions (Fig. 4). The most striking feature of the observed CS grain-size distributions, in general, is their bimodality which refers to two clearly separated populations of particles, i.e. large and small ones. What is behind all this becomes obvious from the SEM observations of selected bulk silt samples (Plate 1). The SEM reveals that mainly fragments of planktic foraminifers accompanied by few juvenile tests create the coarse mode, whereas coccoliths produce the fine peak in the CS grain-size distributions. Calcareous dinoflagellate cysts only contribute increased numbers in the Central MAR province. In this province these cysts consist of hollow spheres with a diameter of about 11 µm. Hence, their effective bulk density is reduced, and therefore they settle slower than a solid quartz sphere of the same size. Because of this their equivalent spherical diameter must be smaller than the original size diameter, supposedly smaller than 8 µm. Therefore, calcareous dinoflagellates contribute to the fine peak of the CS.

The coarse part of the silt size window predominantly is composed of foraminifer fragments and juvenile tests. These fragments result from broken tests originally derived in the sand fraction. Therefore, the coarse carbonate population can be extended to the sand fraction, then including planktic foraminifers completely. Additionally, this ultimate coarse carbonate population then comprises the entire zooplankton. This includes also pteropods and, in most cases, only very minor amounts of various calcareous benthic particles, e.g. benthic foraminifers, gastropods, bivalves, echinoderms, ostracods, etc.. Since pteropods virtually are the only planktic organisms that secrete aragonite the measurement of the aragonite content is the tool of choice in most studies to estimate the pteropod contribution. For South Atlantic MAR surface-sediments it has been shown by Baumann et al. (in press) that only at shallow sites aragonite contributes about 10 to 30 % to the total carbonate budget. Furthermore, the aragonite content rapidly decreases below the aragonite lysocline (at about 2500 m water depth in the South Atlantic) to vanish completely below the aragonite compensation depth (around 3400 m water depth according to Gerhardt and Henrich (2001) and Henrich et al. (in press)). Only a low number of samples (16) used in this study is situated at water depths above the aragonite compensation depth. At these shallow sites pteropods might contaminate the coarse carbonate fraction and account for up to 20 wt.-%.

The fine share of the silt fraction mainly comprises relatively large coccoliths with nominal diameters of > 4 µm (Fig. 7). The smaller species (*E. huxleyi*, *F. profunda*) occur in the clay fraction (< 2 µm ESD, Figs. 6, 7, Plate 1). Summing up the coccolith values from the fine CS population and those from the clay fraction therefore will include the whole

calcareous phytoplankton, e.g. all coccoliths and the contamination by calcareous dinoflagellates.

The coccolith population and the foraminifer population (named according to the main contributors in each population) in South Atlantic MAR sediments are clearly separated by a low frequency size zone in the silt size window (Fig. 4). Beyond this CS minimum zone (ranging from 10 to 7 μm, average 8 μm = 7 Φ) both populations thin out. It is assumed that in and beyond this minimum zone particles of both populations are present but rapidly decreasing within the "hostile" population. Therefore a separation of the carbonate of these samples at 8 μm ESD (settling technique) will provide the most precise separation of calcareous zoo- and phytoplankton possible (Fig. 9a, b). A similar grain-size distribution pattern was detected by Paull et al. (1988), who found a general minimum at about 4-6 μm in the size fraction 38-2 μm for pelagic calcareous sediments. We attribute the shift observed in the absolute values of the minimum zone detected in this study and in the study by Paull et al. (1988) to methodical differences in the measuring techniques applied. This includes differences in measuring principle (i.e. determination of vol.-% with a Coulter Counter used by Paull et al. (1988) versus wt.-% with the SediGraph used in this study), and differences in size resolution of 1/3 Φ (Paull et al., 1988) versus 1/10 Φ (this study). On the other hand, this study can confirm the observations from the Pleistocene NE Atlantic (Robinson and McCave, 1994; McCave et al., 1995). In both study areas and monitored time intervals prominent minima in the carbonate silt fraction are observed in almost perfect agreement (10 μm in the Pleistocene NE Atlantic compared to 8 μm in the South Atlantic).

Hitherto, foraminifer studies (isotope investigations, fragmentation indices, assemblage analyses etc.) usually refer to discrete "coarse" fractions ranging from > 200 μm (Beiersdorf et al., 1995) to > 63 μm (Sarnthein, 1971). On the one hand, identification is easier the larger the particles are. On the other hand, small tests and fragments are strongly underestimated. Beyond question, changes of sand contents itself in pelagic environments with no dilution by coarse terrigenous input may provide a good estimate for changes in zooplankton carbonate, because most of the adult foraminifers fall in this size range (Brummer, 1988; Giraudeau et al., 2000). In doing so, carbonate estimates from foraminifer census data and carbonate measurements of this size fraction are in good agreement (Stuut et al., 2002; Baumann et al., in press). Additionally, taking the coarse CS fraction into account the sand fraction underestimates the foraminifer carbonate by about 10-20 % (Fig. 8a, compare Fig. 3a with 8c). Already arguing about this, a number of studies used smaller fractions for the determination of foraminifer contents, e.g. the sieve fraction > 32 μm (van Kreveld et al., 1996; Ziveri et al., 2000) or > 25 μm (Divakar Naidu and Malmgren, 1999).

Fine carbonate fraction is referred to consist mainly of coccoliths. "Fine carbonate fraction" can comprise completely different size fractions ranging from < 63 μm to

< 25 µm (see introduction). Nowadays commonly mass estimates of individual coccolith species are extrapolated to the bulk number of individuals according to Young and Ziveri (2000). However, these mass estimates only cover a part (55-60 %) of the carbonate of the fraction < 32 µm (Broerse et al., 2000c). Possible error sources are the mass estimate error for coccolith species of ± 50 % (Young and Ziveri, 2000), and that coccolith fragments mostly are not regarded (Broerse et al., 2000c) and, according to this study, also fine foraminifer fragments. An example, that the latter error source is important, becomes obvious from a comparison of the measured CS grain-size distribution in the Southern MAR province (Fig. 4c) and observations of its composition by SEM studies (Plate 1). Here, even though the number of foraminifer fragments is low these few but relatively large particles produce a low but considerable peak in the coarse CS.

For comparison, the contribution of the plankton groups determined in this study is opposed to the results of studies that use conventional proxies (Fig. 8).

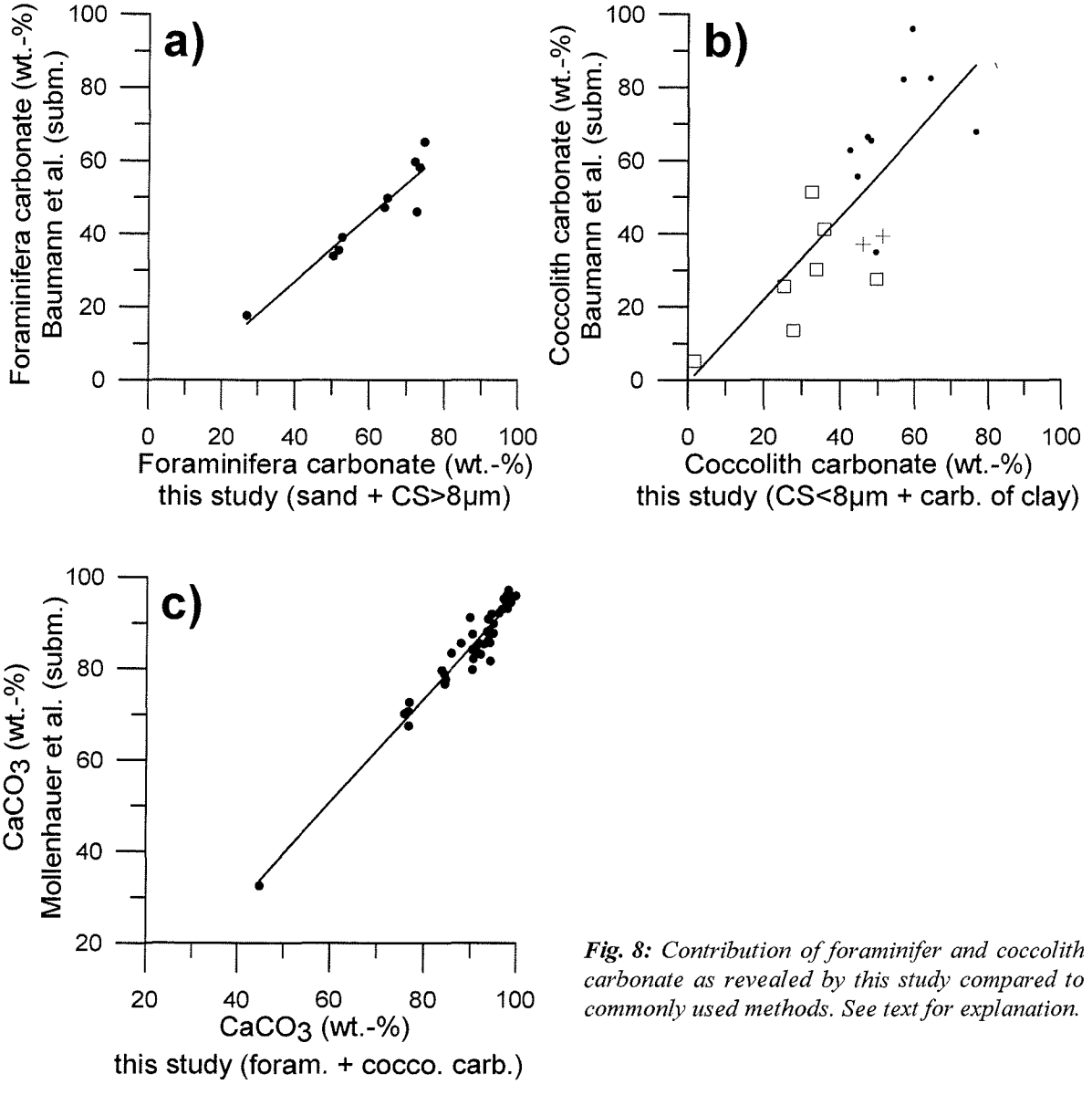

Fig. 8: Contribution of foraminifer and coccolith carbonate as revealed by this study compared to commonly used methods. See text for explanation.

Generally, the carbonate contribution of foraminifers analysed by Baumann et al. (in press) using the carbonate content of the sand fraction is in good agreement to our findings (Fig. 8a). However, in comparison our results are generally increased by about 10-20 %. This can clearly be attributed to the presence of relatively small foraminifer fragments that are not recognised in the sand fraction, however they are detected by means of silt grain-size analyses.

The coccolith carbonate calculated on the basis of mass estimates of individual species compared to the carbonate content of the size fraction < 8 µm do roughly agree (Fig. 8b). However, deviations of ± 20 % are common. Besides general analytical errors of both methods, mainly the extrapolation of individual coccolith masses to the huge number of individuals is held responsible to cause the observed deviations. Because this error may be as high as 50 % (Young and Ziveri, 2000) the observed range of deviation suggests to favour the method of this study to infer the contribution of coccolith carbonate in marine sediments.

The carbonate content of the silt and clay fractions together with the sand content as a measure for the bulk carbonate content is generally increased by about 5 % compared to bulk carbonate measurements (Mollenhauer et al., submitted, Fig. 8c). This surprisingly slight enhancement is attributed to an overestimation of the carbonate contents of the silt and clay fractions due to loss of material during the repeated decanting procedures.

4.2 Evaluation of regional trends in the contribution of coccolith versus planktic foraminifer carbonate in South Atlantic MAR sediments

The regional distribution of foraminifer and coccolith carbonate (Fig. 9a, b) confirms the trend that mesotropic regions (Equatorial province) are the favoured habitats of foraminifers, whereas coccolithophores prefer oligotrophic regions (Central and Southern provinces, Baumann et al., in press), if one assumes comparable production within one province. Additionally, this pattern is a mirror for differences in ecological conditions from tropical (Equatorial province) to likely subantarctic (Southern province).

The similarity of the CS grain-size composition within the provinces bases on the shape and the position of the two peaks, respectively (Fig. 4). The coarse peak represents mainly foraminifer fragments. Its broader distribution is the expression of the individuality of size and shape of every fragment, in comparison to the narrow distributed coccolith peak in the fine CS. In contrast to the fine peak that is very stable, the coarse modal value decreases with water depth (Fig. 5), more or less parallel to the general decrease in foraminifer carbonate (Fig. 9c). This coarse CS size decrease indicates dissolution by increasing fragmentation and the higher dissolution susceptibility of foraminifers compared to coccoliths. For the Equatorial province an escalating decrease of the modal value indicates enhanced dissolution only below 5000 m water depth, displaying the tropical depression of the modern calcite lysocline. In the Equatorial province this dissolution indicator works best because of the high relative contribution of foraminifer carbonate. In the Central

province two individual branches of decrease are obvious (Fig. 5). From Fig. 9a it is evident that foraminifer carbonate in this province decreases faster towards the Brazil than towards the Angola Basin. This can be attributed to differences in the vertical water mass distribution and position of the calcite lysocline which is situated at 4200 m in the Brazil Basin (Thunell, 1982) and at about 4400 m water depth in the Angola Basin (Volbers and Henrich, 2002; Henrich et al., in press).

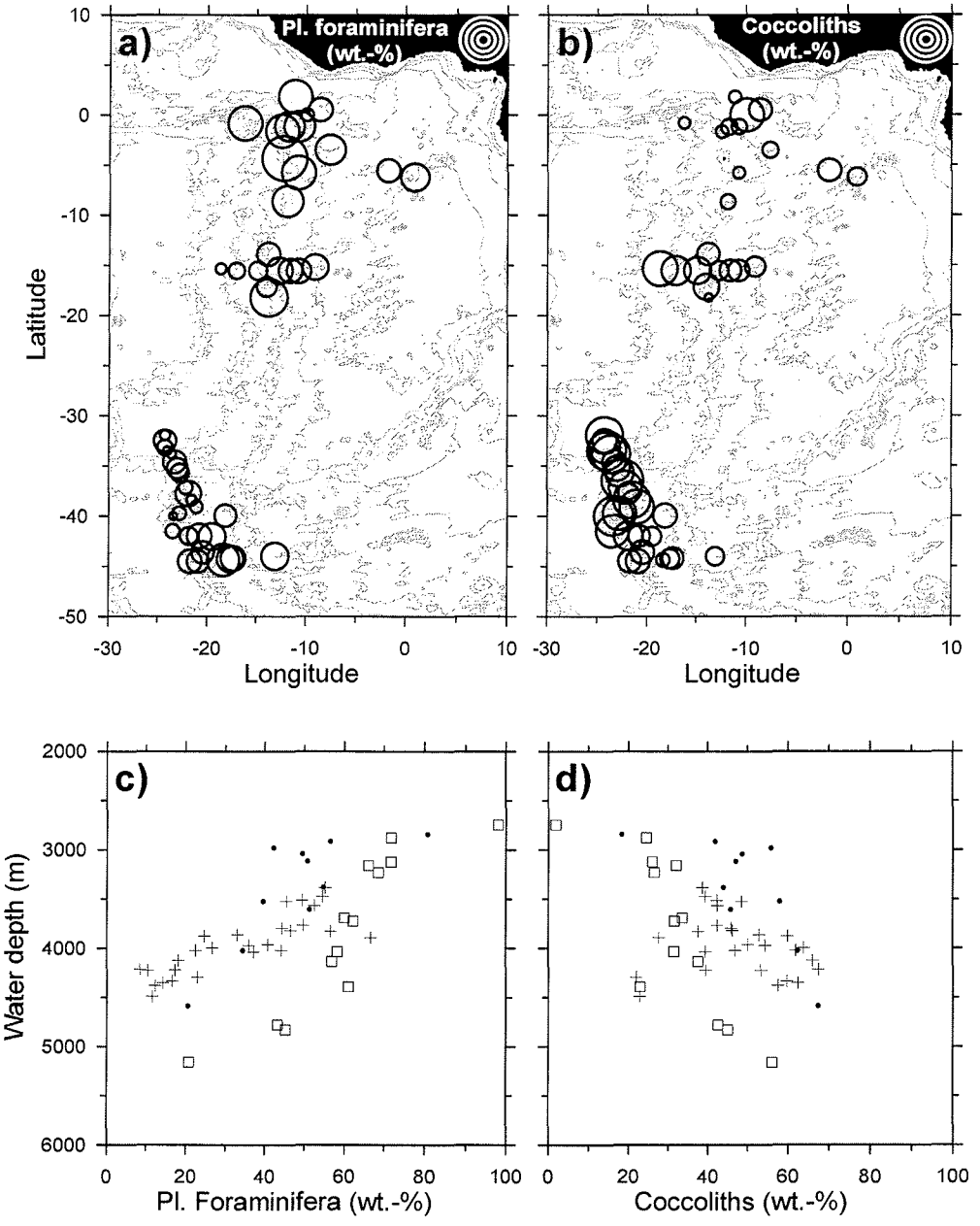

Fig. 9: *Regional distribution of a) foraminifer and b) coccolith carbonate relative to the carbonate content (both add up to 100 %). c) and d) show the same relative to bulk sample (sum of both result in the bulk sample carbonate content) versus water depth. For a) and c) the shallowest ridge crest in the Equatorial and Central MAR provinces may be contaminated by pteropods (20 %). Scale in a) and b) 25, 50, 75 and 100 %.*

By the stability of the fine CS peak per area with increasing water depth the less carbonate dissolution susceptibility of coccoliths is indicated (Fig. 4, 5). If so, then the shift in the modal size from province to province indicates differences in the coccolith assemblages present in the silt fraction, i.e. it represents ecological differences between the provinces.

In the Southern province the well-defined fine CS peak is caused by the more or less monospecific composition of the coccolith assemblage, dominated by *C. leptoporus* (A+C). In contrast, the bulk coccolith assemblage is numerically dominated by *E. huxleyi*, which is almost absent in the silt fraction (Fig. 6). From this follows that accidentally the empirically defined silt/clay border (2 µm/9 Φ ESD) is coarser than the ESD of *E. huxleyi* itself, so that this species as well as *F. profunda* is removed from the silt and enriched in the clay fraction. The barely contaminated composition of the fine CS in the Southern province (Figs. 6, 7, 10) makes these samples be reference samples for *C. leptoporus* (A+C). In contrast to the individual size and shape of foraminifer fragments coccoliths of the same species generally have the same shape and additionally the same size in each ecologic province. This will results in normal grain-size distribution for measurements using settling techniques (SediGraph) with a good sorting (low standard deviation, Tab. 1). In such a normal distribution with only slight disturbance by additional constituents as revealed for the Southern province (Fig. 7) the mean grain size may be influenced by the contaminants whereas the modal grain size represents the mean grain size (ESD) of this main constituent if normal distribution is assumed. The mean ESD of *C. leptoporus* (A+C) for the Southern province is represented by the average modal grain size of the fine CS. This mean ESD corresponds to the average Nominal Diameter (ND) of the coccoliths, for which we take the maximum diameter of the coccolith species, by means of a shape factor (SF) according to the following equation:

$$\overline{ND}(\Phi) \cdot SF = \overline{ESD}(\Phi)$$

For *C. leptoporus* (A+C) in the Southern province this is: $7.29\Phi \cdot 1.136 = 8.28\Phi$. Transformed for this special case this means that the mean ND (6.40 µm) of *C. leptoporus* (A+C) is about twice as large its mean ESD (3.25 µm). The Φ-*C. leptoporus*-shape factor (1.136) is valid for all bodies with the shape and density of *C. leptoporus* (A+C), e.g. for *C. leptoporus* (B), which can be applied for other areas, especially the Equatorial province (see below).

In contrast to the rather simple coccolith composition of the Southern province the Central and Equatorial provinces show a multispecific coccolith assemblage in the silt fraction. Especially the abundance of the small species *E. huxley* and *F. profunda* in the silt samples of these provinces (Figs. 6, 7) gives evidence that the clay separation does not work as excellent as in the Southern province even though both species show similar ND in all provinces. Generally this phenomenon must be attributed to the building of aggregates in the duration time of each Atterberg-settling cycle (17-22 h). The aggregates may be caused by a high terrigenous clay input in association with a different clay mineral composition in the Equatorial and Central provinces compared to the Southern province. According to (Petschick et al., 1996), the content of terrigenous clay increases in the area of interest from the south towards the equator. Additionally, the clay mineral composition changes in

this direction that smectite and chlorite decrease by increasing illite and kaolinite contents (Petschick et al., 1996). On the other hand, organic coatings can cause the building of aggregates as well (S. van der Gaast, pers. comm.), even though the organic carbon content among the samples used in this study is below 0.5 % (Baumann et al., in press). Finally, the generally multifarious coccolith composition with many size-overlapping species may cause a general loss in separation quality.

4.3 A new approach to unravel coccolith populations in South Atlantic MAR sediments

Because the coccolith assemblage in the Equatorial and Central MAR provinces are composed of a number of species their fine CS grain-size distributions must be seen as the sum of a number of populations. To simplify the disentanglement of this system of interference Normal or Gaussian distributions are assumed for each population, respectively (normal for Φ-scale, log-normal for metrical scale). Moreover the numerical frequencies (Fig. 7) must be related to their weights, i.e. at same abundances larger species make a higher peak than smaller ones. For example one platelet of *C. leptoporus* with a length of 7 µm weighs 74 pg in comparison to one platelet of *E. huxleyi* that weighs only 2.3 pg by 3.5 µm length (Young and Ziveri, 2000). In other words, only in the case that the numbers of *E. huxleyi* are enriched thirty-fold in comparison to *C. leptoporus*, both populations would have the same weight with respect to carbonate. In our cases, the CS grain-size distributions do not "see" *E. huxleyi* and, for that matter, *F. profunda* (1.7 pg at 2.5 µm, Young and Ziveri (2000)). This means that even though both species are the most frequent ones in sediments they are probably not the main carriers of phytoplankton carbonate. Therefore the pool of populations causing the observed CS grain-size distributions is reduced to concisely five large species (Figs. 6, 7).

In this section a semi-automated un-mixing technique for coccolith species is introduced which for several reasons can not claim the relative perfection of a fully automated algorithm. By means of the PeakFit program (SPSS science) Gaussian distributions were used to fit the measured grain-size distribution with best possible but reasonable fit. The Gaussian distribution used obey the following function:

$$y = a_0 \exp\left[-\frac{1}{2}\left(\frac{x-a_1}{a_2}\right)^2\right]$$

with

a_0 = amplitude,
a_1 = center (= mean and modal size),
a_2 = width (= standard deviation).

The number of fine peaks used is aligned to the number of coccolith species for the fine CS. The coarse share was fitted with the least possible number of fits (2-3) because it is impossible to distinguish populations of foraminifer fragments due to their individual size and shape.

The initial point for these considerations again is the relative simple coccolith composition of the Southern province (reference sample GeoB 6418). Strictly, the population of *C. leptoporus* (A+C) builds the main peak 1 in the fine CS (Fig. 10). The centre of this peak can be fixed at the fine CS modal size. Because a small amount of *C. leptoporus* (A+C) can be transferred to the clay fraction (Fig. 7) the measured size distribution shows a slight asymmetry. This results in that the fitted normal distribution overlaps the steeper slope of the distribution at the finer end (peak 1, Fig. 10). By neglecting the very rare species *U. sibogae* and *R. clavigera* (Fig. 7), an additional but relatively small peak caused by *C. leptoporus* (B) and *H. carteri* (Fig. 7) is expected to build the coarser peak 2 in the fine CS (Fig. 10). Probably the contribution of the two species is too low to build two individual peaks.

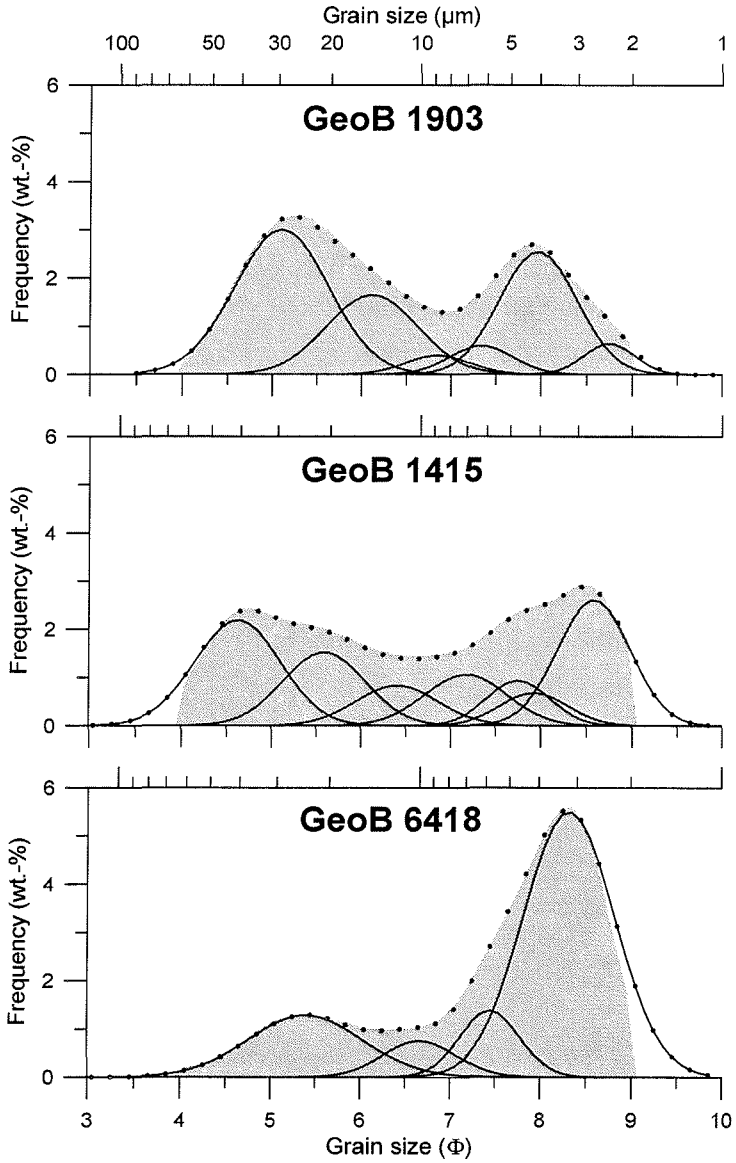

Fig. 10: *Possible solutions for an unravelling of representative CS grain-size distributions into Gaussian distributed subpopulations that represent coccolith species (numbers) in the fine silt (< 8 µm) share. The letters represent unspecified foraminifer fragments. The dots represent the size distribution if all peaks are summed up. The grey background stands for the original CS grain-size distribution. From top to bottom there are the same examples as highlighted in Figures 4 and 7.*

With the help of some of this pre-knowledge we are able to shed some light on the grain-size distributions of the Equatorial province in a further step. In this province the large morphotype of *C. leptoporus* is the most frequent species with high contributions of *H. carteri*. Considering their individual weight the smaller species will have a minor impact on the grain-size distribution. As described above, the shape factor that connects ND and ESD (both in Φ) of bodies with the shape of *C. leptoporus* is 1.136. Therefore, *C. leptoporus* (B) with an average ND of 7.03 Φ (7.7 µm) is expected to build a peak at 7.98 Φ (3.95 µm). And true, this is only 0.02 Φ-units smaller in size compared to the average modal value (7.96 Φ) observed for the fine CS in this province. Therefore the *C. leptoporus* peak (peak 1 Fig. 10a) can be fixed at this position. Together with one coarser peak for *H. carteri* (2) and one finer peak for the bulk smaller species (3) the fine CS is well represented in this province (Fig. 10a).

The CS grain-size distribution of the Central MAR province is the most complicated. The finest modal value compared to the other two provinces (Fig. 5) indicates that relatively small coccolith species dominate the fine silt. These are *C. leptoporus* (A+C) together with *U. sibogae* (Fig. 7). Applying the leptoporus shape factor the *C. leptoporus* (A+C) peak is expected at 2.77 µm in this province. The observed fine CS average modal value is 2.75 µm and therefore almost equal to this size. That this size is slightly finer than expected can be attributed to interference with the smaller species *U. sibogae* which can not be resolved (peak 1, Fig. 10b). That larger coccolith species have an impact on the size distribution in this province is obvious from the pillow-shaped and broad grain-size distribution as well as from relative high numerical contribution of the larger species *C. leptoporus*, *H. carteri* and *R. glavigera* (Fig. 7). Probably the relative large calcareous dinoflagellates that are frequent too (Plate 1) may create an own peak (peak 4 in Fig. 10b). These species built the three more peaks of the fine CS that are necessary to give a reasonable fit (peak 2-4, Fig. 10b).

It is emphasised that the given unmixing solutions are not the only possible combination of Gaussian distributions that fit the observed grain-size distributions. Nevertheless, most of the assumptions are reasonable to the observations, especially the ones based on ND, ESD and SF of *C. leptoporus*. Finally, the area below each of the gaussian curves can be considered as a measure for the carbonate contribution of the species, respectively.

5 Summary and Conclusions

This study presents a synthesis of the results of sedimentological and micropaleontological investigations on a set of surface sediment samples from the Mid-Atlantic Ridge in the South Atlantic. The sedimentological results comprise grain-size distributions of the carbonate compounds that are subsequently set into context with micropaleontological results from numerical abundances and biometrical statistics of different coccolith species.

From the differences in the spatial distribution of the grain-size patterns along the MAR some important general and regional aspects are derived. Three areas with characteristic grain-size distributions appear to be outstanding: the Equatorial, Central and Southern provinces. Generally, the CS grain-size distributions are bimodal distributed with a general minimum at about 8 µm (7 Φ). This minimum defines the transition of foraminifer and coccolith carbonate. Foraminifers display the highest contribution to the sediments in the Equatorial province, whereas coccoliths dominate in the Southern province. The coarse peak of the grain-size distributions decreases in size and amplitude with increasing water depth. This indicates higher dissolution susceptibility for foraminifers as compared to coccoliths, which is also manifested by the fact that the fine CS peak representing coccoliths does not change according to water depth

Coevally, regionally very stable fine CS peaks represent distinct coccolith assemblages. Generally, the numerically most frequent small coccolith species *E. huxleyi* and *F. profunda* are strongly depleted in the silt and therefore enriched in the clay fraction because they have an ESD of < 2 µm. The Southern province is dominated by *C. leptoporus* (A+C). The other two provinces reveal a more complex composition of coccolith species. Their grain-size spectra can be resolved into normal distributed subpopulations using a fit program. The resulting peaks can be attributed to distinct species and the area below each distribution is equal to the carbonate contribution to the carbonate silt respectively.

For practical purposes the following suggestions are made. A size separation at 8 µm ESD using a settling technique reasonably separates calcareous zoo- and phytoplankton in Southern MAR sediments. Variations of this size minimum need to be checked in samples of other origin. *E. huxleyi* and *F. profunda* are enriched in the < 2 µm ESD fraction. For *C. leptoporus* the shape factor of 1.136 is useful to find its modal size and fix a convenient separation window. Hitherto, only this species has a fixed shape factor. For other species other reference areas need to be found. Because in samples that are composed of many species the peaks broadly overlap, it is hardly possible to separate them purely for further use. We suspect a considerable enrichment of coccolith species with settling techniques if the size window is fixed carefully and the samples are suitable.

Acknowledgements

We would like to thank the shipboard and scientific crews of the RV METEOR that were involved in the sediment coring. Furthermore we thank B. Diekmann who comprised the clay weights and a major part of the quantitative clay decarbonisation data and S. van der Gaast for giving valuable introductory help to the Peakfit program. This research was funded by the Deutsche Forschungsgemeinschaft (Sonderforschungsbereich 261 at the University of Bremen). This is SFB contribution no. ###. All data presented in this publication are archived in the PANGAEA database at www.pangaea.de (search string: FrenzM).

6 References

Andruleit, H., 1996. A filtration technique for quantitative studies of coccoliths. Micropaleontology, 42: 403-406.

Baumann, K.-H., Böckel, B., Donner, B., Gerhardt, S., Henrich, R., Vink, A., Volbers, A.N.A., Willems, H. and Zonneveld, K.A.F., in press. Contribution of calcareous plankton groups to the carbonate budget of South Atlantic surface sediments. In: S. Mulitza, V. Ratmeyer and G. Wefer (Editors), The South Atlantic in the late Quaternary: Reconstruction of material budget and current systems. Springer, Berlin Heidelberg New York.

Beiersdorf, H., Bickert, T., Cepek, P., Fenner, J., Petersen, N., Schonfeld, J., Weiss, W. and Won, M.-Z., 1995. High-resolution stratigraphy and the response of biota to Late Cenozoic environmental changes in the central equatorial Pacific Ocean (Manihiki Plateau). Marine Geology, 125(1-2): 29-59.

Bickert, T. and Wefer, G., 1996. Late Quaternary deep-water circulation in the South Atlantic: Reconstruction from carbonate dissolution and benthic stable isotopes. In: G. Siedler (Editor), The South Atlantic: Present and past circulation. Springer, Berlin Heidelberg, pp. 599-620.

Boeckel, B., Baumann, K.-H., Henrich, R. and Kinkel, H., submitted. Distribution patterns of coccoliths in South Atlantic and Southern Ocean surface sediments in relation to environmental gradients.

Broerse, A.T.C., Brummer, G.-J.A. and Hinte, J.E.V., 2000a. Coccolithophore export production in response to monsoonal upwelling off Somalia (northwestern Indian Ocean). Deep Sea Research Part II: Topical Studies in Oceanography, 47(9-11): 2179-2205.

Broerse, A.T.C., Ziveri, P. and Honjo, S., 2000b. Coccolithophore (-$CaCO_3$) flux in the Sea of Okhotsk: seasonality, settling and alteration processes. Marine Micropaleontology, 39(1-4): 179-200.

Broerse, A.T.C., Ziveri, P., van Hinte, J.E. and Honjo, S., 2000c. Coccolithophore export production, species composition, and coccolith-CaCO3 fluxes in the NE Atlantic (34°N 21°W and 48°N 21°W). Deep Sea Research Part II: Topical Studies in Oceanography, 47(9-11): 1877-1905.

Brummer, G.-J.A., 1988. Ocean carbonate-CO_2 cycle. In: G.-J.A. Brummer and D. Kroon (Editors), Planktonic Foraminifers as tracers of ocean-climate history. Free University Press, Amsterdam, pp. 322-334.

Conan, S.M.-H. and Brummer, G.J.A., 2000. Fluxes of planktic foraminifera in response to monsoonal upwelling on the Somalia Basin margin. Deep Sea Research Part II: Topical Studies in Oceanography, 47(9-11): 2207-2227.

Conan, S.M.-H., Ivanova, E.M. and Brummer, G.-J.A., 2002. Quantifying carbonate dissolution and calibration of foraminiferal dissolution indices in the Somali Basin. Marine Geology, 182(3-4): 325-349.

Diekmann, B., Fütterer, D.K., Grobe, H., Hillenbrand, C.D., Kuhn, G., Michels, K., Petschick, R. and Pirrung, M., 2003. Terrigenous sediment supply in the polar to temperate South Atlantic: Land-ocean links of environmental changes during the late Quaternary. In: S. Mulitza, V. Ratmeyer and G. Wefer (Editors), The South Atlantic in the late Quaternary: Reconstruction of material budget and current systems. Springer, Berlin Heidelberg New York.

Divakar Naidu, P. and Malmgren, B.A., 1999. Quaternary carbonate record from the equatorial Indian Ocean and its relationship with productivity changes. Marine Geology, 161(1): 49-62.

Ennyu, A., Arthur, M.A. and Pagani, M., 2002. Fine-fraction carbonate stable isotopes as indicators of seasonal shallow mixed-layer paleohydrography. Marine Micropaleontology, 46(3-4): 317-342.

Frenz, M., Höppner, R., Stuut, J.-B., Wagner, T. and Henrich, R., in press. Surface sediment bulk geochemistry and grain-size composition related to the oceanic circulation along the South American continental margin in the Southwest Atlantic. In: S. Mulitza, V. Ratmeyer and G. Wefer (Editors), The South Atlantic in the late Quaternary: Reconstruction of material budget and current systems. Springer, Berlin Heidelberg New York.

Gerhardt, S. and Henrich, R., 2001. Shell preservation of Limacina inflata (Pteropoda) in surface sediments from the Central and South Atlantic Ocean: a new proxy to determine the aragonite saturation state of water masses. Deep Sea Research Part I: Oceanographic Research Papers, 48(9): 2051-2071.

Giraudeau, J., Bailey, G.W. and Pujol, C., 2000. A high-resolution time-series analyses of particle fluxes in the Northern Benguela coastal upwelling system: carbonate record of changes in biogenic production and particle transfer processes. Deep Sea Research Part II: Topical Studies in Oceanography, 47(9-11): 1999-2028.

Haidar, A.T., Thierstein, H.R. and Deuser, W.G., 2000. Calcareous phytoplankton standing stocks, fluxes and accumulation in Holocene sediments off Bermuda (N. Atlantic). Deep Sea Research Part II: Topical Studies in Oceanography, 47(9-11): 1907-1938.

Henderiks, J., Freudenthal, T., Meggers, H., Nave, S., Abrantes, F., Bollmann, J. and Thierstein, H.R., 2002. Glacial-interglacial variability of particle accumulation in the Canary Basin: a time-slice approach. Deep Sea Research Part II: Topical Studies in Oceanography, 49(17): 3675-3705.

Henrich, R., 1998. Dynamics of Atlantic water advection to the Norwegian-Greenland Sea -- a time-slice record of carbonate distribution in the last 300 ky. Marine Geology, 145(1-2): 95-131.

Henrich, R., Baumann, K.-H., Gerhardt, S., Gröger, M. and Volbers, A.N.A., in press. Carbonate preservation in deep and intermediate water masses in the South Atlantic: evaluation and geological record (a review). In: S. Mulitza, V. Ratmeyer and G. Wefer (Editors), The South Atlantic in the late Quaternary: Reconstruction of material budget and current systems. Springer, Berlin Heidelberg New York.

Henrich, R., Kassens, H., Vogelsang, E. and Thiede, J., 1989. Sedimentary facies of glacial-interglacial cycles in the Norwegian Sea during the last 350 ka. Marine Geology, 86: 283-319.

Henrich, R., Wagner, T., Goldschmidt, P. and Michels, K., 1995. Depositional regimes in the Norwegian-Greenland Sea: the last two glacial to interglacial transitions. Geologische Rundschau, 84(1): 28-48.

Krumbein, W.C., 1936. Application of logarithmic moments to size frequency distributions of sediments. Journal of Sedimentary Petrology, 6: 35-47.

Krumbein, W.C. and Pettijohn, F.J., 1938. Manual of sedimentary petrography. The century earth science series. Appleton-century-crofts, inc., New York, 549 pp.

McCave, I.N., Manighetti, B. and Robinson, S.G., 1995. Sortable silt and fine sediment size/composition slicing: Parameters for palaeocurrent speed and palaeoceanography. Paleoceanography, 10(3): 593-610.

Michels, K., 2000. Inferring maximum current velocities in the Norwegian-Greenland Sea from settling-velocity measurements of sediment surface samples: methods, application, and results. Journal of Sedimentary Research, 70(5): 1036-1050.

Milliman, J.D., 1993. Production and accumulation of calcium carbonate in the ocean: budget of nonsteady state. Global Biogeochemical Cycles, 7(4): 927-957.

Mollenhauer, G., Jennerjahn, T., Müller, P.J., Schneider, R.R. and Wefer, G., submitted. Spatial distribution and accumulation of organic carbon in the South Atlantic Ocean: Its modern and glacial contribution to the carbon cycle. Global and Planetary Change.

Paull, C.K., Hills, S.J. and Thierstein, H.R., 1988. Progressive dissolution of fine carbonate particles in pelagic sediments. Marine Geology, 81: 27-40.

Paull, C.K. and Thierstein, H.R., 1987. Stable isotopic fractionation among particles in Quaternary coccolith-sized deep-sea sediments. Paleoceanography, 2(4): 423-429.

Peeters, F., Ivanova, E., Conan, S., Brummer, G.-J., Ganssen, G., Troelstra, S. and van Hinte, J., 1999. A size analysis of planktic foraminifera from the Arabian Sea. Marine Micropaleontology, 36(1): 31-63.

Petschick, R., Kuhn, G. and Gingele, F., 1996. Clay mineral distribution in surface sediments of the South Atlantic: sources, transport, and relation to oceanography. Marine Geology, 130(3-4): 203-229.

Pflaumann, U., Duprat, J., Pujol, C. and Labeyrie, L.D., 1996. SIMMAX: A modern analog technique to deduce Atlantic sea surface temperatures from planktonic foraminifera in deep-sea sediments. Paleoceanography, 11(1): 15-35.

Robinson, S.G. and McCave, I.N., 1994. Orbital forcing of bottom-current enhanced sedimentation on Feni Drift, NE Atlantic, during the mid-Pleistocene. Palaeogeography, 9(6): 943-972.

Sarnthein, M., 1971. Oberflächensedimente im Persischen Golf und Golf von Oman: II. Quantitative Komponentenanalyse der Grobfraktion. Meteor-Forschungsergebnisse, Reihe C(5): 1-113.

Stoll, H.M. and Ziveri, P., 2002. Separation of monospecific and restricted coccolith assemblages from sediments using differential settling velocity. Marine Micropaleontology, 46(1-2): 209-221.

Stuut, J.-B.W., Prins, M.A. and Jansen, J.H.F., 2002. Fast reconnaissance of carbonate dissolution based on the size distribution of calcareous ooze on Walvis Ridge, SE Atlantic Ocean. Marine Geology, 190(3-4): 581-589.

Thunell, R.C., 1982. Carbonate dissolution and abyssal hydrography in the Atlantic Ocean. Marine Geology, 47: 165-180.

van Kreveld, S.A., Knappertsbusch, M., Ottens, J., Ganssen, G.M. and van Hinte, J.E., 1996. Biogenic carbonate and ice-rafted debris (Heinrich layer) accumulation in deep-sea sediments from a Northeast Atlantic piston core. Marine Geology, 131(1-2): 21-46.

Volbers, A.N.A. and Henrich, R., 2002. Present water mass calcium carbonate corrosiveness in the eastern South Atlantic inferred from ultrastructural breakdown of Globigerina bulloides in surface sediments. Marine Geology, 186(3-4): 471-486.

Young, J.R. and Ziveri, P., 2000. Calculation of coccolith volume and it use in calibration of carbonate flux estimates. Deep Sea Research Part II: Topical Studies in Oceanography, 47(9-11): 1679-1700.

Ziveri, P., Broerse, A.T.C., van Hinte, J.E., Westbroek, P. and Honjo, S., 2000. The fate of coccoliths at 48°N 21°W, Northeastern Atlantic. Deep Sea Research Part II: Topical Studies in Oceanography, 47(9-11): 1853-1875.

Appendix

Plate 1: SEM images of isolated size fractions representing the three outstanding MAR provinces in the South Atlantic: **a)** and **b)** Equatorial, **c)** Central, **d)** Southern province (Fig. 1). The images of the right column (indexed 2) are magnifications of the images on the left hand side (indexed 1). For information on composition and size of the coccolith assemblage compare the Figures 6 and 7. The variations in particle coverage are caused by differences in the grain-size composition, since equal sample weights are used and much more finer particles are necessary to equalise the same sample weight.

bar for images if not given separately: $\mathbf{b_1}$, $\mathbf{c_1}$, $\mathbf{d_1}$: 50 µm, $\mathbf{b_2}$, $\mathbf{c_2}$, $\mathbf{d_2}$: 10 µm

a) Clay fraction of GeoB 1903 (Equatorial MAR province). The clay fraction of the calcareous oozes consist almost exclusively of relatively small coccoliths, that have an equivalent spherical diameter (ESD) of < 2 µm although their nominal diameter can exceed 5 µm. The blurry image ($\mathbf{a_1}$) illustrates the effect of higher particle density at lower grain sizes at same amount of sample material. Prominent species found in this province in the clay fraction are *E huxleyi, F. profunda* and *U. sibogae*. Small abundances of larger species are observed as well. [bar of $\mathbf{a_1}$ 50 µm, bar of $\mathbf{a_2}$ 5 µm]

b) Silt fraction of GeoB 1903 (Equatorial MAR province). These images illustrate, what the fine and coarse silt peaks are composed of, respectively. The few foraminifer fragments observed equal the weight of much more coccoliths present to grain size distributions observed in upper Figure 4. **$\mathbf{b_2}$)** The coccolith assemblage is inhomogeneous with high contributions of *C. leptoporus* large (B), *Helicosphera carteri* and *Umbilicosphera sibogae*.

c) Silt fraction of GeoB 1415 (Central MAR province). The inhomogeneous particle composition causes the pillow shaped size distributions observed in the Central MAR province (Fig. 4). In this multi-species sample *C. leptoporus* intermediate and small (A+C), *R. clavigera* and *U. sibogae* are prominent.

d) Silt fraction of GeoB 6418 (Southern MAR province). This sample represents an almost pure powder of *C. leptoporus* intermediate and small (A+C), which makes up about 80 % of the assemblage (Fig. 6). The most frequent species of the whole sample (*E huxleyi, F. profunda*) are almost completely excluded by removing the clay fraction (< 2 µm) in settling tubes.

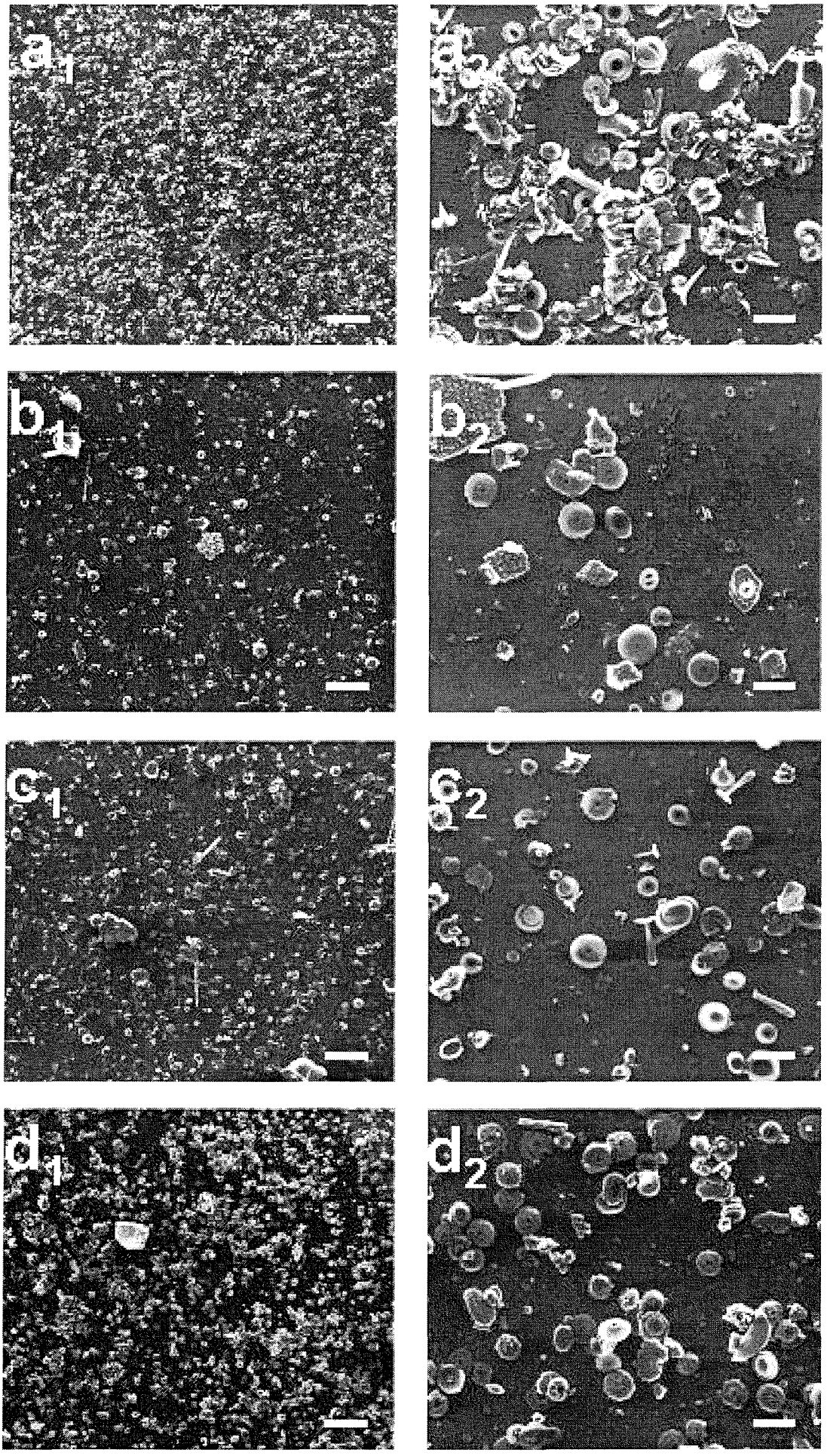
a1
a2
b1
b2
c1
c2
d1
d2

CARBONATE DISSOLUTION REVEALED BY SILT GRAIN-SIZE DISTRIBUTIONS: COMPARISON OF HOLOCENE AND LAST GLACIAL MAXIMUM SEDIMENTS FROM THE PELAGIC SOUTH ATLANTIC

M. Frenz * and R. Henrich

FB Geowissenschaften, Universität Bremen, Postfach 330440, D-28334 Bremen, Germany

** corresponding author, e-mail: mfrenz@uni-bremen.de*

Abstract

South Atlantic pelagic sediments from the Holocene and the Last Glacial Maximum (LGM) were investigated with respect to their grain-size composition (sand/silt/clay relation and grain-size distributions of the carbonate silt). This approach deals with two major aspects of the pelagic sedimentation: carbonate production and dissolution, and how these processes are reflected in the grain-size distributions of the sediments. For the Holocene time slice at water depths above a certain critical level the size composition reveals high contribution of calcareous zooplankton (mainly foraminifers) in the mesotrophic regions at and beyond the equator. In the oligotrophic Central South Atlantic coccoliths contribute most to the carbonate budget of the sediments. The size composition of the calacareous sediment compounds changes significantly below a certain critical water depth, which is therefore referred to as the sedimentary lysocline. For the Holocene its vertical position indicates the expected asymmetry between the Brazil and Cape Basins on the one hand (≈ 4200 m water depth) and the Angola Basin on the other hand (≈ 4600 m water depth) according to the modern watermass distribution. The size composition of LGM sediments suggests that, compared to the modern situation, the sedimentary lysocline was raised to water depths of about 3000 m during this time interval. An asymmetry in the water mass distribution as observed for the modern situation did not exist for the LGM. Additionally, in all investigated open ocean settings supralysoclinal dissolution was observed by a constant decrease of foraminifer carbonate of about 5-10 % per 1000 m water depth for the benefit of the more dissolution resistant coccolith carbonate.

Keywords: South Atlantic, Holocene, Last Glacial Maximum, calcareous sediments, carbonate dissolution, foraminifers, coccoliths, grain size

submitted to Sedimentology

1 Introduction

1.1 Objectives and Motivation

In the focus of the ongoing climate discussion, large efforts have been devoted to evaluate the role of the ocean in the global exchange of CO_2. This requires the development of solid budgets for marine carbonate production and dissolution under different oceanic regimes. Dissolution is a complex process being affected by various factors, e.g. hydrostatic pressure, differential pCO_2 and CO_3^{2-} concentrations of intermediate and deep water masses as well as grain size, mineralogy, crystallography and texture of carbonate tests (Henrich and Wefer, 1986). Various approaches to assess the influence of these different factors and to reconstruct the lysocline and compensation depth levels for aragonite and calcite in various parts of the oceans were carried out already in the sixties and seventies of the nineteenth century (see review by Berger, 1979). Depending on the proxies used, the reconstructions of the dissolution levels differ considerably (see review by Henrich et al., in press). In addition, there is an ongoing discussion regarding the magnitude and the intensity of supralysoclinal dissolution at various levels of the oceans. Supralysoclinal dissolution is induced by the degradation of organic matter in the water column as well as close to or at the sediment/water interface (Jahnke et al., 1994; Archer, 1996). Recently, Milliman et al. (1999) suggested that as much as 60 to 80% of the originally produced carbonate might be dissolved by biological mediation in the upper water masses above the hydrographic lysocline.

Benefits and pitfalls of different conventional dissolution proxies based on sedimentologic and micropalaeontologic properties are discussed by Henrich et al. (in press). The basic idea behind all these bulk sediment and microfossil parameters is the progressive breakdown of carbonate particles during dissolution. By this: (1) The amount of carbonate is diminished, i.e. bulk carbonate contents, sand percentages and the grain size of the particles decrease, whereas the number of fragments increases. (2) Planktic foraminifer species assemblages are modified by preferentially removing surface dwellers with thin porous walls and enriching deep-dwelling thick-walled more robust shells. (3) The more soluble planktic foraminifers are preferentially removed, passively enriching benthic foraminifers and radiolarians. However, in many cases the above mentioned conventional proxies fail or produce incorrect and misleading results. The processes responsible for this failure are manifold: (1) The bulk sediment parameters might be affected by dilution with non-carbonate material (e.g. input of dust material, river supply of terrigenous fine grained sediments), downslope re-suspension and lateral advection, or by winnowing of sediment by bottom currents. (2) The microfossil parameters might respond to changes in ecology through time. In order to avoid these discrepancies new SEM and light microscope dissolution proxies were developed for planktic foraminifers (Henrich et al., 1989; Volbers and Henrich, 2002b) and pteropods (Gerhardt and Henrich, 2001). These are the only

proxies that determine the state of calcium carbonate preservation on at least semi-quantitative scales and are not affected by other factors beside dissolution.

1.2 General aspects on the composition of calcareous pelagic sediments and their grain-size distributions

Pelagic carbonate consists of the following three main particle groups: planktic foraminifers and pteropods contributing to sand and coarse silt size classes, and coccoliths contributing to the fine silt and clay size spectra. Hence, it is obvious that variations in production rates of these particle groups will change the grain-size characteristic in the silt fraction of pelagic carbonate sediments. On the other hand, it is also clearly evident from the above mentioned processes, that intensified fragmentation during dissolution will result in a progressive transfer of particles from coarser to finer size classes. Hence, by analysing grain-size characteristics of the CS fraction the influence of these two differentially operating processes may be assessed. Up to now, such an approach has been considered only in very few studies, and, in particular, a calibration study in modern environments is still lacking.

Recently the potential to deduce the state of carbonate preservation from grain-size parameters was independently discovered by Gröger et al. (submitted) and Stuut et al. (2002) using different size fractions and methods. Gröger et al. (in press) investigated calcareous silt grain-size spectra in the Quaternary record of ODP Sites in the equatorial Atlantic at the Ceará Rise with a Micromeritics SediGraph 5100. They show by comparison with planktic foraminifer fragmentation proxies that with progressive dissolution the overall calcareous silt content and the coarse calcareous silt mode decreases and that values for the mean and modal grain size in the coarse silt fraction diminishes consistently. Parallel to this, the amount of calcareous clay increases indicating a continuous transfer of particles from coarser to finer grain sizes. Stuut et al. (2002) used a laser-particle sizer for measurements of grain-size characteristics in Quaternary calcareous sediments from the Walvis Ridge. They defined a new dissolution index as the log-ratio of two coarse modes, mode A (25-90 μm) and mode B (> 90 μm). Similar to Gröger et al. (submitted), they related the decrease in the coarsest mode to progressive carbonate dissolution. Both studies assume that the production rates of the contributing particle groups remained constant through time. That this is not always the case becomes clearly evident from studies of South Atlantic surface sediments by Baumann et al. (in press) and Frenz et al. (submitted).

Baumann et al. (in press) compiled the contribution of the various calcareous plankton groups to the carbonate budget of surface sediments in the South Atlantic. They attributed the spatial variations in the distribution pattern to differences in production which is induced by the fertility of the upper ocean environment and differences in the solubility of the diverse plankton groups. According to these authors, foraminifers and coccoliths are the major components of pelagic carbonate. Coccolith carbonate dominates the sediments

below the oligitrophic gyres of the South Atlantic, while carbonate derived from foraminifers increases in mesotropic areas like the equatorial divergence zone. The general decrease of foraminifer carbonate in relation to that of coccoliths with increasing water depth is ascribed to the higher dissolution susceptibility of foraminifers compared to coccoliths.

Frenz et al. (submitted) found a general bimodality in the carbonate silt fraction (CS) of pelagic surface sediments in the South Atlantic using a SediGraph, as was observed in earlier studies (Robinson and McCave, 1994; McCave et al., 1995) for Pleistocene drift sediments in the NE Atlantic. By means of SEM investigations it was concluded that the prominent minimum at 8 µm separates foraminifer fragments and juvenile tests from coccoliths. Extending this division to the carbonate of the sand and clay fraction respectively, the division at 8 µm allows a differentiation of foraminifer and coccolith carbonate with high precision, given that the sediments do not contain appreciable amounts of pteropods and calcareous dinoflagellate cysts. The inclusion of the coarse CS to the foraminifer population increases this plankton group by about 10 to 20 % in comparison to the foraminifer carbonate estimated by Baumann et al. (in press) based on the sand fraction. As will be shown here, the coarse mode strongly varies with water depth indicating the influence of carbonate dissolution. In contrast, the grain size of the fine carbonate mode shows a high size stability within one region. This is assumed to result from the similarity of the coccolith assemblage within one region. The differences in the fine mode size between the provinces are attributed to regional variations in the nannoplankton assemblage in the South Atlantic as recorded by, e.g. McIntyre and Bé (1967) as well as Boeckel et al. (submitted-b).

In conclusion, investigations of silt grain-size spectra clearly bear a high potential to evaluate variations in production and preservation patterns of pelagic carbonates, at least at semi-quantitative scales. However, studies considering both processes adequately and calibrating them on the modern environmental settings are still lacking. In this study we intend to fill this gap by investigating silt grain-size characteristics of pelagic South Atlantic surface sediments. In addition, the results attained from analysing modern settings will be compared with those determined for Last Glacial Maximum (LGM) sediments at the same locations.

1.3 Modern and LGM ocean circulation in the South Atlantic

Since the distribution pattern of the different water masses and their physical and chemical properties have a crucial influence on the preservation of carbonate, in this paragraph the modern and Last Glacial Maximum (LGM) oceanography of the South Atlantic is introduced shortly.

The modern circulation of the Atlantic Ocean is characterised by a net northward movement of water masses of southern source and a compensating southward movement of water masses of northern origin. In general, the density stratification of the water masses

is steered by their physical and chemical properties. It results in the classical four-level structure of the water column (Wüst, 1935). The Thermocline Water of the upper ocean follows roughly the atmospheric circulation pattern, building the subtropical gyres. At intermediate water depths Antarctic Intermediate Water (AAIW) and the upper branch of Circumpolar Deep Water (UCDW) flow northward. Roughly, below 4000 m water depth Antarctic Bottom Water (AABW) moves northward as the densest and deepest water body. It is composed of Weddell Sea Deep Water (WSDW) and the lower branch of Circumpolar Deep Water (LCDW). Between both water bodies the North Atlantic Deep Water (NADW) flows south at water depth between about 1500 and 4000 m (Fig. 1).

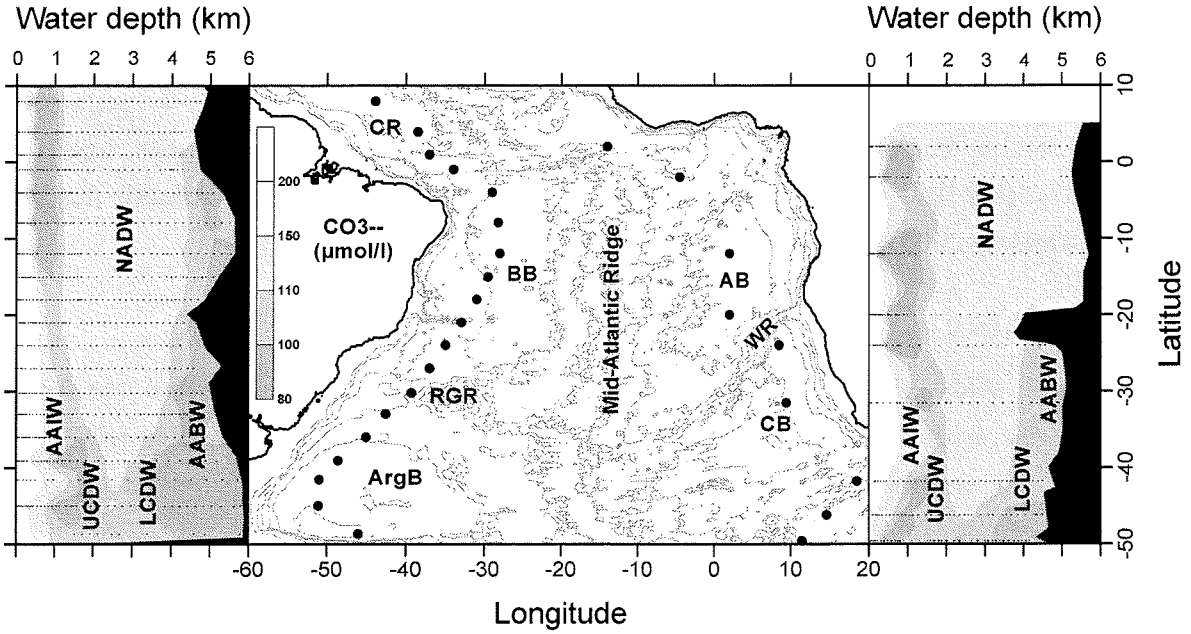

Fig. 1: *Present water mass distribution of the eastern and western South Atlantic according to interpolated carbonate-ion concentrations taken from GEOSECS (1999). Note the asymmetry between the Brazil and Angola Basins. The dots in the centered map indicate the position of the GEOSECS stations along which the profiles run. Essential bathymetric features are indicated as follows: AB – Angola Basin, ArgB – Argentine BB – Brazil Basin, CB – Cape Basin, CR – Ceará Rise, RGR – Rio Grande Rise, WR – Walvis Ridge.*

Besides temperature and pressure the most important water-mass property with respect to carbonate dissolution is the state of carbonate-ion saturation. The intermediate and deep water masses of southern origin display weak to strong undersaturation of carbonate ions ($CO_3^{2-} < 90$ µmol kg^{-1}). The NADW, in contrast, is oversaturated with respect to CO_3^{2-} ($CO_3^{2-} > 110$ µmol kg^{-1}, (Broecker and Peng, 1982; Dittert et al., 1999)). Therefore, the dissolution of carbonate is increased in AAIW, CDW and AABW water levels, whereas NADW fosters enhanced carbonate preservation (Fig. 1).

Additionally, the distribution of AABW in the South Atlantic is controlled by submarine barriers like the Mid-Atlantic and Walvis Ridges. Since only small quantities of AABW are able to cross the sills of the Romanche Fracture Zone and Walvis Passage, the eastern Guinea and Angola Basins are predominantly filled with NADW (e.g. Shannon and Chapman (1991) and Warren and Speer (1991)).

There exists a prominent vertical boundary in the water column where carbonate dissolution increases significantly, leaving highly corroded carbonate compounds. This level is referred to as the sedimentary lysocline. In the modern western South Atlantic and the Cape Basin the sedimentary lysocline is predominantly tied to the interface between NADW and AABW (Volbers and Henrich, 2002b).

It is assumed that during the LGM the circulation pattern differed considerably from the pattern described above. A reduced production in combination with a southward shift of the formation region of NADW (Stocker, 1998) lead to the formation of a less dense water mass referred to as Glacial North Atlantic Intermediate Water (GNAIW, Boyle and Keigwin (1987), Oppo and Lehman (1995)). On the other hand, corrosive waters of southern origin expanded vertically, which enabled these water masses to intrude the Angola and Guinea Basins. Consequently, the position of the hydrographic lysocline was raised to shallower water depth. Recent studies using benthic stable isotopes, however, indicate that this shift was restricted to the sector of the eastern marginal Atlantic (Bickert and Mackensen, 2003).

2 Methods

The present study bases on grain-size analyses of sediment samples from the South Atlantic. The samples were recovered during several cruises with the RV METEOR between 1988 and 1998 using multi-, box- and gravity corers. The sampled sites are grouped into four provinces (Fig. 2):

A) Ceará Rise (A1) and Northwestern Mid-Atlantic Ridge (A2)
B) Equatorial Mid-Atlantic Ridge
C) Mid-Atlantic Ridge of the Central South Atlantic
D) Walvis Ridge

Furthermore, the provinces B to D are subdivided into the flanks that slope to different Atlantic basins (Fig. 2). This is necessary since a different water mass structure has to be considered in the four sub-basins of the South Atlantic. Particularly significant differences are evident between the Brazil and Angola Basins (Fig. 1).

Generally, the investigated sediments originate from tops and beyond bathymetric highs. The samples fulfil important requirements: (1) relatively high carbonate contents (> 20 %, see concluding remarks) to allow the derivation of reasonable carbonate grain-size distributions from bulk and carbonate-free measurements, (2) relatively high spatial coverage of surface samples for calibration, (3) the availability of corresponding LGM samples for comparison.

All surface samples are assumed to be of Holocene age. Variations up to several hundred to thousand years may occur depending on the local sedimentation rate (Gerhardt and Henrich, 2001).

The time interval of the LGM was fixed at 19-23 ka B.P. (calendar years) following the recommendations of the EPILOG group (Mix et al., 2001). The sampling on this time

interval is based on the so called "LGM-Liste" whose stratigraphic control is given by Niebler et al. (submitted). The depth of this time interval for dated GeoB cores is available at the internet site http://www.pangaea.de/Institutes/GeoB/Cores/LGM.html. Because the thickness of this time interval depends on the sedimentation rate, the sampling strategy was to have at least one LGM sample where this interval is rather thin, and up to 5 samples spaced at narrow distances (2-10 cm) within the intervals which have higher LGM thickness. Additionally, one sample above and below the LGM interval were included. Altogether, 89 surface samples and 94 samples from 27 sites where the LGM was recovered were analysed for this study (Fig. 2).

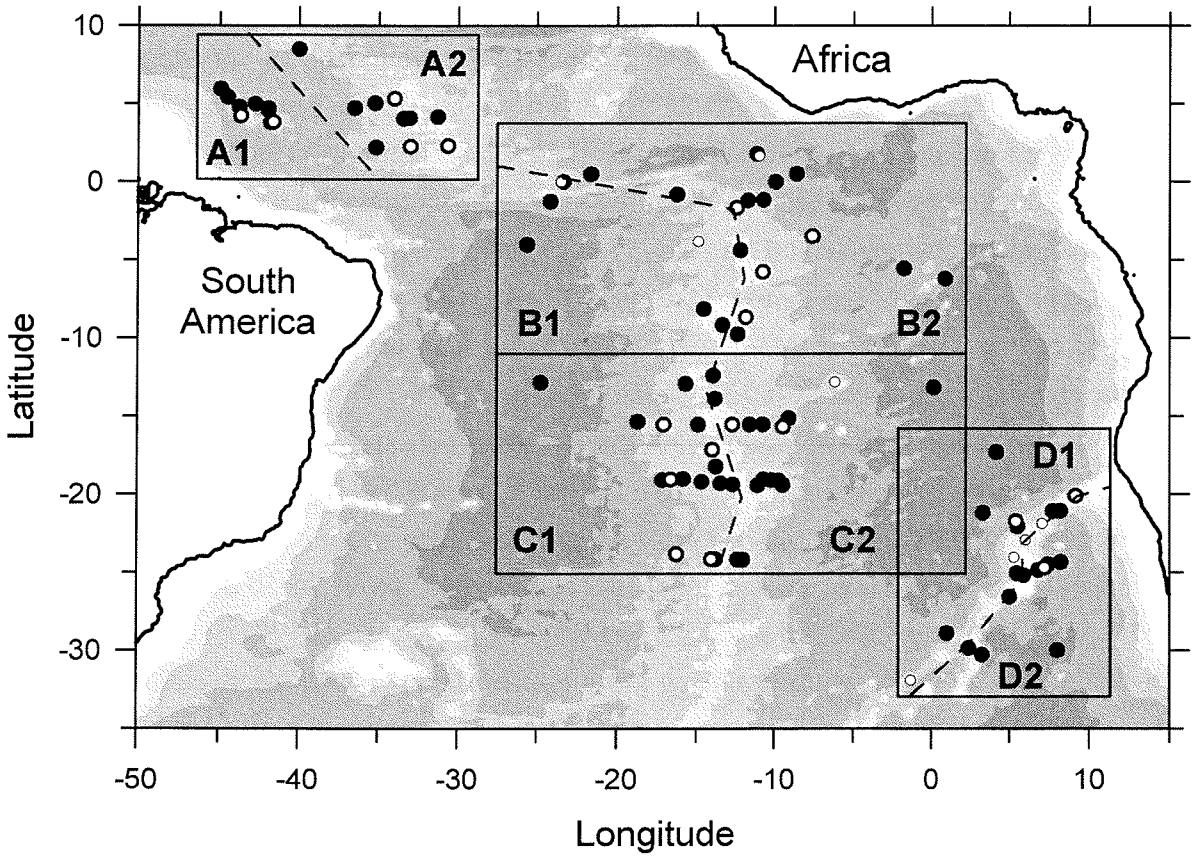

Fig. 2: Basic bathymetry of the South Atlantic including sample locations for Holocene (•) and LGM samples (○) analysed in this study. The boxes with letters indicate the provinces: A_1 – Ceará Rise, A_2 – NW' MAR, B – Equatorial MAR, C – Central MAR, D – Walvis Ridge. The latter three are subdivided into eastern/western or northern/southern slopes as indicated by the dashed line.

All samples underwent the analytical procedure described in detail in Frenz et al. (submitted). This procedure briefly comprised the splitting of the bulk sediments into sand (> 63 µm), silt (63-2 µm) and clay (< 2 µm) size fractions, the repeated grain-size analysis of the silt fraction using a SediGraph 5100 including a quantitative decarbonisation between the two runs, and the calculation of the carbonate silt (CS) grain-size distribution from the two measurements. Finally, the statistical parameters of the size distributions were calculated according to Krumbein (1936).

3 Results

3.1 General characteristics of Holocene grain-size signatures

Generally, the bulk sand and clay contents of the surface sediments reveal a negative correlation. With increasing water depth sand decreases while clay increases (Fig. 3). Above a certain critical water depth this change preceeds gradually (sand decreases from 70 to 50 %, clay increases from 10 to 40 %). Below the critical water depth minimum (< 10 % sand) and maximum values (> 90 % clay) are approached. Regionally this critical water depth level varies broadly between 4000 and 5000 metres (Fig. 3). In contrast to the contents of sand and clay, the silt content remains relatively stable throughout all water depths (10-30%). The carbonate content of the silt fraction remains very high (> 90 %, except Ceará Rise/NW' MAR: 70-80 %) down to a critical water depth, as already observed for sand and clay. Below it decreases significantly to 10-20 % (Fig. 3).

Generally, the CS reveals a bimodal size frequency distribution with a prominent minimum at about 8 μm, where coarse and fine CS is separated (Fig. 4). Above the mentioned critical depth the proportions of coarse (63-8 μm) and fine CS (8-2 μm) are relatively constant (i.e. 50-80 % coarse CS). Below this distinct water depth the proportion shifts significantly to the fine share leaving about 20-60 % coarse CS (Fig. 3).

Above the mentioned critical water depth the size distribution of the coarse CS (referred to as "coarse mode") is more or less stable (Ceará Rise/NW' MAR) to slightly decreasing with increasing water depth (i.e. other provinces). Besides a slight decrease in amplitude the mean grain size of the coarse mode decreases from about 25-30 μm to 20 μm, the modal grain size from about 40 μm to 25 μm (Fig. 5).

Below the critical water depth the mean grain size of the coarse CS decreases to < 20 μm. As a clear shift this decline in coarse mean size is only obvious in the Ceará Rise/NW' MAR province, whereas in the other provinces the size decrease is further continued down to the deeper parts of the basins. Taking the modal grain size into account also in the Equatorial province a considerable decrease in the grain size of the coarse mode is observed, e.g. as a drop of mean and modal size from > 20 μm to < 15 μm (Fig. 5).

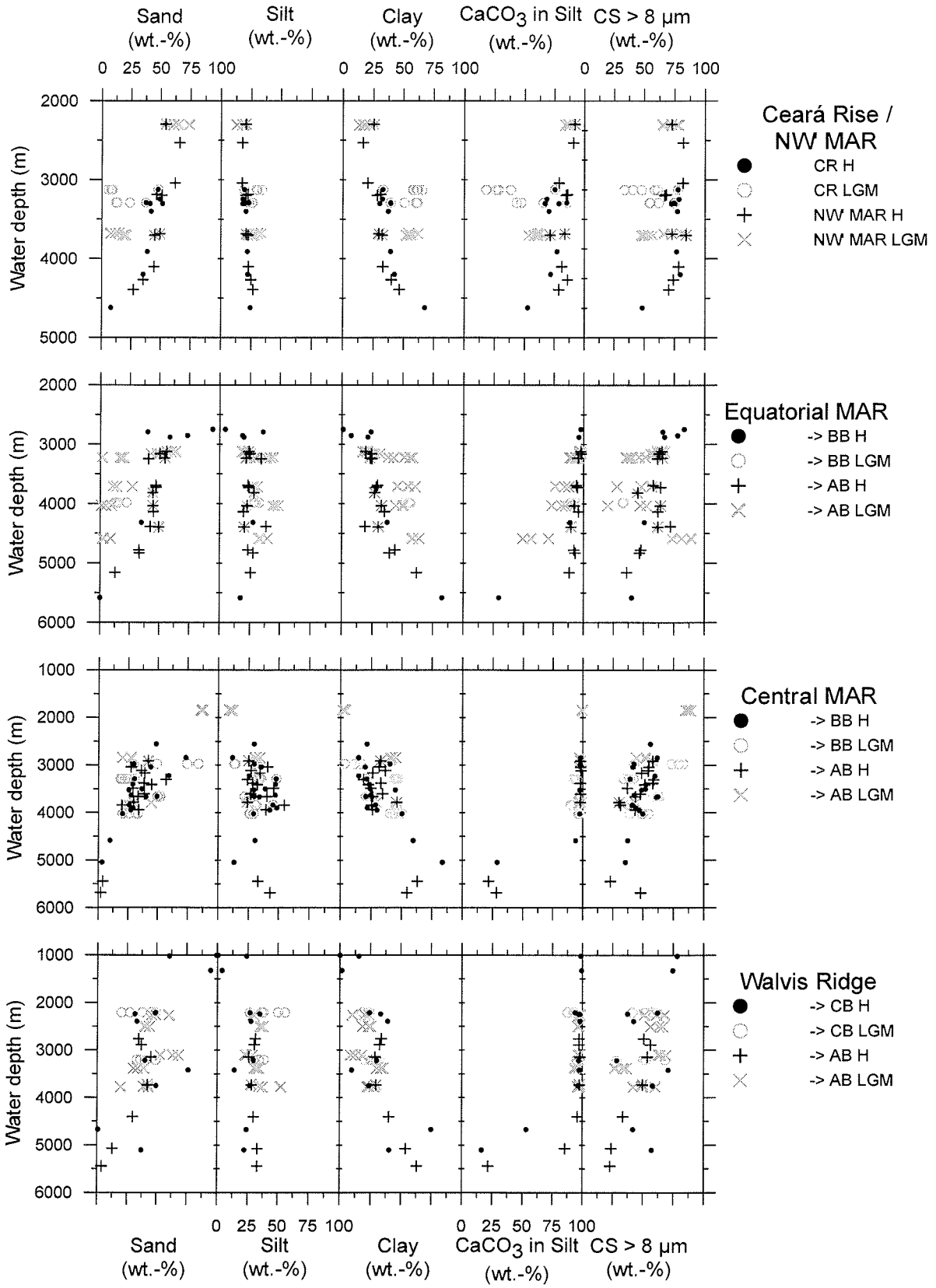

Fig. 3: Bulk sedimentological parameters for the provinces as indicated by Fig. 2 in relation to water depth. Black symbols represent the Holocene (H) time slice, light symbols represent samples from the LGM which, aligned at one water depth, belong to the same sediment core. Data for the Holocene of the Equatorial and Central MAR provinces (except below 4000 m) taken from Frenz et al. (submitted).

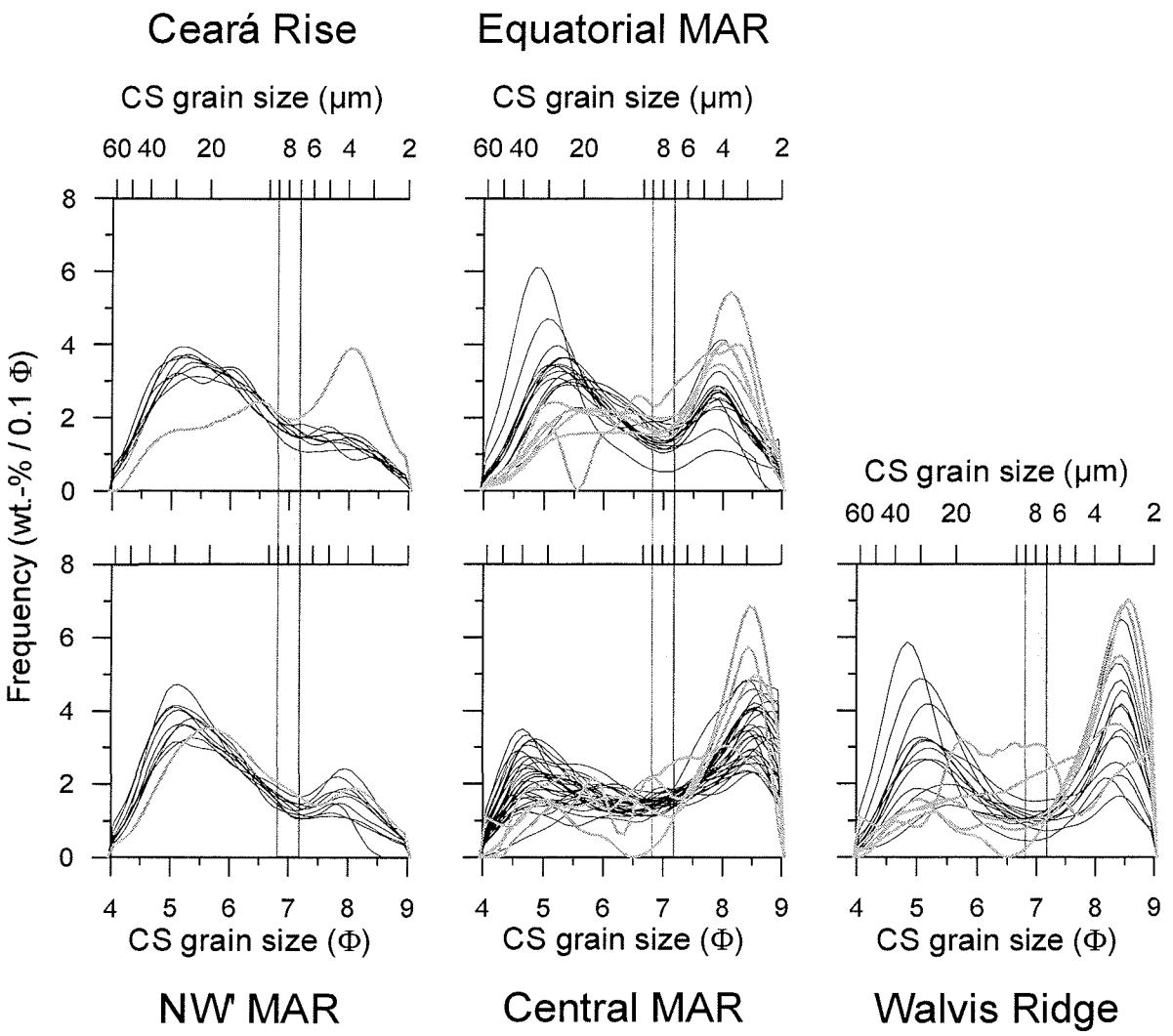

Fig. 4: *CS grain-size distributions for the provinces as indicated by Fig. 2. The grey bar indicates the position of the generally observed frequency minimum (8 µm/7 Φ) which separates the coarse (foraminifer fragments) from fine CS (coccoliths). The grey indicated samples originate from below the critical water depth. These samples reveal a decrease in size and amplitude of the coarse mode, while the fine silt shows highest amplitudes at constant size. The upper axes generally give µm while the lower axes show Φ-units. Size distributions of the Equatorial and Central MAR provinces (except grey ones) taken from Frenz et al. (submitted).*

Due to the closed sum relation for the frequency distributions (i.e. sum of all classes = 100 %) the decrease in the coarse mode is connected with an increase in the fine mode. However, this increase affects almost exclusively the amplitude as indicated by the size parameters of the fine CS (Figs. 4, 5). All samples from below the critical water depth show the highest amplitudes in the fine mode, while the modal as well as the mean grain size remains almost constant (Fig. 4)

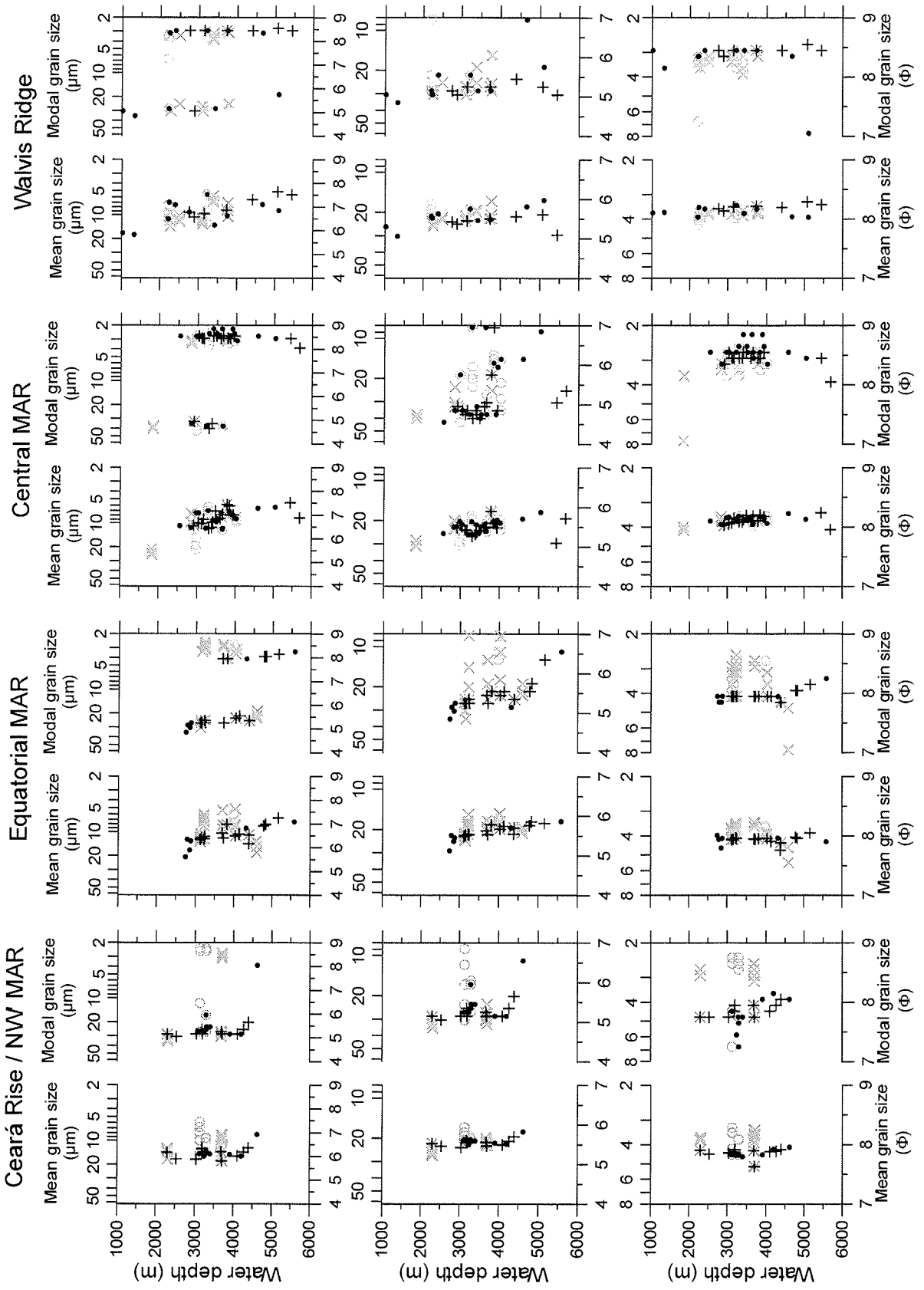

Fig. 5: *Statistical mean and modal grain size for the whole (upper), the coarse (middle) and fine size range of the CS (lower panel) of samples from the four provinces as indicated in Figure 2. The upper axes generally give µm while the lower axes show Φ-units. For legend compare Figure 3. Data for the Equatorial and Central MAR provinces (except below 4000 m) taken from Frenz et al. (submitted).*

With regard to the total silt size-spectrum the increase of the fine CS on the expense of the coarse share with increasing water depth is recorded by a decrease of the mean size and a switch of the modal size from coarse to fine (Fig. 5). Depending on the proportion of fine and coarse CS at shallow water depths this switch occurs already well above the critical water depth (Figs. 5).

To infer the critical water depth for each of the South Atlantic sub-basins the samples need to be differentiated according to their position at the western / eastern (MAR), or southern / northern slopes (Walvis Ridge) and not simply according to their regional settings.

Table 1: *Vertical position (water depth) of observed significant change in sediment composition of surface samples from the Brazil, Angola and Cape Basins*

Basin	Province and depth level of observed change		Confined depth
Brazil Basin	Ceará Rise/NW' MAR	4100-4200 m	**4100-4200 m**
	Equatorial MAR	insuff. Data coverage	
	Central MAR	4100-4500 m	
Angola Basin	Equatorial MAR	4400-4700 m	**4500-4700 m**
	Central MAR	4000-5400 m	
	Walvis Ridge	4500-5000 m	
Cape Basin	Walvis Ridge	3700-4500 m	insuff. Data coverage

3.2 Comparison of Holocene and LGM sediment grain-size characteristics

LGM sediments at water depths between about 3000 and 4000 m reveal a size composition which is very different from Holocene samples of the same locations (Fig. 3). For the Ceará Rise/NW' MAR and Equatorial MAR provinces the sand content is reduced from about 50 % in the Holocene sediments to less than 10 % in LGM sediments, whereas the clay content increases from about 30 % (Holocene) to considerable 70 % (LGM). In addition, the LGM samples reveal an overall silt increase by about10-20 % compared to their Holocene counterparts. The carbonate content of the silt fraction can be reduced to below 50 % in LGM sediments. The prevalence of the coarse silt share in the Holocene is reversed so that in LGM sediments only about one third to one fourth of the CS is coarser than 8 μm.

In the Central MAR province a similar trend is observed for the same water depth interval, however in a alleviated manner. Compared to the Holocene here the sand content of LGM samples decreases to 20 %, whereas clay increases to 50 %, leaving generally about 30 % silt. At least on the western flank of the Central MAR the carbonate content in the silt fraction decreases from Holocene values of 99 % to 90 % in the LGM. The slight predominance of coarse CS in the Holocene for most of the samples is reversed in the LGM. For the Walvis Ridge province clear deviations from Holocene to LGM are observed only in a general increase of the silt from 30 % in the Holocene to 40 % during the LGM and a decrease in the clay content from 30 % (Holocene) to below 10 % (LGM).

All other bulk parameters may deviate hardly, or be inconsistently both, negatively or positively, correlated to Holocene patterns.

However, differences between Holocene and LGM samples appear much more pronounced with regard to the CS grain-size distributions (Figs. 6-9). The down-core variation of the CS grain-size distributions of most cores reveals a distinct decrease of the coarse mode and an increase of the fine mode, particularly regarding a clear rise in amplitude. This pattern manifests as a complete disappearance (e.g. GeoB 1041, Fig. 7) or considerable weakening (e.g. GeoB 1023, Fig. 9, GeoB 1101, Fig. 7) of the coarse mode, which in turn may be partly connected with a shift to finer grain sizes (e.g. GeoB 5140, Fig. 8). If not already recognised in Holocene samples, in most cases a fine silt mode develops (e.g. GeoB 1505, Fig. 6) or is amplified in the LGM samples (e.g. GeoB 2215, Fig. 7).

In the grain-size parameters this pattern is expressed by a switch from the coarse to the fine modal grain size for most of the LGM samples (Fig. 5). Additionally, the mean grain size of the coarse share in the LGM sediments reveals values below 20 μm, i.e. values recorded only for deepest samples in the Holocene sample set. Especially in the Equatorial and Central MAR provinces the coarse modal grain size shows a strong decrease [Equatorial MAR: 30 μm (Holocene) to 10 μm (LGM), Central MAR: 40 μm (Holocene) to < 20 μm (LGM)]. At the Ceará Rise/NW' MAR and Equatorial MAR provinces LGM samples display normally a size decrease for the fine mode (i.e. by about 1 μm for the mean and by about 2 μm for the modal size). In contrast, in the Central MAR and Walvis Ridge provinces the mean grain size of the fine mode increases slightly by about 0.5-1 μm from Holocene to LGM.

Very shallow LGM samples are of exceptional relevance for the discussion. In the provinces Ceará Rise/NW' MAR (GeoB 1503), Equatorial (GeoB 1112 and 1903) and Central MAR (GeoB 1408) the LGM samples from the shallowest sites reveal almost no differences relative to the Holocene trends, concerning all parameters studied (Figs. 3, 5). These samples show high contents of sand, high carbonate values in the silt, a high proportion of the > 8 μm fraction, but low clay contents. The relative coarse CS grain-size distributions in these LGM samples compare well with those from shallow Holocene sites. At the Walvis Ridge no sample was available to confirm such a pattern for this province.

Analogue to the Holocene, the water depth interval between the shallow samples that follow the coarse Holocene trend and the deviating LGM trend can be used to trace the critical water depth for the LGM (Tab. 2).

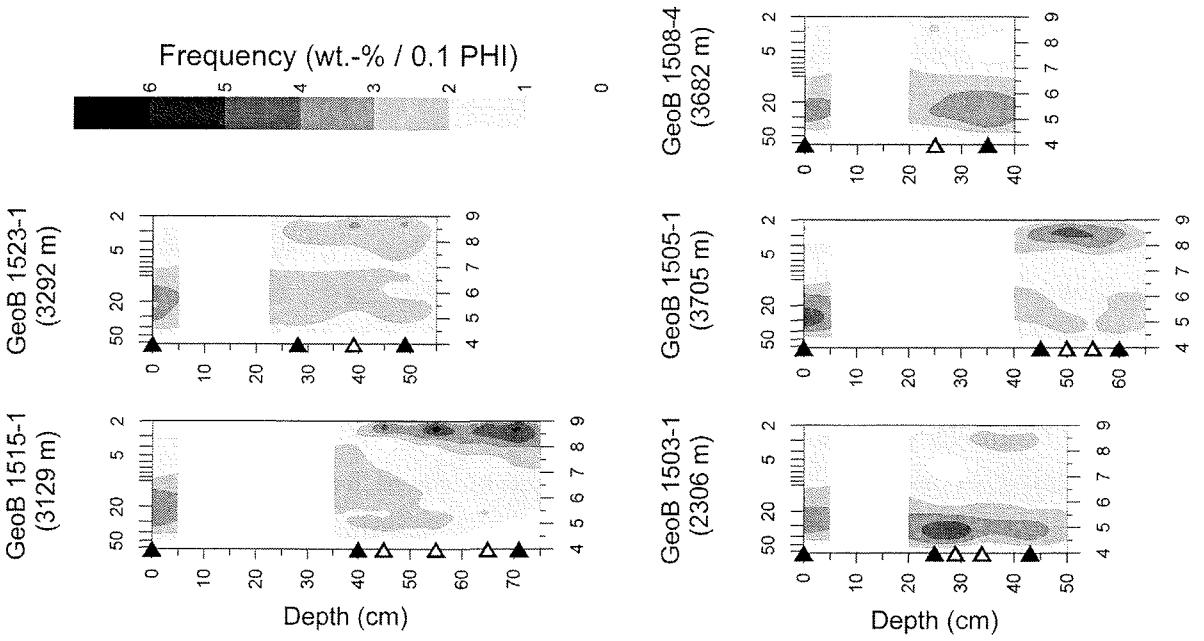

Fig. 6: *Downcore-presentation of the grain-size frequency distributions for the CS fraction of LGM-bearing GeoB-cores from the Ceará Rise (upper two) and Northwestern MAR provinces (lower three). The numbers below the core ID shows the modern water depth. Triangles on the depth scale indicate the sampling depth in the cores along which the variations in size frequency are most reliable. Open symbols indicate strict LGM samples. Areas of low sample coverage are blanked. Darker colours indicate higher frequency as given by the scale. Upper scale shows the grain size in μm the lower scale in Φ-units*

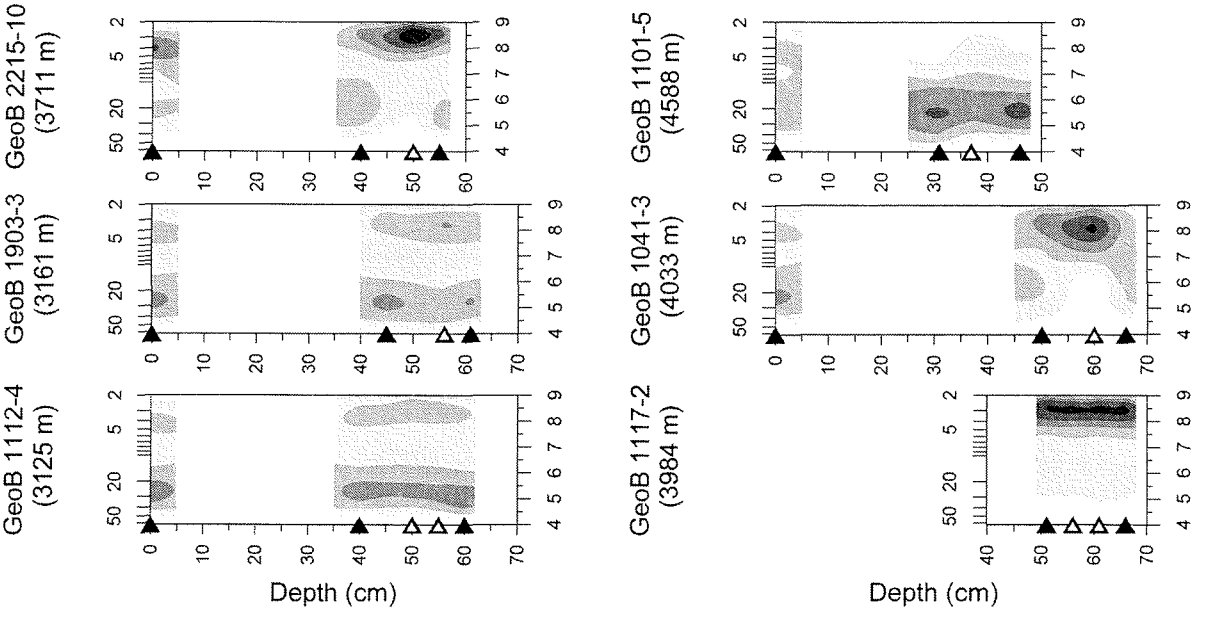

Fig. 7: *Same as Figure 6 for samples from the equatorial MAR province. Scales refer to Figure 6 as well.*

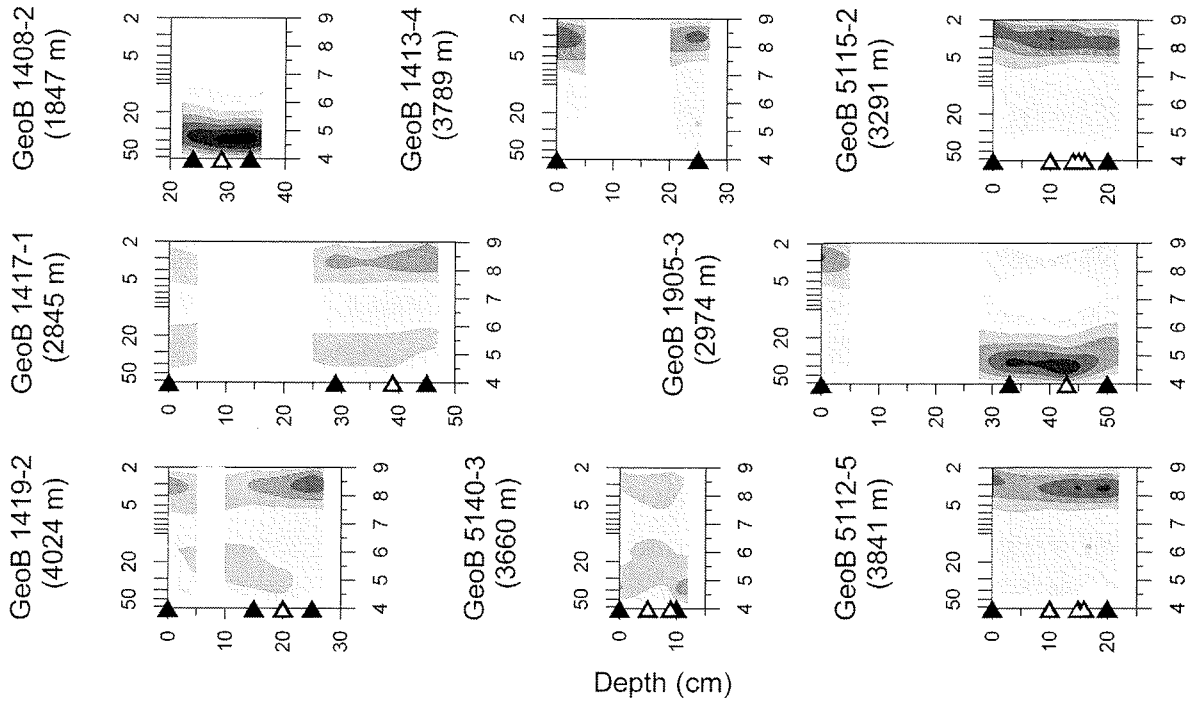

Fig. 8: *Same as Figure 6 for samples from the central MAR province. Scales refer to Figure 6 as well.*

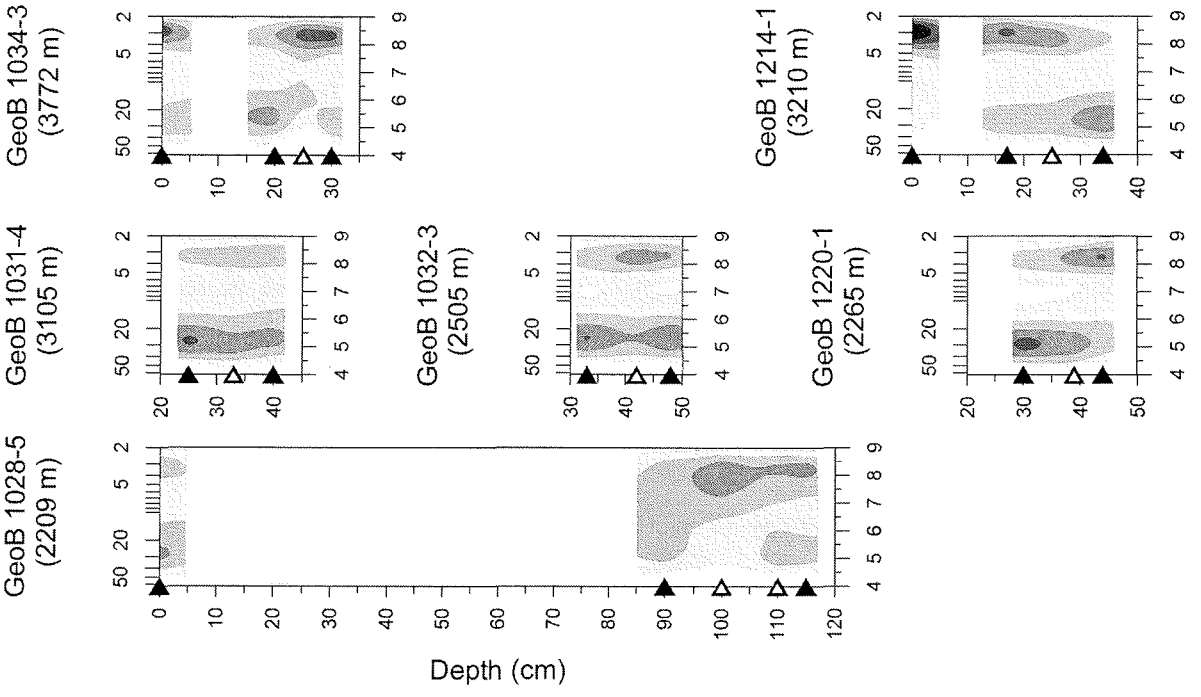

Fig. 9: *Same as Figure 6 for samples from the Walvis Ridge province. Scales refer to Figure 6 as well.*

Table 2: Vertical position (water depth) of observed significant change in sediment composition of LGM samples from the Brazil and Angola Basins

Basin	Province and depth level of observed change		Confined depth
Brazil Basin	Ceará Rise/NW' MAR	2300-3100 m	**3000-3100 m**
	Equatorial MAR	insuff. Data coverage	
	Central MAR	3000-3300 m	
Angola Basin	Equatorial MAR	3200 m	**< 3200 m**
	Central MAR	1900-2900 m	
	Walvis Ridge	insuff. Data coverage	
Cape Basin	Walvis Ridge	insuff. Data coverage	insuff. Data coverage

Altogether, there exists a critical water level in the LGM comparable to that observed in modern conditions below which the sediment (grain-size) composition differs significantly from that of shallower sites. Compared to the Holocene, this level is determined at shallower water depths between 3000 and 3200 m, showing only minor variances between the different sub-basins of the South Atlantic. In contrast to the modern situation the asymmetry between the Brazil and Angola Basins is not existent in the LGM.

4 Discussion

4.1 Regional characteristics of carbonate production and sedimentation in the South Atlantic

The characteristic grain-size patterns observed in the investigated provinces (Figs. 3, 4) are primarily related to differential production and sedimentation rates of planktic organism remains, mainly foraminifer shells and coccoliths. Above the critical water depth mentioned, carbonate dissolution is primarily of minor importance, because the investigated provinces are not situated in eutrophic areas with high accumulation rates of organic carbon. Therefore the sediment composition can be assumed to be the direct imprint of the particles produced within the upper ocean.

In the Ceará Rise sub-province generally low carbonate contents are observed (60-80 %, Fig. 10). The biogenic opal content together with organic carbon does not exceed 1 % (Rühlemann et al., 1996). Therefore, the relatively low carbonate contents are predominately attributed to terrigenous dilution originating from the Amazon river. Its discharge of suspended matter was estimated to about 1200 Mt a^{-1} (Gaillardet et al., 1997). By means of clay mineral composition Rühlemann et al. (2001) excluded appreciable input of eolian dust from Saharan sources. The distribution of the very fine-grained terrigenous constituent (Fig. 11) is controlled by the Amazon fresh water plume and the equatorial surface-current system (Rühlemann et al., 2001). The terrigenous export is mainly carried by the Northern Brazil Current to the northwest. A minor proportion of the Amazon input reaches the NW' MAR sub-province via the North Equatorial Counter Current (Zabel et

al., 1999). However, the longer distance from the source results in lower terrigenous dilution and therefore higher carbonate contents compared to the Ceará Rise sub-province (Fig. 10).

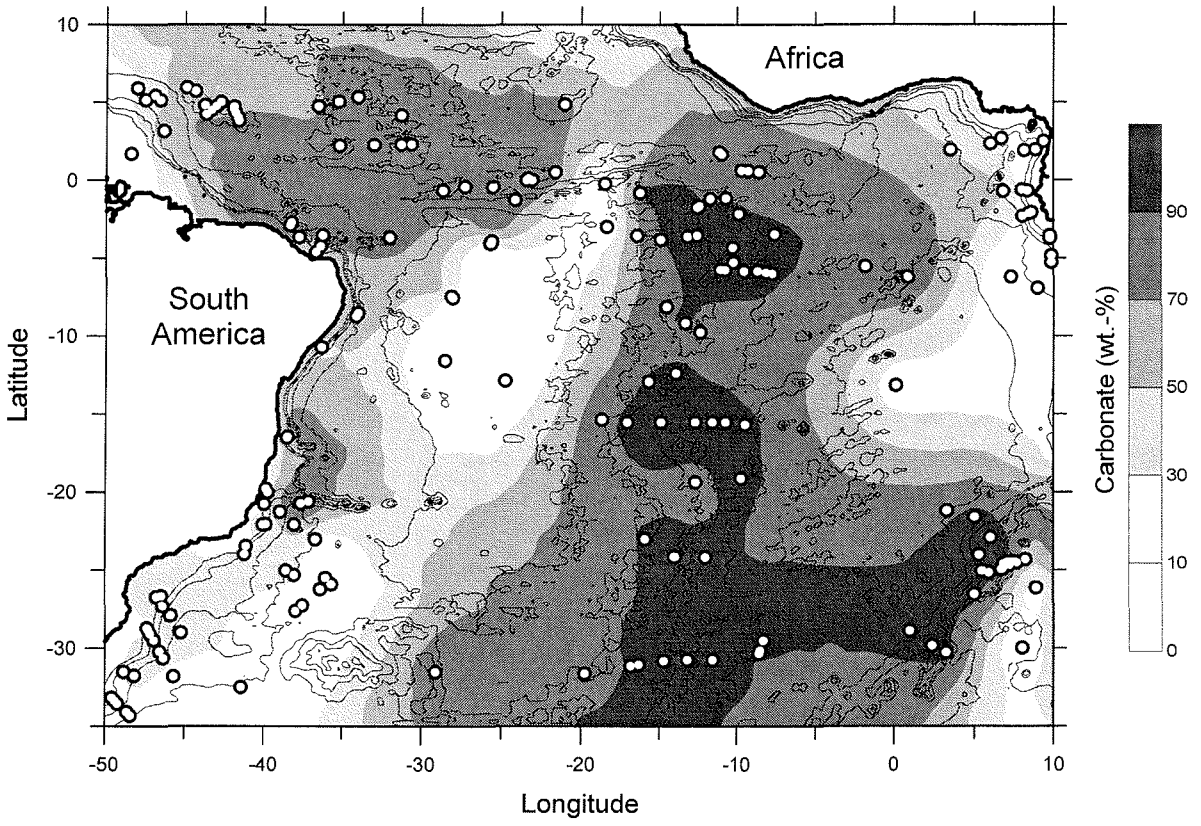

Fig. 10: *The carbonate content of South Atlantic surface sediments redrawn from Baumann et al. (in press). Sediments from the Mid-Atlantic Ridge and Walvis Ridge consist almost purely of carbonate. In contrast, the carbonate contents at the Ceará Rise are relatively low.*

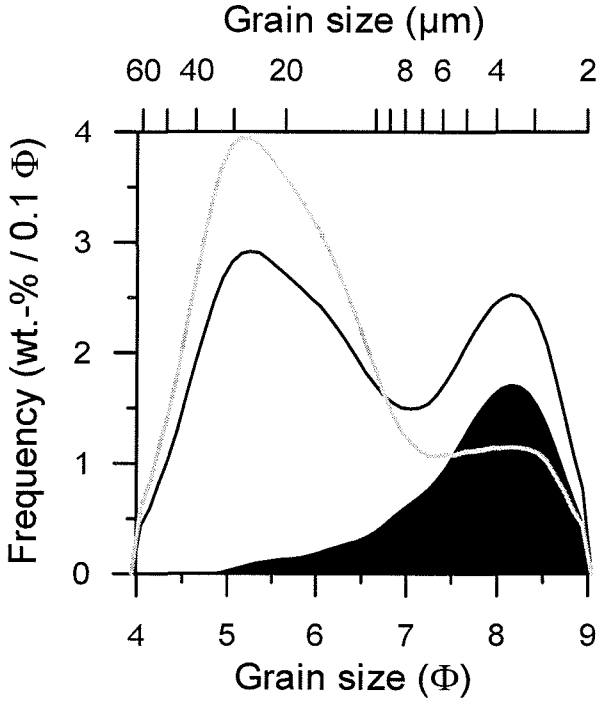

Fig. 11: *Grain-size distributions of GeoB 1519 (surface) from the Ceará Rise. The Figure illustrates the high fine terrigenous silt (black filled area) from the Amazon river which makes up a major portion of the fine peak of the bulk silt size distribution (black line). The resulting and rescaled CS size distribution reveals a predominance of foraminifer fragments in the silt fraction.*

Most striking for all low-latitude provinces (i.e. Ceará Rise, NW' MAR, Equatorial MAR) is the high contribution of foraminifer carbonate that amounts to 60 to 90 % of the bulk carbonate (Fig. 12). This high contribution indicates the favoured habitat of the calcareous zooplankton in mesotropic, i.e. relatively nutrient-enriched ocean areas. The nutrient supply for the Ceará Rise/NW' MAR province is assumed to originate from the Amazon river (e.g. Muller-Karger et al., 1988), probably supported by eddie-generated upwelling (Longhurst, 1993). In the Equatorial MAR province the higher nutrients are attributed to upwelling at the equatorial divergence zone (e.g. Fischer et al., 2000).

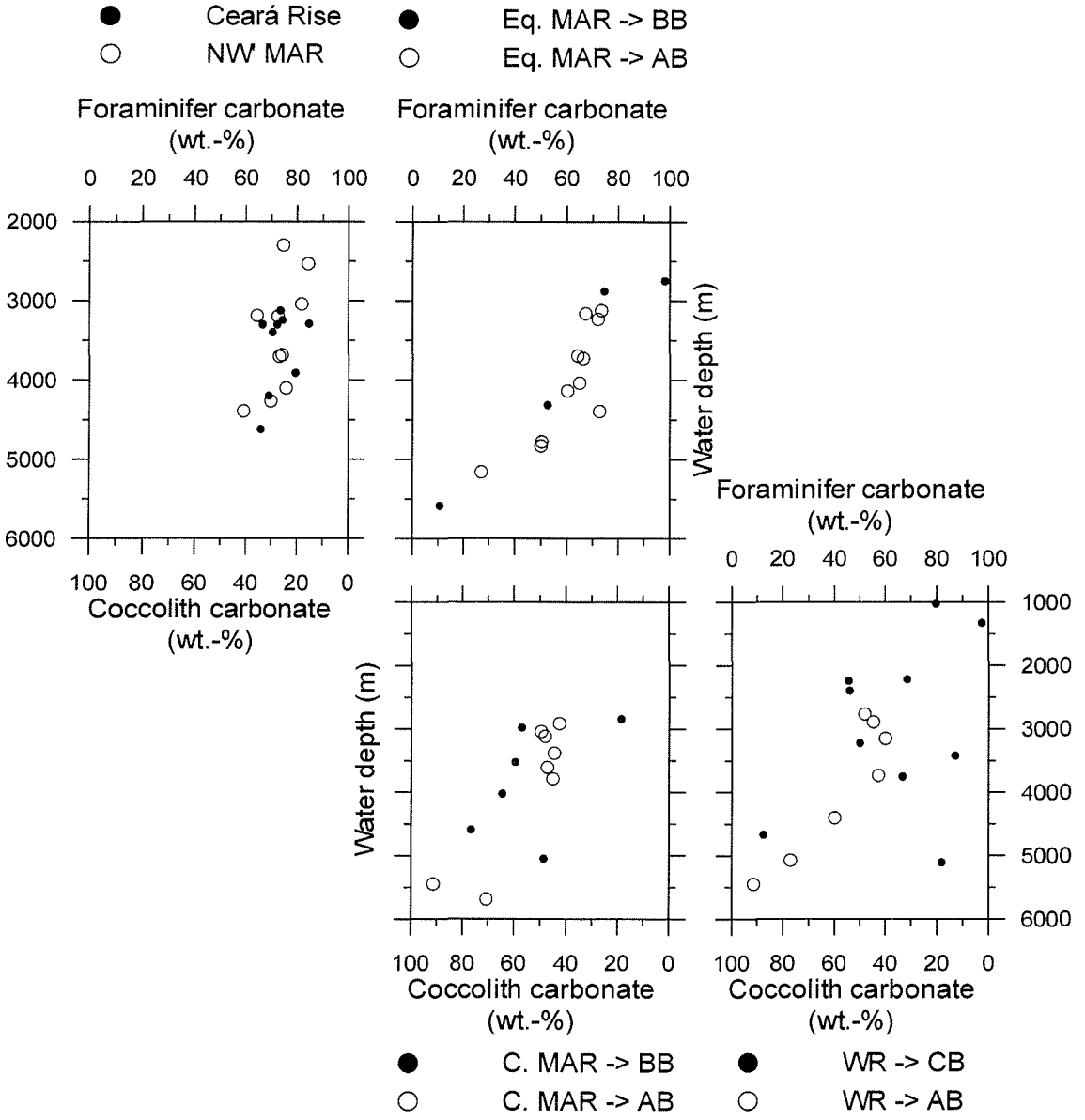

Fig. 12: Modern carbonate contribution of foraminifers (carbonate > 8 µm) and coccoliths (carbonate < 8 µm) relative to the bulk carbonate contents given in Figure 10. The signatures indicate different slopes of the ridges that dip to the Angola (AB), Brazil (BB) and Cape Basins (CB).

The Central MAR and Walvis Ridge provinces reveal a contrasting production pattern with only about 40 to 60 % foraminifer carbonate contribution (Fig. 11). For the Central MAR province the increase of coccolith carbonate relative to the provinces at low latitudes is

typical for production patterns within the nutrient-poor centres of subtropical ocean gyres (Hulburt, 1963). These oligotrophic habitats are avoided by zooplanktic organisms because of low food supply. Hence, this results in a relative increase of calcareous phytoplankton remains in the sediments below (Baumann et al., in press). An increase in nutrients closer to the southwest African upwelling areas increases the overall carbonate production affecting both, phytoplankton as primary producers and zooplankton which feed on it. This assumption is supported by differences in the sedimentation rates which are about two times higher on the Walvis Ridge in comparison with the Central MAR. On average the LGM interval is reached within the upper 20 cm in the Central MAR compared to 40 cm at Walvis Ridge province.

4.2 Regional variability of carbonate preservation patterns in South Atlantic pelagic sediments

4.2.1 Holocene

For the investigated Holocene pelagic deposits from water depths shallower than about 4000 m distinct carbonate sedimentation patterns within each province (Fig. 12) refer to overall comparable production rates in the upper ocean in the respective province. This "primary" composition is changed significantly at a certain water depth, i.e. the above mentioned "critical water depth", as can be seen by a broad number of parameters (Figs. 3-5, 11). Since the shift in sediment composition appears at relative high water depths, it is attributed to carbonate dissolution. Hence, the critical water depth represents a close approximation to the depth level of the sedimentary lysocline. The vertical position of the critical water depth for the latest Holocene (i.e. surface sediments) is recorded at water depth of about 4100 to 4200 m in the Brazil Basin, and at water depth of about 4500 to 4700 m in the Angola Basin (Tab. 1). In the Cape Basin low sample coverage leaves a broad possible water-depth interval of 3700-4500 m. However, relating the values observed at 4700 m water depth in the Cape Basin to comparable results in the Angola Basin (e.g. % sand, % carbonate in Silt, Fig. 3) would place this critical level about 600 m shallower at a water depth of about 4100 m. The modern position of the sedimentary lysocline recorded by means of grain-size composition agrees well with the positions as detected by Volbers and Henrich (2002b) using ultrastuctural breakdown of *G. bulloides* (BDX' = 3.0). For the Brazil and Cape Basins this position is tied to the interface of low corrosive NADW and highly corrosive AABW (Fig. 1). In the Angola Basin AABW is virtually absent which increases the importance of pressure in relation to carbonate dissolution. In contrast to the findings of Volbers and Henrich (2002b) who fixed the sedimentary lysocline for the Angola Basin at a water depth of 4400 m from the Walvis Ridge, the grain size data support earlier studies which reported rather deeper positions (i.e. 4700 m, Berger, 1968; 5000 m, Thunell, 1982).

Apart from dissolution in abyssal depths, supralysoclinal or respiratory carbonate dissolution became a focus in the last two decades. Even though sediments above the hydrographic lysocline are exposed to water masses that are supersaturated with respect to [CO_3^{-2}] a proportion of the calcium carbonate can be dissolved. This supralysoclinal dissolution is attributed to the oxidation of organic compounds (respiration) which increases the pCO_2 and drives carbonate dissolution (Emerson and Bender, 1981; Archer et al., 1989; Hales et al., 1994; Jahnke et al., 1994; Milliman et al., 1999). Most records of this phenomenon are based on sediments which originate from areas of high C_{org} deposition for example the upwelling areas off southwest Africa (Pfeifer et al., 2002; Volbers and Henrich, 2002a) and the Brazil Malvinas Confluence zone (Frenz et al., in press).

For the pelagic sediments of the South Atlantic that are bathed in NADW a relatively good and uniform carbonate preservation is observed (compare Figs. 1, 3, 5, 11). However, already in this water level gradual changes occur. As illustrated in Figure 3 the sand content in most provinces decreases at relatively shallow water depths (< 4000 m), anticipating a decrease in foraminifer carbonate of 5 to 10 % per 1000 m water depth in all low latitude provinces (Fig. 11). Additionally, there exists a gradient in this rate between the eastern Equatorial MAR province (higher rates: 10 %/1000 m) and the western Ceará Rise/NW' MAR province (lower rates: 5 %/1000 m, Fig. 11). This E-W gradient can be attributed to higher accumulation rates of organic carbon in more eastern parts of the equatorial upwelling compared to areas further west and beyond (e.g. Antoine et al., 1996; Fischer et al., 2000).

Due to the vertical position well above the sedimentary lysocline this shift is attributed to supralysoclinal dissolution, which here for the first time is reported in open ocean conditions. Since comparable production rates within the respective provinces are assumed, the relative increase of coccolith carbonate with increasing water depth confirms, that, compared to foraminifers, coccoliths are less susceptible for carbonate dissolution (Honjo, 1976).

4.2.2 LGM

The results from relative shallow LGM sites (< 3000 m) agree well with the Holocene trend at same water depths. Therefore, the significant differences of LGM relative to Holocene sediments (e.g. the decrease in sand content and the size decrease in the coarse CS) at water depths between 3000 and 4000 m are attributed to carbonate dissolution (Figs. 3, 5). The strong changes approach values which are observed for Holocene samples from below the sedimentary lysocline. Therefore, the differences in LGM can not be explained by increased supralysoclinal dissolution. Instead we favour a raise in the sedimentary lysocline level of about 1000 m from water depths of (below) 4000 m today to about 3100 m in the LGM (Tab. 2). Thereby our data confirm the results of earlier studies claiming a similar raise of the sedimentary lysocline level and an extinction of the modern

east-west asymmetry as recorded by Bickert (1992), Bickert and Wefer (1996), Duplessy et al. (1988) and Volbers and Henrich (submitted). Compared to the BDX'-based reconstructions by Volbers and Henrich (submitted) our method detects the depth of the sedimentary lysocline for the LGM generally only about 100-200 m shallower. This minor discrepancy may be attributed to general methodical differences. In contrast to these authors a depression of the lysocline depth at the equatorial divergence during the LGM was not observed. Our results support LGM circulation models for the South Atlantic with a reduced NADW, being present as a carbonate conservative Northern Component Water or GNAIW. Furthermore, from the south the NADW extent is to a great replaced by a carbonate corrosive Southern Component Water (Duplessy et al., 1988; Bickert, 1992; Labeyrie et al., 1992).

There is little knowledge about how ecological changes might have affected the planktic foraminifer or coccolith assemblages during the LGM in the South Atlantic. For the foraminifers, we refer to the samples which are situated above the sedimentary lysocline in the LGM, revealing similar grain sizes for their fragment (coarse CS mean and modal values, Fig. 5) relative to Holocene. Therefore we conclude that the size decrease at greater water depths (> 3000 m) are not attributed to an increase of more fragile species, but to carbonate dissolution. For the Holocene in the Equatorial provinces (Ceará Rise, NW' MAR, Equatorial MAR) besides the coarse CS also the fine carbonate shows a slight decrease in grain size below the sedimentary lysocline (Fig. 5). This decrease of the fine CS modal grain size might be as low as 1.0 to 1.5 µm. However, in relation to the "primary" size (above the lysocline) this shift represents one fifth of the diameter. For the Holocene the observed size decrease of the fine CS therefore is attributed to carbonate dissolution as well, since primary input is considered to be similar within each province. In the appropriate LGM samples of the Equatorial province in all samples there is a general size decrease in the fine CS mode of up to 2 µm. This size decrease even affects the shallowest samples believed to be situated above the sedimentary lysocline of the LGM. Since in these shallow samples the coarse silt and sand share does not indicate enhanced carbonate dissolution, and the coccoliths are assumed to be even less susceptible for dissolution this points to a general difference in the coccolith assemblage between Holocene and LGM. According to Frenz et al. (submitted) this fine CS size decrease can be caused by a relatively lower abundance of larger and a higher abundance of smaller species. However, Baumann et al. (1999) showed a relative increase of *C. leptoporus* in a core from the equatorial Atlantic (GeoB 1117-2) from about 15 % in the Holocene to about 25 % in stage 2. Smaller species stay relatively constant or decrease in the assemblage. Following another result of Frenz et al. (submitted) the observed size decrease can also be caused by a shift from the large (B) to the medium and small morphotype (A+C) of *C. leptoporus* although this relatively coarse species increases. However, up to now there are no biometrical data of this site availlable. At deeper positions, carbonate dissolution may

support the observed size decrease, however close to the lower border of the silt fraction (< 2.5 µm) silt size parameters lack in sensitivity.

In contrast to the findings at low latitudes, the fine silt grain size in the Central MAR and Walvis Ridge province is slightly increased in the LGM in contrast to the Holocene (Fig. 5). For one site of the Walvis Ridge (GeoB 1028-5) Baumann et al. (1999) showed a decrease for *C. leptoporus* in the coccolith assemblage. Probably a case inverse to that of the Equatorial province may cause this incident, i.e. a change-over from smaller to larger morphotypes of *C. leptoporus*. However without biometry proof is lacking. A recent study (Boeckel et al., submitted-a) recorded an increase of the coccolith species *C. pelagicus* from about 1 % in Holocene to 4 % of the coccolith assemblage in stadium 2 in a sediment core off Namibia. Because this species supplies about two times more carbonate per placolith than *C. leptoporus* (74 pg *C. leptoporus* vs. 143 pg *C. pelagicus*, Young and Ziveri (2000)) already a slight increase can cause or support significant increases in grain size.

5 Concluding remarks

In the present study we have shown that the grain-size composition of the calcareous sediment component is sensitive for carbonate dissolution. Other way round: carbonate dissolution significantly modifies the grain-size distribution of the calcareous sediment compounds (towards finer grain sizes). Therefore it is possible to trace such important (palaeo-) oceanographic features as the sedimentary lysocline and its variations spatially and temporarily. Besides, there are still open questions, uncertainties and handicaps which are addressed here and proposals to overcome are made.

Very constant silt contents are curious at a first glance (Fig. 3). However they may indicate a continuous breakdown and transfer of particles between the size fractions. An input of particles by transfer of fragments from the sand into the coarse silt fraction is documented (Frenz et al., submitted). However, the transfer from the silt into the clay fraction to balance this input can be caused by a continuous size decrease and transfer to the fine silt and clay fractions. The proceeding dissolution of foraminifer fragments increases their loss in weight so far, that the coccoliths population overwhelms the fragment population. Furthermore, the slight size decrease indicated even for coccoliths (Fig. 5) can lower their equivalent spherical diameter significantly, so that the relative increase in clay carbonate is more attributed to coccoliths than to transferred foraminifer fragments. Quantitative SEM investigations which record abundance and size of fragments in silt and clay separates of dissolution influenced samples will shed some light on this.

In contrast to the spatial pattern, to decide whether temporal decrease in carbonate grain size is attributed to dissolution or an increase in more fragile or smaller species, knowledge about the latter is necessary. For this approach samples from above the reconstructed sedimentary lysocline in the LGM have to represent the relative primary composition. This leads to the major problem of spatial sample coverage, concerning both time slices. For the

Holocene good coverage is given above the sedimentary lysocline. However, there is a gap or low coverage for the depth of and below the sedimentary lysocline. For the LGM the mesh width of sample distribution is even increased.

As obvious from Figure 3 the silt fraction itself makes up about 20 to 30 % of the samples. Out of this 50 to 75 % is coarse silt (63-8 µm, 4-7 Φ), representing foraminifer fragments and assumed to be the most sensible fraction for carbonate dissolution. From the percentages of this size fraction and microscopical observations in the sand fraction it can be concluded that the coarse silt acquires only a minor proportion of the foraminifer fragments of a given sample (e.g. Stuut et al., 2002). According to this study, a size decrease of 0.5 Φ in the coarse silt is indicative for significant carbonate dissolution. To improve the sensibility of our method it is suggested to extend the upper limit of 63 µm to 125 µm (plus of 1 Φ) to record grain-size changes of a higher proportion of fragments. The size fraction < 125 µm should smoothly pass the tubing system of the SediGraph. According to Gibbs et al. (1971) deviations from Stokes' diameters to measured diameter increases in the size fraction > 100 µm (Stokes' law predicts faster settling/coarser diameters). However, treating the samples equally, relative differences are recorded and the increased size spectrum makes the method more sensitive.

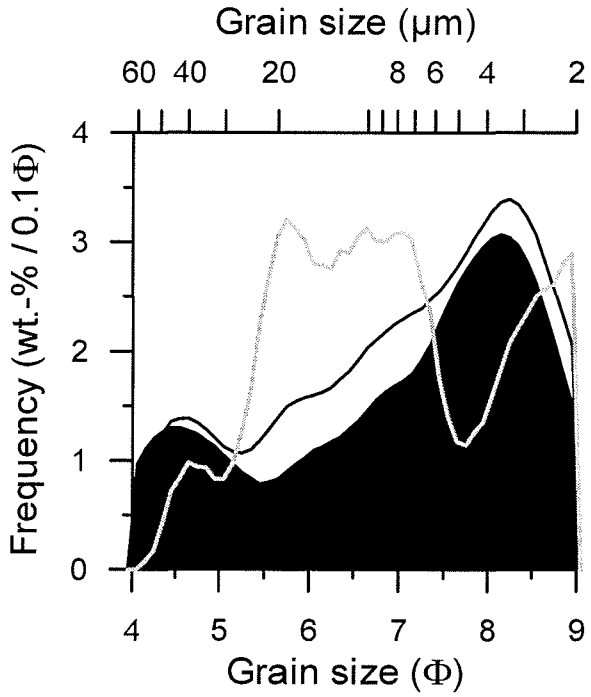

Fig. 13: Grain-size distributions of GeoB 1724 (surface) from the deep Cape Basin (Walvis Ridge province). The illustration shows an example for the noisy CS grain-size distributions (grey) that results from samples with relatively low carbonate contents in the silt fraction (here 12.6 %). See text for further explanation. Signatures as in Figure 11.

A major limiting factor for the calculation of the CS grain-size distributions is the carbonate content of the silt fraction. Low carbonate contents in this fraction cause the relative carbonate-free grain-size size distributions (sum of all classes = 100 % – % carbonate of silt) to be close to that of the absolute bulk silt (sum of all classes = 100 %). The difference between both curves, the relative CS size distribution (sum of all classes = % carbonate of silt), rescaled to 100 % then is a very noisy signal. In Figure 13 an example from the deep Cape Basin with 13 % carbonate in silt is given. It raises the question how far one can trust the resulting statistical parameters for carbonate-poor

samples. This difficulty was reported by Robinson and McCave (1994) stating that the CS size distribution of samples containing 5 % carbonate in silt are hard to interpret. This limits the presented method to carbonate-rich sediments, away from the continental margin with additionally high terrigenous dilution. According to our results samples with more than 20 % carbonate in the silt fraction show size distributions with a reliable and interpretable shape.

The calcareous components acquired comprise the aragonite compounds too. In pelagic settings pteropods are virtually the only aragonite contributors. Because upper NADW is supersaturated with respect to aragonite, in contrast to AAIW above and lower NADW below, there are two aragonite lysoclines (Gerhardt and Henrich, 2001). In the upper NADW level (≈ 2000-3000 m) pteropods are well preserved and can reach proportions of more than 50 % of the carbonate budget (Gerhardt and Henrich, 2001; Baumann et al., in press). However, geographically the distribution of pteropods is rather restricted to the western margin of the South Atlantic, whereas in pelagic sediments their contribution is below 10 % of the carbonate content (Baumann et al., in press). This proportion is assigned to the proportion of the coarse (foraminifer) carbonate. Therefore, in relatively shallow samples a potential contamination of up to 20 % must be considered.

Acknowledgements

We are grateful to the shipboard and scientific crews of the RV METEOR involved in the sediment coring offshore. Furthermore we thank B. Diekmann who comprised the clay weights and a major part of the quantitative clay decarbonisation data. This research was funded by the Deutsche Forschungsgemeinschaft (Sonderforschungsbereich 261 at the University of Bremen). This is SFB contribution no. ###. All data presented in this study are archived in the PANGAEA database at www.pangaea.de (search string: FrenzM).

6 References

Antoine, D., André, J.-M. and Morel, A., 1996. Oceanic primary production-2. Estimation at global scale from satellite (coastal zone colour scanner) chlorophyll. Global Biogeochemical Cycles, 10: 57-69.

Archer, D.E., 1996. An atlas of the distribution of calcium carbonate in sediments of the deep sea. Global Biogeochemical Cycles, 10(1): 159-174.

Archer, D.E., Emerson, S. and Reimer, C., 1989. Dissolution of calcite in deep-sea sediments: pH and O_2 microelectrode results. Geochimica et Cosmochimica Acta, 53: 2831-2845.

Baumann, K.-H., Böckel, B., Donner, B., Gerhardt, S., Henrich, R., Vink, A., Volbers, A.N.A., Willems, H. and Zonneveld, K.A.F., in press. Contribution of calcareous plankton groups to the carbonate budget of South Atlantic surface sediments. In: S. Mulitza, V. Ratmeyer and G. Wefer (Editors), The South Atlantic in the late Quaternary: Reconstruction of material budget and current systems. Springer, Berlin Heidelberg New York.

Baumann, K.-H., Cepek, M. and Kinkel, H., 1999. Coccolithophores as indicators of ocean water masses, surface-water temperature, and paleoproductivity - examples from the South Atlantic. In: G. Fischer and G. Wefer (Editors), Use of proxies in paleoceanography - examples from the South Atlantic. Springer, Berlin Heidelberg.

Berger, W.H., 1968. Planktonic foraminifera: selective solution and paleoclimatic interpretation. Deep-Sea Research, 15: 31-43.

Berger, W.H., 1979. Preservation of foraminifera., SEPM Short Course No. 6. Society for Sedimentary Geology, Houston TX, pp. 105-155.

Bickert, T., 1992. Rekonstruktion der spätquartären Bodenwasserzirkulation im östlichen Südatlantik über stabile Isotope benthischer Foraminiferen. Berichte, Fachbereich Geowissenschaften, 27. Universität Bremen, Bremen, 205 pp.

Bickert, T. and Mackensen, A., 2003. Last glacial to Holocene changes in South Atlantic deep water circulation. In: S. Mulitza, V. Ratmeyer and G. Wefer (Editors), The South Atlantic in the late Quaternary: Reconstruction of material budget and current systems. Springer, Berlin Heidelberg New York.

Bickert, T. and Wefer, G., 1996. Late Quaternary deep-water circulation in the South Atlantic: Reconstruction from carbonate dissolution and benthic stable isotopes. In: G. Siedler (Editor), The South Atlantic: Present and past circulation. Springer, Berlin Heidelberg, pp. 599-620.

Boeckel, B., Baumann, K.-H. and Henrich, R., submitted-a. Late Quaternary coccolith assemblages from the south-eastern South Atlantic Ocean: implications for the paleoceanographic evolution of the Benguela and Agulhas Current systems during the past 259kyr.

Boeckel, B., Baumann, K.-H., Henrich, R. and Kinkel, H., submitted-b. Distribution patterns of of coccoliths in South Atlantic and Southern Ocean surface sediments in relation to environmental gradients. Deep-Sea Research.

Boyle, E. and Keigwin, L.D., 1987. North Atlantic thermohaline circulationduring the past 20,000 years linked to high-latitude surface temperature. Nature, 30: 35-40.

Broecker, W.S. and Peng, T.H., 1982. Tracers in the sea. Eldigio Press, New York, 689 pp.

Dittert, N., Baumann, K.-H., Bickert, T., Henrich, R., Huber, R., Kinkel, H. and Meggers, H., 1999. Carbonate dissolution in the deep-sea: methods, quantification and paleoceanographic application. In: G. Fischer and G. Wefer (Editors), Use of proxies in paleoceanography: examples from the South Atlantic. Springer, Berlin Heidelberg.

Duplessy, J.C., Shackleton, N.J., Fairbanks, R.G., Labeyrie, L., Oppo, D. and Kallel, N., 1988. Deepwater source variations during the last climatic cycle and their impact on the global deepwater circulation. Paleoceanography, 3(3): 343-360.

Emerson, S. and Bender, M., 1981. Carbon fluxes at the sediment-water interface of the deep sea: calcium carbonate preservation. Journal of Marine Reserach, 39: 139-162.

Fischer, G., Ratmeyer, V. and Wefer, G., 2000. Organic carbon fluxes in the Atlantic and the Southern Ocean: relationship to primary production compiled from satellite radiometer data. Deep Sea Research II, 47(9-11): 1961-1997.

Frenz, M., Baumann, K.-H., Boeckel, B., Höppner, R. and Henrich, R., submitted. Quantification of foraminifer and coccolith carbonate in South Atlantic surface sediments by means of carbonate grain-size distributions.

Frenz, M., Höppner, R., Stuut, J.-B., Wagner, T. and Henrich, R., in press. Surface sediment bulk geochemistry and grain-size composition related to the oceanic circulation along the South American continental margin in the Southwest Atlantic. In: S. Mulitza, V. Ratmeyer and G. Wefer (Editors), The South Atlantic in the late Quaternary: Reconstruction of material budget and current systems. Springer, Berlin Heidelberg New York.

Gaillardet, J., Dupré, B. and Allègre, C.J., 1997. Chemical and physical denudation in the Amazon river Basin. Chemical Geology, 142(141-173).

GEOSECS, 1999. Pangaea data set ID: 55389.

Gerhardt, S. and Henrich, R., 2001. Shell preservation of Limacina inflata (Pteropoda) in surface sediments from the Central and South Atlantic Ocean: a new proxy to determine the aragonite saturation state of water masses. Deep Sea Research Part I: Oceanographic Research Papers, 48(9): 2051-2071.

Gibbs, R.J., Matthews, M.D. and Link, D.A., 1971. The relationship between sphere size and settling velocity. Journal of Sedimentary Petrology, 41(1): 7-18.

Gröger, M., Henrich, R. and Bickert, T., submitted. Glacial-interglacial variability and long-term changes in the lower circulation loop of North Atlantic Deep Water: Inference from silt grain-size analysis and carbonate preservation studies at Ceará Rise, western equatorial Atlantic.

Hales, B., Emerson, S. and Archer, D., 1994. Respiration and dissolution in the sediments of the western North Atlantic: estimates from models of in situ microelectrode measurementsof pore water oxygen and pH. Deep Sea Research I, 41(4): 695-719.

Henrich, R., Baumann, K.-H., Gerhardt, S., Gröger, M. and Volbers, A.N.A., in press. Carbonate preservation in deep and intermediate water masses in the South Atlantic: evaluation and geological record (a review). In: S. Mulitza, V. Ratmeyer and G. Wefer (Editors), The South Atlantic in the late Quaternary: Reconstruction of material budget and current systems. Springer, Berlin Heidelberg New York.

Henrich, R., Kassens, H., Vogelsang, E. and Thiede, J., 1989. Sedimentary facies of glacial-interglacial cycles in the Norwegian Sea during the last 350 ka. Marine Geology, 86: 283-319.

Henrich, R. and Wefer, G., 1986. Dissolution of biogenic carbonates: effects of skeletal structure. Marine Geology, 71: 341-362.

Honjo, S., 1976. Coccoliths: production, transportation and sedimentation. Marine Micropaleontology, 1(1): 65-79.

Hulburt, E.M., 1963. The diversity of phytoplanktonic populations in oceanic, coastal, and estuarine regions. Journal of Marine Reserach, 21: 81-93.

Jahnke, R.A., Craven, D.B. and Gaillard, J.-F., 1994. The influence of organic matter diagenesis on CaCO3 dissolution at the deep-sea floor. Geochimica et Cosmochimica Acta, 58(11): 2799-2809.

Krumbein, W.C., 1936. Application of logarithmic moments to size frequency distributions of sediments. Journal of Sedimentary Petrology, 6: 35-47.

Labeyrie, L.D., Duplessy, J.C., Duprat, J., Juillet-Leclerc, A., Moyes, J., Michel, E., Kallel, N. and Shackleton, N.J., 1992. Changes in the vertical structure of the North Atlantic Ocean between glacial and modern times. Quaternary Science Reviews, 11: 401-413.

Longhurst, A., 1993. Seasonal cooling and blooming in tropical oceans. Deep-Sea Research I, 40(11/12): 2145-2165.

McCave, I.N., Manighetti, B. and Robinson, S.G., 1995. Sortable silt and fine sediment size/composition slicing: Parameters for palaeocurrent speed and palaeoceanography. Paleoceanography, 10(3): 593-610.

McIntyre, A. and Bé, A.W.H., 1967. Modern coccolithophorids of the Atlantic Ocean - I. Placoliths and cyrtoliths. Deep Sea Research I, 14: 561-597.

Milliman, J.D., Troy, P.J., Balch, W.M., Adams, A.K., Li, Y.-H. and Mackenzie, F.T., 1999. Biologically mediated dissolution of calcium carbonate above the chemical lysocline? Deep Sea Research I, 46(10): 1653-1669.

Mix, A.C., Bard, E. and Schneider, R., 2001. Environmental processes of the ice age: land, oceans, glaciers (EPILOG). Quaternary Science Reviews, 20(4): 627-657.

Muller-Karger, F.E., McClain, C.R. and Richardson, P.L., 1988. The dispersal of the Amazon's water. Nature, 333: 56-59.

Niebler, H.-S., Mulitza, S., Donner, B., Arz, H., Pätzold, J. and Wefer, G., submitted. Sea-Surface Temperatures in the Equatorial and South Atlantic Ocean during the Last Glacial Maximum (23-19 ka). Paleoceanography.

Oppo, D.W. and Lehman, S.J., 1995. Suborbital timescale variability of North Atlantic Deep Water during the past 200,000 years. Paleoceanography, 10(5): 901-910.

Pfeifer, K., Hensen, C., Adler, M., Wenzhfer, F., Weber, B. and Schulz, H.D., 2002. Modeling of subsurface calcite dissolution, including the respiration and reoxidation processes of marine sediments in the region of equatorial upwelling off Gabon. Geochimica et Cosmochimica Acta, 66(24): 4247-4259.

Robinson, S.G. and McCave, I.N., 1994. Orbital forcing of bottom-current enhanced sedimentation on Feni Drift, NE Atlantic, during the mid-Pleistocene. Palaeogeography, 9(6): 943-972.

Rühlemann, C., Diekmann, B., Mulitza, S. and Frank, M., 2001. Late Quaternary changes of western equatorial Atlantic surface circulation and Amazon lowland climate recorded in Ceará Rise deep-sea sediments. Paleoceanography, 16(3): 293-305.

Rühlemann, C., Frank, M., Hale, W., Mangini, A., Mulitza, S., Muller, P.J. and Wefer, G., 1996. Late Quaternary productivity changes in the western equatorial Atlantic: Evidence from 230Th-normalized carbonate and organic carbon accumulation rates. Marine Geology, 135(1-4): 127-152.

Shannon, L.V. and Chapman, P., 1991. Evidence of Antarctic Bottom Water in the Angola Basin at 32°S. Deep-Sea Research, 38(10): 1299-1304.

Stocker, T.F., 1998. A glimpse of the glacial. Nature, 391: 338-339.

Stuut, J.-B.W., Prins, M.A. and Jansen, J.H.F., 2002. Fast reconnaissance of carbonate dissolution based on the size distribution of calcareous ooze on Walvis Ridge, SE Atlantic Ocean. Marine Geology, 190(3-4): 581-589.

Thunell, R.C., 1982. Carbonate dissolution and abyssal hydrography in the Atlantic Ocean. Marine Geology, 47: 165-180.

Volbers, A.N.A. and Henrich, R., 2002a. Late Quaternary variations in calcium carbonate preservation of deep-sea sediments in the northern Cape Basin: results from a multiproxy approach. Marine Geology, 180(1-4): 203-220.

Volbers, A.N.A. and Henrich, R., 2002b. Present water mass calcium carbonate corrosiveness in the eastern South Atlantic inferred from ultrastructural breakdown of Globigerina bulloides in surface sediments. Marine Geology, 186(3-4): 471-486.

Volbers, A.N.A. and Henrich, R., submitted. Calcium carbonate corrosiveness in the South Atlantic during the Last Glacial Maximum as inferred from changes in the

preservation of *Globigerina bulloides*: A proxy to determine deep water circulation pattern?

Warren, B. and Speer, K.G., 1991. Deep circulation in the eastern South Atlantic ocean. Deep-Sea Research, 38(1): 281-322.

Wüst, G., 1935. Schichtung und Zirkulation des Atlantischen Ozeans: Die Stratosphäre, Wissenschaftliche Ergebnisse der Deutschen Atlantischen Expedition auf dem Forschungs- und Vermessungsschiff "Meteor" 1925-1927. de Gruyter, Berlin, pp. 109-288.

Young, J.R. and Ziveri, P., 2000. Calculation of coccolith volume and it use in calibration of carbonate flux estimates. Deep Sea Research Part II: Topical Studies in Oceanography, 47(9-11): 1679-1700.

Zabel, M., Bickert, T., Dittert, L. and Haese, R., 1999. Significance of the sedimentary Al:Ti ration as an indicator for variations in the circulation patterns of the equatorial North Atlantic. Palaeoceanography, 14(6): 789-799.

PART III

SUMMARY AND CONCLUSIONS

The present PhD thesis is the result of intense analysis of grain-size distributions of South Atlantic sediments. The samples cover a large variety of sedimentary settings and climatic environments. They vary between predominantly terrigenous sediments at the South American continental margin and almost pure calcareous ooze at the Mid-Atlantic Ridge, and cover the region from the equator to subpolar areas. The sampled sediments represent two periods: the recent and the LGM time slices. Therefore, a large variety of sedimentary processes needs to be considered in order to interpret the measured grain-size distributions correctly. In this study bulk texture parameters and the detailed grain-size distributions of the terrigenous and calcareous silt fractions are analysed using sieve, settling and SediGraph techniques.

From the terrigenous grain-size distribution in combination with bulk geochemical parameters at the South American continental margin modern sediment input and distribution are deduced in accordance to the oceanographic framework. The sedimentary imprint of the Brazil Malvinas Confluence was traced by a corridor with sediments rich in organic carbon and a typical grain-size distribution. This corridor represents a discontinuity of relatively carbonate-rich sediments which reflect the southward flow of North Atlantic Deep Water at water depths between 2000 and 4000 m. Four distinct depositional settings were detected by the terrigenous silt grain-size distributions. At the Argentine outer shelf and continental slope sediments experience strong winnowing by the vigorous Malvinas Current. A very coarse tongue aligned downslope off the mouth of the Rio de la Plata represents the sandy bedload of this large river. Coarse silty deposit are observed in an area congruent to the corridor containing high amounts of organic carbon. Here the suspended river discharge is deposited. Very fine sediments accumulate under obviously low energetic conditions at the southern rise of the Santos Plateau and the southern Brazil Basin.

The size distribution of the carbonate fraction of the sediments is analysed in strong linkage to the calcareous particles it represents. A generally bimodal grain-size distribution suggests to distinguish foraminifer and coccolith carbonate at 8 μm equivalent spherical diameter. The fine silt represents relatively large coccoliths. The ecological variations of

the coccolith assemblages can be followed by variations in the size distribution of the fine mode. Additionally, when fitting Gaussian distributions to the relatively stable size frequencies, single peaks can be attributed to single coccolith species. Due to the clay-silt size splitting the relatively large coccolith species (especially *C. leptoporus*) are enriched in the silt fraction. In contrast, the most frequent species (*E. huxleyi, F. profunda*) are caught methodically in the clay fraction. The coarse silt mode represents foraminifer fragments and juvenile foraminifer tests. Its grain-size distribution can be used to trace carbonate dissolution by the simple assumption that more intense carbonate dissolution causes smaller fragments. Using this causality, for the modern situation and for that of the Last Glacial Maximum (LGM) the vertical position of the sedimentary lysocline is traced. In agreement with the modern water mass distribution the sedimentary lysocline was found at 4100 m in the Brazil and Cape Basins and at 4600 m in the Angola Basin. According to this study during the LGM the sedimentary lysocline was situated at about 3100 m, which agrees with a reduced NADW production during this time period and a compensation by corrosive Southern Component Water.

From the results of this study it is concluded that silt grain-size distributions of sediments is a powerful tool to deduce the spatial distribution of sediment input variables and carbonate dissolution. However, there is enough left for future studies with respect to spatial sample coverage and methodical improvement.

The spatial resolution of samples is an important point. For the results of terrigenous sediment grain-size distributions only the presented dense sample grid off South America enabled detailed discrimination and spatial configuration of sedimentary facies in adequate accuracy. The N-S alignment of the sedimentary trace of the intermediate-scale oceanographic feature of the Brazil Malvinas Confluence could be traced only in this relatively high-resolution with one more downslope transect in this region compared to previous studies (Benthien and Müller, 2000; Hensen et al., 2000). At the eastern side of the South Atlantic the sample coverage is by far too low to relate the samples to each other in this highly variable and complex setting (cf. Rogers and Bremner, 1991). For the carbonate-rich sediments of the pelagic open ocean the measurement of the terrigenous grain-size distribution frequently failed due to low amount of terrigenous material left after decarbonisation. Assuming about 1/3 of silt in these samples and a carbonate content of 95-99 % in the silt fraction, then a sample amount of 60-300 g is needed to gain the 1 g of terrigenous silt necessary for size analysis by the SediGraph. Therefore for this environment only sporadic terrigenous size data are available.

The main limitation of the method used in this study is that the SediGraph measures the grain-size distribution of the artificially restricted size window of the silt fraction. This restriction results in artificial alteration of the grain-size distributions (cf. Frenz et al., in press, Manuscript #1). To avoid significant disturbance by the cohesive behaviour of clay-sized particles and distinct clay minerals (Stein, 1985) the clay fraction is generally excluded. However, in some areas this is not necessary due to low amounts of clay and low

smectite occurrence. In such areas smaller size classes could be included in the size spectrum, providing information on the grain-size distribution of finer fractions, e.g. that of smaller coccolith species. The upper boundary is set by the empirical silt/sand border at 63 µm. Hitherto, the sand fraction was not taken into account when analysing grain size by means of the SediGraph technique. The measuring range of the SediGraph 5100 is 300-0.1 µm (Micromeritics, 1996). However, the validity range of Stokes' Law is restricted to < 100 µm (Gibbs et al., 1971). Expanding the grain-size range measured to the (equally treated) fraction < 125 µm (+ 1 Φ compared to the method used) would compromise both requirements. The innovation is to include coarser grain-size ranges to the spectrum that are sensitive for input or sorting variability and especially for the dissolution proxy. For example, the terrigenous sediments of the bedload tongue of the La Plata river and the winnowed sediments at the Argentine outer shelf and slope are predominantly sandy (90 % sand, 10 % silt). By the suggested grain-size expansion a more representative portion of the samples would be characterised. Carbonate dissolution inferred from the carbonate silt fraction bases of a grain-size variability of 0.5 Φ for the coarse silt mean (about 25-17 µm). Measurements using laser techniques indicated a dissolution-sensible size range of 90 to 25 µm (Stuut et al., 2002). Therefore, expanding the upper limit by one more Φ-unit would collect valuable size data of more fragments and finally increase the reliability of the method. Another way to include the sand fraction is the use of a sedimentation balance. As Michels (2000) has shown, sand grain-size data collected with such a device are useful to infer current intensities and can even be used to detect single foraminifer species as applied in the present study to coccolith species. The combined use of two settling techniques may avoid steps occurring at methodical borders, e.g. between sieve (> 63 µm) and SediGraph techniques (e.g. Dahlgren and Vorren, 2003).

Finally, the link of grain-size distribution with the coccolith assemblage needs to be verified and advanced. Hitherto, the relation of nominal and equivalent spherical diameter exists only for *C. leptoporus*. If this relation is verified for other species, their equivalent settling size could be fixed and used to separate single coccolith species or samples containing a restricted coccolith assemblage. Additionally, the mass estimation of single species as suggested in this study (area below fitted Gaussian distribution) needs to be cross-checked with the volume-estimation method of Young and Ziveri (2000).

All data used for the manuscripts are archived in the PANGAEA database at www.pangaea.de (search string: FrenzM).

References

Benthien, A. and Müller, P.J., 2000. Anomalously low alkenone temperatures caused by lateral particle and sediment transport in the Malvinas Current region, western Argentine Basin. Deep-Sea Research I, 47: 2369-2393.

Dahlgren, K.I.T. and Vorren, T.O., 2003. Sedimentary environment and glacial history during the last 40 ka of the Voring continental margin, mid-Norway. Marine Geology, 193(1-2): 93-127.

Frenz, M., Höppner, R., Stuut, J.-B., Wagner, T. and Henrich, R., in press. Surface sediment bulk geochemistry and grain-size composition related to the oceanic circulation along the South American continental margin in the Southwest Atlantic. In: S. Mulitza, V. Ratmeyer and G. Wefer (Editors), The South Atlantic in the late Quaternary: Reconstruction of material budget and current systems. Springer, Berlin Heidelberg New York.

Gibbs, R.J., Matthews, M.D. and Link, D.A., 1971. The relationship between sphere size and settling velocity. Journal of Sedimentary Petrology, 41(1): 7-18.

Hensen, C., Zabel, M. and Schulz, H.D., 2000. A comparison of benthic nutrient fluxes from deep-sea sediments off Namibia and Argentina. Deep Sea Research Part II: Topical Studies in Oceanography, 47(9-11): 2029-2050.

Michels, K., 2000. Inferring maximum current velocities in the Norwegian-Greenland Sea from settling-velocity measurements of sediment surface samples: methods, application, and results. Journal of Sedimentary Research, 70(5): 1036-1050.

Micromeritics, 1996. SediGraph 5100 Particle size analysis system, Operator's manual, pp. 238.

Rogers, J. and Bremner, J.M., 1991. The Benguela Ecosystem. Part VII. Marine-geological Aspects. Oceanography and Marine Biology Annual Review, 29: 1-85.

Stein, R., 1985. Rapid grain-size analyses of clay and silt fraction by Sedigraph 5000D: comparison with Coulter Counter and Atterberg methods. Journal of Sedimentary Petrology, 55(4): 590-615.

Stuut, J.-B.W., Prins, M.A. and Jansen, J.H.F., 2002. Fast reconnaissance of carbonate dissolution based on the size distribution of calcareous ooze on Walvis Ridge, SE Atlantic Ocean. Marine Geology, 190(3-4): 581-589.

Young, J.R. and Ziveri, P., 2000. Calculation of coccolith volume and it use in calibration of carbonate flux estimates. Deep Sea Research Part II: Topical Studies in Oceanography, 47(9-11): 1679-1700.

Dank

Ich danke Herrn Prof. Dr. Rüdiger Henrich für die Vergabe und Betreuung dieser Arbeit, sowie für den Rückenwind in der Endphase ihrer Entstehung. Außerdem danke ich Herrn Dr. Rüdiger Stein für die freundliche Übernahme des Zweitgutachtens.

Besonders möchte ich meiner Arbeitsgruppe Sedimentologie/Paläozeanographie danken, in der ich mich in Bremen gut aufgehoben gefühlt habe. Frau Helga Heilmann und Frau Renate Henning danke ich für die stets hervorragend organisierte Materialbeschaffung und die technische Hilfestellung, ohne welche der Arbeitsfluss doch häufiger ins Stocken geraten wäre. Ich danke meiner „Hiwine" Meike Rohde für ihren Einsatz bei der Probenaufbereitung.

Anregende Diskussionen mit vielen Kollegen des Fachbereichs 5, des SFB 261, des AWI und des RCOM sowie von außerhalb haben ebenfalls zum Gelingen dieser Arbeit beigetragen. Ein besonderer Dank geht dabei an Jan-Berend Stuut, dessen Hilfsbereitschaft und Teamgeist Vorbild sind, und das, obwohl er in der „Schlacht der Methoden" ein Laser-Fan ist.

Ich danke allen Kollegen und Freunden für ihre Geduld und das dicke Fell, das manchmal nötig war, um die Kommunikation aufrecht zu erhalten. Jetzt wird alles wieder gut!

Meinen Eltern danke ich für die moralische Unterstützung im Hintergrund und manche klingende Injektion.

Ich danke meiner geliebten „eierlegenden WollmilchLAUS" Katrin! Jetzt bist Du dran mit Deiner Dr.-Arbeit und ich mach' die Wäsche, versprochen (☺/☹).